**Distribution Agreement**

In presenting this thesis or dissertation as a partial fulfillment of the requirements for an advanced degree from Emory University, I hereby grant to Emory University and its agents the non-exclusive license to archive, make accessible, and display my thesis or dissertation in whole or in part in all forms of media, now or hereafter known, including display on the world wide web. I understand that I may select some access restrictions as part of the online submission of this thesis or dissertation. I retain all ownership rights to the copyright of the thesis or dissertation. I also retain the right to use in future works (such as articles or books) all or part of this thesis or dissertation.

Signature:

_____ _____

Michael Brandon Ware Date

Dynamic Immune and Stromal Modulation by Therapeutic Targeting of IL-6 in Pancreatic Cancer
By

Michael Brandon Ware
Doctor of Philosophy

Cancer Biology

_____ [Advisor's signature]
Gregory Lesinski, Ph.D., MPH
Advisor

_____ [Member's signature]
Adam Marcus, Ph.D.
Committee Member

_____ [Member's signature]
Curtis Henry, Ph.D.
Committee Member

_____ [Member's signature]
Dolores Hambardzumyan, Ph.D., M.B.A.
Committee Member

_____ [Member's signature]
Haydn Kissick, Ph.D.
Committee Member

Accepted:

_____
Lisa A. Tedesco, Ph.D.
Dean of the James T. Laney School of Graduate Studies

_____
Date

# Dynamic Immune and Stromal Modulation by Therapeutic Targeting of IL-6 in Pancreatic Cancer

By

Michael Brandon Ware
B.S., Mercer university, 2014

Advisor: Gregory Lesinski, Ph.D., MPH

An abstract of
A dissertation submitted to the Faculty of the
James T. Laney School of Graduate Studies of Emory University
in partial fulfillment of the requirements for the degree of
Doctor of Philosophy
in Cancer Biology
2020

Abstract

Dynamic Immune and Stromal Modulation by Therapeutic Targeting of IL-6 in Pancreatic Cancer
By Michael Brandon Ware

Pancreatic ductal adenocarcinoma (PDAC) is a highly aggressive malignancy with a 5-year survival rate of only 10%. This cancer progresses silently in early stages, resulting in many patients presenting with metastatic disease. The aggressive and inherit drug resistant nature of PDAC is heavily influenced by the unique fibrotic stroma of PDAC, sometimes comprising up to 90% of the tumor by volume. This stroma contains dense matrices of collagen and fibronectin which harbor immune suppressive myeloid cells, regulatory T-lymphocytes and cancer associated fibroblasts (CAFs). Our research has revealed the highly heterogeneous populations of CAFs in PDAC to be key mediators of disease progression. Specifically, we previously identified interleukin-6 (IL-6) to be the most highly transcribed soluble factor by these cells, driving suppressive myeloid cells expansion while blunting T-cell responses to PDAC. Here, my thesis research sought to expand our knowledge of CAFs in PDAC by investigating the role of these cells in metastasis of pancreatic cancer. I hypothesized that IL-6 secreting CAFs are essential to pancreatic cancer cells, not only governing the TME of the primary tumor, but also mediating establishment of metastatic PDAC lesions in the liver. I chose to pursue this hypothesis through two projects. First, to understand how these cells enable metastasis, and seeking to unveil novel therapeutic targets for the treatment of late stage pancreatic cancer. I found PDAC associated CAFs to promote pancreatic cancer spheroid invasion through production of soluble factors and when in co-culture with tumor cells. Our lab previously utilized murine models of PDAC, and demonstrated IL-6 blockade significantly enhanced PD-1/PD-L1 blockade therapy. Therefore, my second project sought to leverage IL-6 blockade to disrupt dynamic interactions between IL-6 secreting CAFs and tumor cells to enhance CTLA-4 blockade efficacy in PDAC. Herein, I describe mechanisms by which this therapeutic combination elicits a potent anti-tumor response dependent upon $CD4^+$ T cells and CXCR3 which is unique to this strategy. The data I present here has the potential for future and immediate clinical translation for the benefit of patients with PDAC.

Dynamic Immune and Stromal Modulation by Therapeutic Targeting of IL-6 in Pancreatic Cancer

By

Michael Brandon Ware
B.S., Mercer University, 2014

Advisor: Gregory Lesinski, Ph.D., MPH

An abstract of
A dissertation submitted to the Faculty of the
James T. Laney School of Graduate Studies of Emory University
in partial fulfillment of the requirements for the degree of
Doctor of Philosophy
in Cancer Biology
2020

Acknowledgements

Certainly this thesis is not a reflection of what I have accomplished, rather a reflection of how blessed I was to have an unbelievable support system throughout my graduate career. I owe a great deal of gratitude to many mentors, but specifically to Dr. Greg Lesinski who took every opportunity to mentor me on how to be a scientist, a dad and a husband. I would also like to thank Dr. Bernardo Mainou who gladly gave his time to advise me on the many decisions I was faced with throughout these years. To my committee, Dr. Hambardzumyan, Dr. Henry, Dr. Kissick and Dr. Marcus, I am so thankful for your openness and willingness to give me advice and guidance as I sought to develop my scientific thoughts and pursue this doctoral degree. To my lab mates and friends Matt, Hannah, Mohammad, Brian, Amanda, Jerry, Jacklyn, Emily, Turgeon, Maggie, and Jess, thank you all for helping me maintain my sanity and helping me every step along the way. You guys are the real MVP. Thank you to my cohort Jameson, Rae, Cara, and Carey for your encouragement, support and friendship from the very first day in ethics class to the last.

To the members of the Integrated Cellular Imaging Core and the Emory + Pediatrics'/Winship Flow Cytometry Core, thank you all for your patience, flexibility and teaching. Especially thanks to Will Giang who took every opportunity to delve into the weeds of an explanation and never balked at my many many many questions, to the 99!

While a thank you could never do it thank you to Grandmama and Nonna for the many hours you babysat, loved, taught and nurtured Hannah and Maggie while I was in lab. I love you both. Thank you to the rest of my family who asked me about my work and maintained eye contact even though you probably wanted to stop listening. To my Mom and Dad, thank you both for listening to me and learning about what I was doing, you'll never know how much that meant.

To Hannah and Maggie, I am so thankful for you making zoom meetings more interesting, watching/listening to many webinars from home and trying to rewrite papers when I walked away from my computer. I love you both so much!

To my beautiful, intelligent and thoughtful wife Madeline. Thank you doesn't even cut it. This work is dedicated to you, and without you I really don't think any of it would have happened. For pushing me to chase this dream, for the time spent without me because I was working late to run sample or at a conference, for the innumerous hours spent trying to make my life easier at home, for sometimes listening to what I was doing at work, for loving me and being there at every moment, this is for you. Above all, I owe all my success to God. Thank you for orchestrating our move to Atlanta, my admission to Emory and continuously blessing us and watching over us.

Table of Contents

List of Figures

**List of Abbreviations**

| Abbreviation | Full Term |
|---|---|
| **ADAM17** | A Disintegrin and Metalloprotease-17 |
| **ADM** | Acinar-to-Ductal Metaplasia |
| **apCAF** | antigen-presenting Cancer Associated Fibroblast |
| **ARID1A** | AT rich interactive domain 1A |
| **BIRC** | Baculoviral IAP repeat-containing protein |
| **BLI** | Biluminescent Imaging |
| **BRAF** | v-raf murine sarcoma viral oncogene homolog B1 |
| **BRCA** | BReast CAncer gene |
| **BTLA** | B and T Lymphocyte Attenuator |
| **CAF** | Cancer Associated Fibroblast |
| **CAR T** | Chimeric Antigen-Receptor T cell |
| **CCR** | C-C Chemokine Receptor |
| **CD** | Cluster of Differentiation |
| **CDKN2A** | Cyclin Dependent Kinase 2A |
| **ConA** | Concanavalin A |
| **CTLA-4** | Cytotoxic T-Lymphocyte-Associated Protein 4 |
| **CTNNB1** | Catenin beta-1 |
| **CXCR** | C-X-C Chemokine Receptor |
| **E2F1** | E2F Transcription Factor 1 |
| **ECM** | Extracellular Matrix |
| **EDTA** | Ethylenediamine tetraacetic acid |
| **ELISA** | Enzyme-Linked Immunoassay |

| | |
|---|---|
| **ENA-78** | Epithelial Cell-Derived Neutrophil-Activating Peptide 78 |
| **EOT** | End Of Treatment |
| **FACS** | Fluorescence-Activated Cell Sorting |
| **FAPα** | Fibroblast Activation Protein alpha |
| **FBS** | Fetal Bovine Serum |
| **FFPE** | Formalin Fixed Paraffin Embedded |
| **FGF2** | Fibroblast Growth Factor 2 |
| **FOLFIRINOX** | Folic acid, Five-Fluoruracil, Irinotican, Oxaliplatin |
| **FOXP3** | Forkhead box P3 |
| **FSP-1** | Fibroblast Specific Protein - 1 |
| **GATA3** | GATA3 binding protein |
| **GEMM** | Genetically Engineered Mouse Model |
| **Gli-1** | Glioma-Associated Oncogene Homolog 1 |
| **GNAS** | Guanine Nucleotide Binding Protein, Alpha Stimulating |
| **GP130** | Glycoprotein 130 |
| **HA** | Hyaluronic Acid |
| **hTERT** | human Telomerase Reverse Transcriptase |
| **IACUC** | Institutional Animal Care and Use Committee |
| **iCAF** | inflammatory Cancer Associated Fibroblast |
| **ICI** | Immune Checkpoint Inhibition |
| **IHC** | Immunohistochemistry |
| **IL-** | Interleukin |
| **JAK** | Janus Kinase |
| **KLF5** | Krüppel-like factor 5 |

| | |
|---|---|
| **KRAS** | Kirstin Rat Sarcoma |
| **LAG3** | Lymphocyte-activation gene 3 |
| **Lif** | Leukemia inhibitory factor |
| **LSD** | Least Significant Difference |
| **Ly6C** | Lymphocyte Antigen 6C |
| **Ly6G** | Lymphocyte Antigen 6 Complex Locus G6D |
| **MAPK** | Mitogen-activated protein kinase |
| **MCP-1** | Monocyte Chemoattractant Protein-1 |
| **MDC** | Macrophage-derived Chemokine |
| **MDSC** | Myeloid Derived Suppressor Cell |
| **MHC** | Major Histocompatibility |
| **MSI** | Microsatellite Instable |
| **MYC** | Master Regulator of Cell Cycle Entry and Proliferative Metabolism |
| **myCAF** | myofibroblastic Cancer Associated Fibroblast |
| **NDRG2** | NMYC downstream-regulated gene 2 |
| **NF-κB** | Nuclear Factor Kappa-Light-Chain-Enhancer of Activated B cells |
| **NIH** | National Institutes of Health |
| **Pan-CAF** | Pancreatic Cancer Associated Fibroblast |
| **PanIN** | Pancreatic Intraepithelial Neoplasia |
| **PBRM1** | Protein polybromo-1 |
| **PCC** | Pancreatic Cancer Cell |
| **PD-1** | Programmed cell-Death Receptor 1 |
| **PDAC** | Pancreatic Ductal Adenocarcinoma |
| **PDGF-β** | Platelet Derived Growth Factor Beta |

| | |
|---|---|
| **PD-L1** | Programmed cell-Death Ligand 1 |
| **PI3K** | Phosphatidylinositol-3-Kinase |
| **PLC** | Phosopholipase C |
| **PSC** | Pancreatic Stellate Cell |
| **PSC** | Pancreatic Stellate Cell |
| **PTEN** | Phosphatase and Tensin Homolog |
| **RAL-GEP** | Ras-like Guanine Exchange Factor |
| **RNF43** | Ring finger protein 43 |
| **RORγt** | Retinoic Acid-Related Orphan Receptor γt |
| **RREB1** | Ras-responsive element-binding protein-1 |
| **SC** | Stellate Cell |
| **SDF-1α** | Stromal Cell Derived Factor 1 alpha |
| **SMAD4** | Small Mothers Against Decapentaplegic 4 |
| **STAT** | Signal Transducer and Activator of Transcription |
| **TARC** | Thymus and Activation Regulated Chemokine |
| **TBET** | T-Box Expressed in T Cells |
| **TCF1/7** | T-Cell Factor 1/7 |
| **TCR** | T-Cell Receptor |
| **TEAD2** | TEA Domain Family Member 2 |
| **Tfk** | T follicular helper cell |
| **TGF-β** | Tumor Growth Factor Beta |
| **TGFβR2** | Tumor Growth Factor β Receptor 2 |
| **Th1** | T-helper type 1 |
| **Th17** | T-helper type 17 |

| | |
|---|---|
| **Th2** | T-helper type 2 |
| **Th22** | T-helper type 22 |
| **Th9** | T-helper type 9 |
| **TIG-2** | Tazarotene Induced Gene 2 Protein |
| **TIM3** | T-cell Immunoglobulin and Mucin-Domain Containing-3 |
| **TME** | Tumor Microenvironment |
| **TNFγ** | Tumor Necrosis Factor gamma |
| **TP53** | tumor protein 53 |
| **TRD** | Time from Relapse to Death |
| **Treg** | T-regulatory |
| **Tyr** | Tyrosine |
| **YAP1** | yes-Associated Protein 1 |
| **αSMA** | Alpha-Smooth Muscle Actin |

## Chapter 1: Pancreatic Cancer

### 1.1 Introduction.

Pancreatic ductal adenocarcinoma (PDAC) is an aggressive malignancy, with a 5-year survival rate of only 10%[1,2]. Current models predict that PDAC will soon become the second leading cause of cancer-related deaths in the United States by 2030[3], surpassing both breast and colon cancer. Patients often present with late stage metastatic disease due to the silent progression of this cancer in its early stages, disqualifying the majority of patients from surgical resection. Aggressive chemotherapy regimens such as FOLFIRINOX and the combination of gemcitabine plus nab-paclitaxel are utilized as standard of care treatment in clinical settings[4]. These chemotherapeutics only extend survival by mere months, but are used to debulk the tumor in preparation for surgical resection (**Figure 1.1**). Given the dismal survival rate and extremely limited treatment options for patients diagnosed with PDAC, I have chosen to focus my research on expanding our knowledge of PDAC, while simultaneously developing novel treatment strategies to fight this malignancy. Here, I will review our current understanding of multi-cellular dynamics within PDAC to provide a foundational background for my studies described in the following chapters.

### 1.2 Notable mutations contributing to the underlying biology of pancreatic cancer.

Pancreatic cancer had previously been assumed to harbor an extremely low mutation burden[5,6], aside from the small fraction (0.8%) of cases with high microsatellite instability[7]. Recently, advanced genomic methodologies utilized sequencing approaches preceded by a physical delineation of the bulky stroma from the neoplastic cells within pancreatic tumors. One particular study evaluated 150 PDAC samples and uncovered common mutations in *KRAS, TP53, CDKN2A*, and *SMAD4* among these individual cases[8] (**Figure 1.2**). While *KRAS* was mutated in 93% of cases, other oncogenic

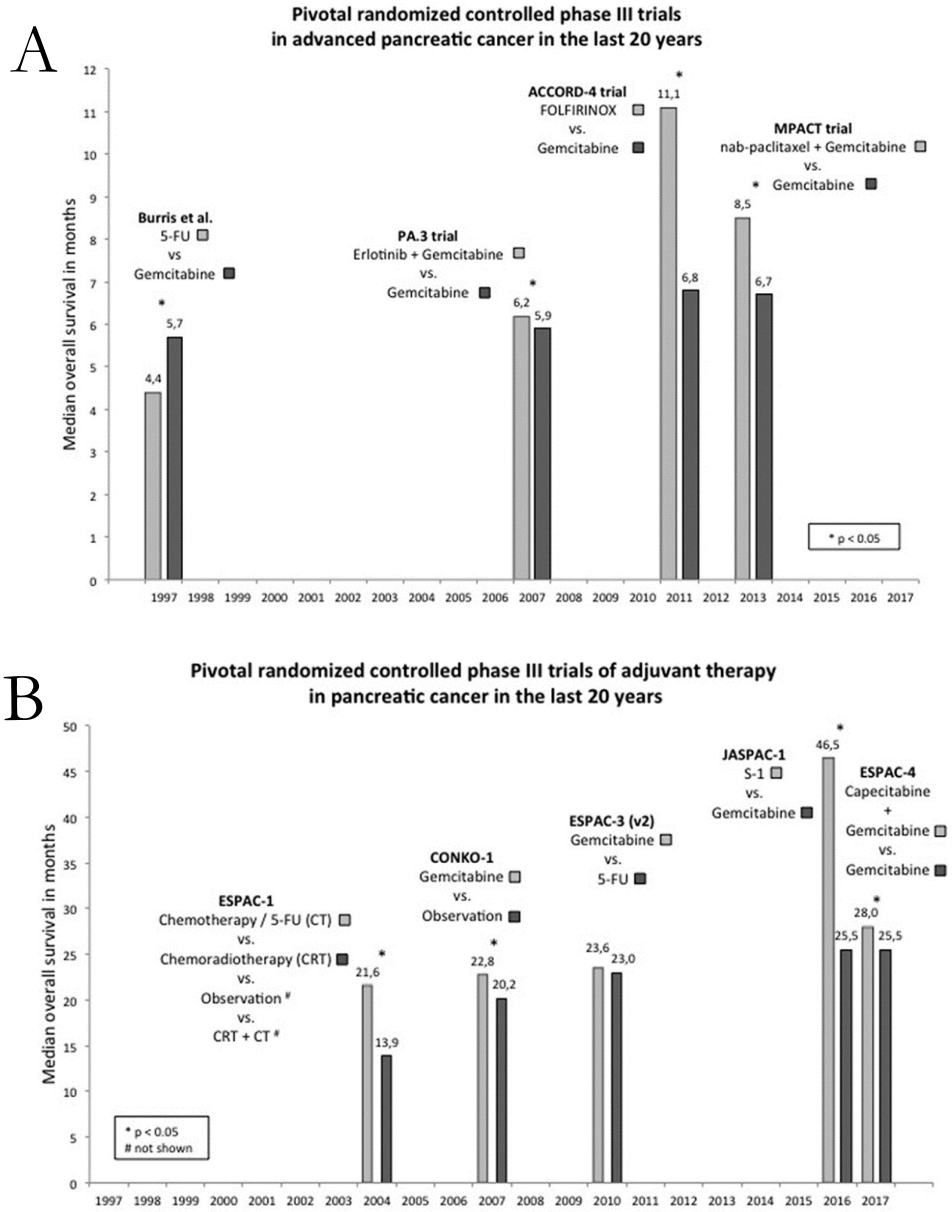


**Figure 1.1 Advancements in the treatment of pancreatic cancer.** (A) Median overall survival, in months, reported from randomize phase III clinical trials of first-line chemotherapy for the treatment of advanced PDAC spanning from 1997 to 2017. (B) Median overall survival, in months, reported from randomized phase III clinical trials of adjuvant chemotherapy for the treatment of pancreatic cancer spanning from 1997 to 2017. Figure adapted from Goess and Friess 2018[9]

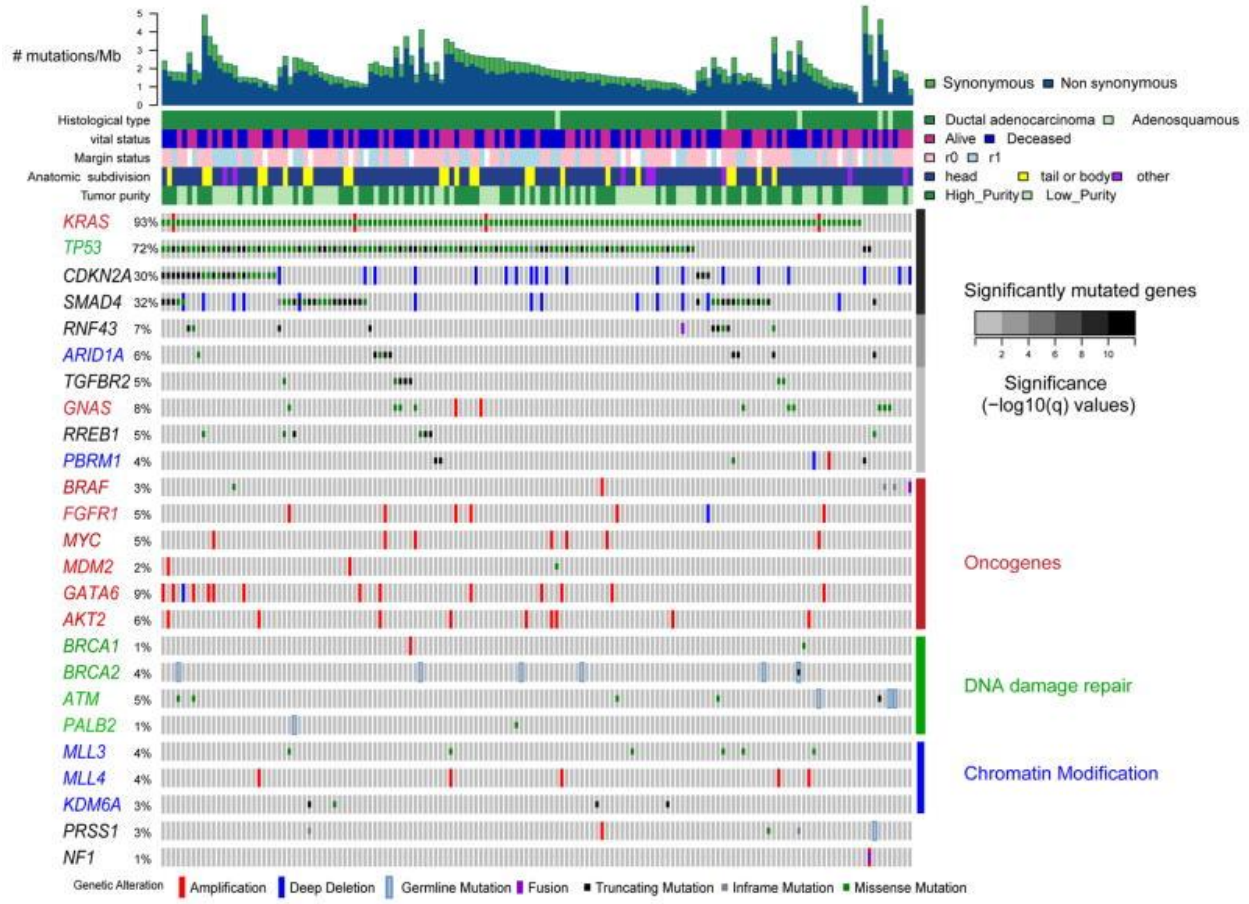


**Figure 1.2. Key mutations in pancreatic ductal adenocarcinoma.** TCGA analysis of 150 PDAC patient samples was performed on whole exome sequencing data. The most significantly mutated genes from these samples were then identified and highlighted here. This figure was originally published by The Cancer Genome Atlas Research Network in *Cancer Cell*[8].

mutations were extremely heterogeneous between patients. This heterogeneity associated with pancreatic cancer creates a difficult scenario for the development of therapeutics against any one genetic target. Thus, attempts to target downstream events of key presumed driver mutations have focused on finding common converging signaling events resulting from these mutations. An overwhelming proportion of patients bearing *KRAS* mutations present with a G12D alteration in this gene[10]. This mutation results in constitutive activation of this pathway culminating in downstream signaling via MAPK, PI3K, NF-κB and STAT pathways. Collectively, these signaling events promote proliferation, metastasis, survival, inflammation and changes in metabolism of these tumors[11-13]. Further, many patients demonstrate significant copy number gains in $KRAS^{G12D}$ which amplifies many of these phenotypic properties[14].

Innovative genetically-engineered mouse models (GEMM) of PDAC and careful evaluation of human disease have furthered identified $KRAS^{G12D}$ mutations in the earliest malignant precursors to PDAC known as pancreatic intraepithelial neoplasias (PanINs) [15,16]. Subsequent studies reveal this mutation facilitates production of factors that dramatically reshape and alter the surrounding tumor microenvironment (TME) of PDAC with influences on stromal fibroblasts, immune cells and vasculature. Mutations in *KRAS* drive aberrant secretion of CXCL2, CXCL5, CXCL1, GM-CSF among other cytokine and chemokines. These inflammatory factors promote infiltration of neutrophils and macrophages while simultaneously expanding suppressive myeloid cells within the TME. Infiltrating myeloid cells directly suppress the activity of CTLs and secrete their own profile of soluble factors which promote fibrosis and immune suppressive effects. Throughout PDAC progression, other mutations are acquired which are necessary for the transition of PanIN into PDAC. These mutations include, but are not limited to, genes such as *TP53, SMAD4, PTEN*, and *INK4a*[23,24]. With the acquisition of additional mutations, the rate of pancreatic cancer progression

heightens along with immunosuppressive cytokine and chemokine secretion and perpetuation of tumor promoting inflammation and fibrosis. Tumor-promoting sequelae generated by these molecular mechanisms provide an ideal microcosm for PanINs to progress into mature PDAC[17-19].

PanINs originate as a result of a process known as acinar-to-ductal metaplasia (ADM) during which the acinar cells of pancreatic ducts differentiate into neoplastic cells[20-23]. Early observations in human PDAC describe a distinct correlation between ductal lesions and mutations in *KRAS*. Observations in human and murine models further suggest acinar cells might be the cell of origin for PDAC[24,25]. Matrix metalloproteinase-7 (MMP-7) overexpression in PDAC is key to ADM and further studies by Crawford et. al. demonstrated acinar cells to be reliant upon this molecule to undergo metaplasia[21,26] and acinar cells are now widely accepted as the cell of origin for PDAC. Extreme inflammation or injury to the pancreas initiates the differentiation of these cells. Aligned with this are observations linking pancreatitis to severe inflammation of the pancreas, leading to eventual ADM and subsequent pancreatic cancer. Early in this process of ADM, the increased expression of Kruppel-like Factor 5 (KLF5) has been noted[27,28]. This downstream effector of KRAS and MAPK is commonly upregulated in fully developed PDAC, where it contributes to the constitutive STAT3 activation in pancreatic tumor cells and surrounding stromal populations[27]. Efforts are ongoing to understand the earliest molecular mechanisms mediating the induction of pancreatic cancer in order to detect PDAC at its earliest stages. The generation of innovative GEM models of PDAC not only allows for studies of PanIN development and subsequent establishment of PDAC, but also provides the field with clinically relevant models for the investigation PDAC biology. Perhaps the most foundational and relevant GEMM of PDAC is the KPC mouse (KrasG12D/+, Tp53R127H/+,Pdx-1-Cre) which is on a C57BL/6 background[29]. These mice express oncogenic Kras with the G12D mutation that is present in an overwhelming portion of patient tumors (70-

90%)[30] and mutant p53 via PDX promoter-mediated Cre[29]. The combined effects of Kras and Tp53 mutations in these mice recapitulate chromosomal instability leading to progressive development of PanINs to fully developed PDAC as is seen in patients[15,29,31] This process occurs over 8-10 weeks once mice reach about 8 weeks of age and leads to wide-spread metastasis to the lungs and livers of these mice, which are the most common sites of metastasis in patients. Notably, this model faithfully recapitulates the stromal reaction observed in human PDAC (**Figure 1.3**).

**1.3 Pancreatic cancer is characterized by a dominant fibrotic stroma.**

Upon resection and histological evaluation of pancreatic tumors, a dominant stromal reaction occurring within this malignancy is overtly evident. Collagenous ECM components and fibronectin are intercalated throughout the tumor and envelop small neoplastic lesions in a thick matrix of fibrosis and desmoplasia. Embedded throughout this fibrotic matrix are a multitude of cellular populations such as fibroblasts, myeloid cells, regulatory lymphocytes and others whose heterogeneity cannot be overestimated. In some cases, this dominant stroma can compose up to 90% of PDAC tumors by volume and is hypothesized to be the driving force behind the immunosuppressive and drug resistant nature of PDAC[32-34]. This stroma not only presents a challenge for the treatment of PDAC, but also represents an obstacle for studying this disease. Namely, this desmoplastic environment can create technical difficulty for extraction of immune and tumor cells must be extracted from this desmoplastic environment to be properly evaluated by cellular, molecular or genetic means.

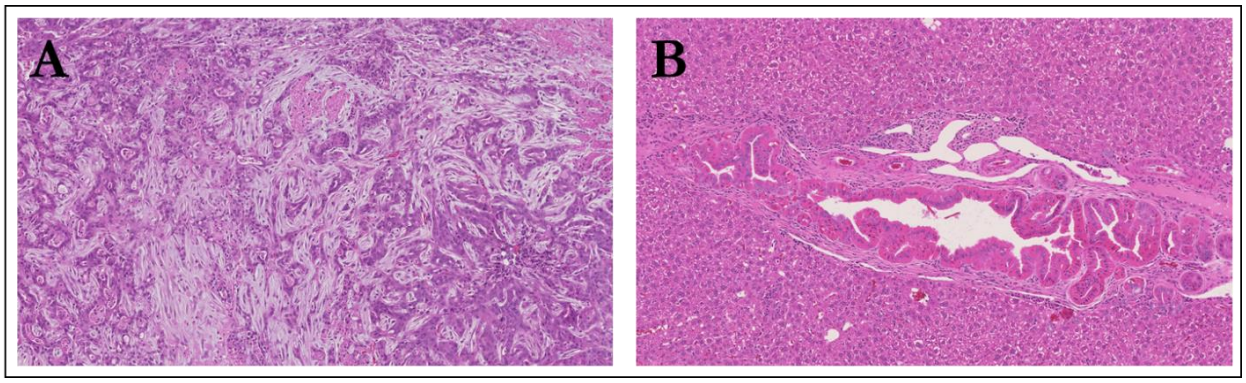


**Figure 1.3. Stromal reaction in primary and metastatic tumors of a KPC mouse. (A)** Representative H&E staining of an advanced, poorly differentiated tumor from a KPC mouse with evident stroma intercalating throughout cancerous lesions. **(B)** Representative H&E staining of an established metastatic site within the liver of the same KPC mouse. A thin border of stroma surrounds the lesion. All images taken at 10x.

Recently, the heterogeneous populations of fibroblasts residing in PDAC tumors have received a great deal of attention. These cells can alter many aspects of PDAC and are key mediators in the development of this unique stroma. Pancreatic cancer associated fibroblasts (CAFs) are heterogeneous, and can be sub-divided into at least three distinct functional and phenotypically defined subsets. This premise is based on histological analysis of tumors, and a series of eloquent organoid-based studies [35,36] (**Figure 1.4**). In identifying the first two subsets, differential αSMA and IL-6 expression were used as distinct markers to define separate "myofibroblastic" and "inflammatory" PSC subsets [35]. Cross-species sequencing of pancreatic tumors in mice and humans further revealed the existence of a third CAF population with the ability to present antigen[36]. These antigen presenting CAFs (apCAFs) express both CD74 and MHC-II and thus present antigen to $CD4^+$ T cells *in vivo*. Although whether this process activates or suppresses T-cell activity is yet to be determined[36]. The plasticity of individual CAF populations and this "Jekyll and Hyde"[37] influence on the immune system presents a complicated case for targeting the stroma to elicit responses against PDAC. Indeed, the stromal targeting agent saridegib, which inhibits sonic hedgehog, failed in the clinic (Infinity Corp reports, 2012) despite encouraging pre-clinical data in GEM models[38]. Further complicating our understanding are conflicting results from murine models indicating that *in vivo* depletion of fibroblasts may accelerate metastasis, but render tumors uniquely susceptible to immune checkpoint blockade[39,40]. Taken together, these data highlight that the fibroblast components of PDAC stroma can be either promoting or suppressive depending on the context of the TME[38,40,41]. Thus, consideration of individual stromal subsets is necessary in the design and approach to treating pancreatic cancer. Although there remains controversy on defining the heterogeneous subtypes of fibroblast cell populations within PDAC, the functional difference between these three well characterized PSC subsets is quite interesting and warrants further discussion below.

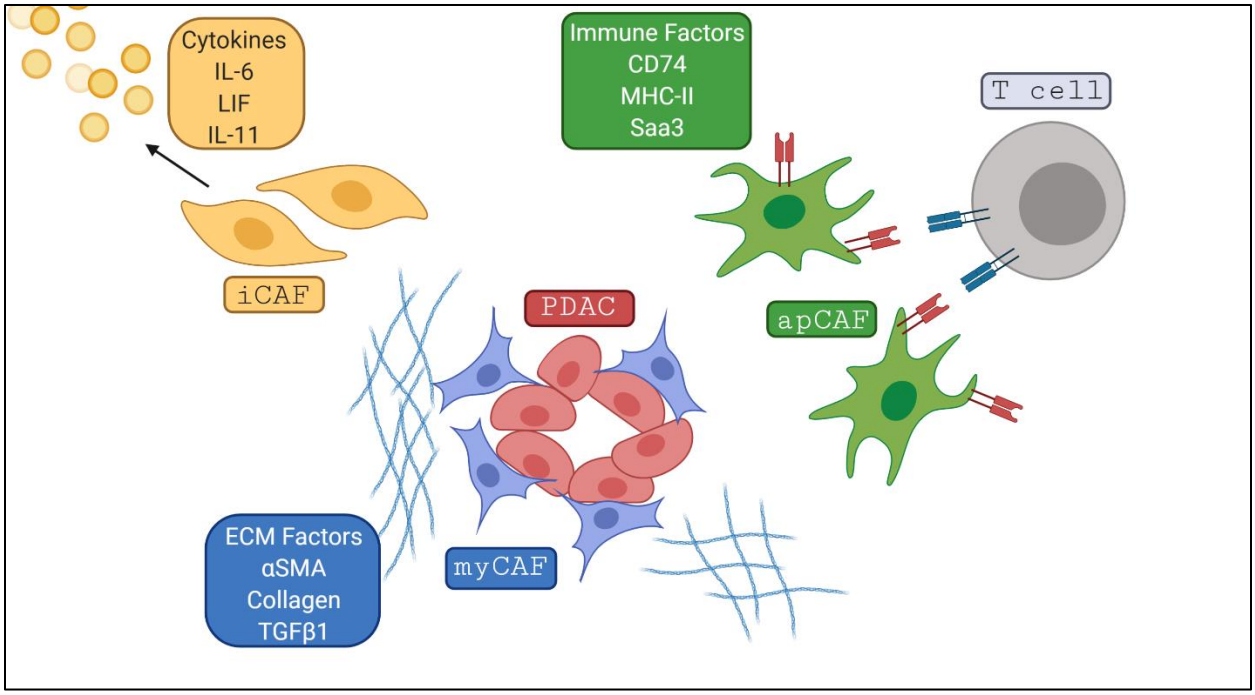


**Figure 1.4. Specialized fibroblast populations in pancreatic tumors.** Depiction of the 3 proposed subtypes of cancer associated fibroblasts; iCAFs, myCAFs and apCAFs. Role of each subtype and its respective interaction with the TME is outlined here. Image created using Biorender.

Immediately surrounding lesions of pancreatic cancer cells, a thin border of myCAFs can be found[35]. These fibroblasts are hypothesized to physically support pancreatic cancer cells and may in fact protect them from immune or pharmacological targeting. Genetic analysis has indicated these fibroblasts are distinguished by elevated secretion of ECM components such as collagen and fibronectin[36]. These elements may further contribute to drug resistance by creating a physical barrier that prevents large molecular drugs or antibodies from actually reaching the tumor cells. While myCAFs express high levels of αSMA and low levels of interleukin-6 (IL-6), iCAFs inversely demonstrate elevated secretion of IL-6 with low expression of the pan-fibroblast marker αSMA[36]. iCAFs are more frequent within pancreatic tumors[35] and embedded within the stroma at a greater distance from pancreatic cancer cells. These two subsets demonstrate surprising plasticity with the ability to convert between iCAFs and myCAFs depending on distinct cytokine signals[35]. Work from Ohlund et. al. defined a unique signaling mechanism mediating the polarization of the CAF subsets. Mechanistically, this involved the secretion of inteleukin-1 alpha (IL-1α) by tumor cells and the presence of transforming growth factor beta (TGFβ) within the TME[42]. IL-1α signaling to iCAFs is disrupted by the high levels of TGFβ within the TME, leading to NF-ϰB activation and the subsequent inflammatory characteristics of iCAFs[42]. These cells secrete high amounts of various immune modulatory cytokines and chemokines which include leukemia inhibitory factor (LIF), interleukin-11 (IL-11) and interleukin-6 (IL-6) [35].

Recently a third major subset of cancer associated fibroblasts has been recognized as having immunomodulatory abilities predicated on the expression of MHC-II and the invariant chain CD74[36]. Genetic analysis of these different subsets in both humans and mice has identified this third subset termed "antigen-presenting CAFs" or apCAFs[36]. This is not surprising given the inflammatory and immunomodulatory nature of iCAFs and the association of both subsets with the

more tumor-distal stroma. apCAFs were first described by the Tuveson lab at Cold Spring Harbor Laboratory and have recently been corroborated by a separate single-cell sequencing experiment of human PDAC[43]. Similar to the myCAF and iCAF subsets, this apCAF subset demonstrates plasticity to switch phenotypes based on the surrounding environment. Together, the data characterizing these three subsets highlight the intricate complexity of the tumor microenvironment influencing pancreatic tumor growth, immune response and disease progression.

**1.4 Metastasis of Pancreatic Cancer**

Most PDAC focused research details characteristics of the primary tumor, yet the majority of patients (85-90%) present with distal or local metastasis. This diagnosis disqualifies them from surgical resection as a treatment option[1,44,45]. Despite these alarming statistics, few studies have pursued detailed investigation of the mechanisms underlying PDAC metastasis. The most common sites of PDAC metastasis are the liver (76-94%), lungs (45-48%), lymph nodes (41%) and peritoneum (41-56%)[45]. The molecular mechanisms underlying metastasis to these different sites are quite different[46], potentially due to the differential physical requirements. Metastasizing cells may have to travel through vasculature (to the liver or lungs), lymphatics (to the lymph nodes or liver) or simply into surrounding organs (peritoneum)[46]. My studies specifically sought to interrogate metastatic spread to the liver, which is the most common site of PDAC metastasis.

Just as fibroblast components of the TME have received special attention in primary PDAC tumors, the influence of immune and fibroblast components of the liver on metastasis is gaining attention. Lee et. al. recently demonstrated hepatocytes with significant STAT3 activation can prime metastatic sites in the liver by secretion of serum amyloid A1 and A2 (SAA)[47]. Interestingly, SAA release by hepatocytes is dependent upon release of IL-6[48-50], which is significantly elevated in PDAC, into

circulation by non-cancerous cells[47]. Similarly, macrophages and MDSCs can prime a "metastatic niche" in the liver by promoting recruitment of suppressive myeloid cells and stimulating hepatic stellate cells to create a fibrotic microenvironment in this organ[51,52]. Taken together, these studies support the notion that many components of primary pancreatic tumors are likely recapitulated in metastatic lesions. Despite this evidence only one published study, to our knowledge, has tested whether cancer associated fibroblasts are directly involved in PDAC metastasis[53]. Notably, this study was not done in immune competent mice or even with species matched CAFs and pancreatic cancer cells. Given the evidence for both stromal and immune involvement in PDAC metastasis, there is a dire need to investigate the potential involvement of PDAC CAFs in the metastasis to the liver.

**1.5 Foundational studies of T-helper cell biology.**

Extensive studies have characterized the immunosuppressive microenvironment created by a dominant stromal reaction, resulting in the realization that this stroma presents a dynamic and frustrating barrier to immunotherapy[32,33]. Current efforts are focused on dissecting the mechanisms by which this stroma drives PDAC immunosuppression, with the idea that targeting the stroma may relieve immune suppression and promote effective anti-tumor immunity. In very recent years, advanced murine models of PDAC and forward-thinking techniques of investigation have begun to reveal key facets of immune suppression in PDAC. Additionally, our ability to generate effective anti-pancreatic responses is advancing with a promising outlook on the future of immunotherapy for this deadly cancer.

Our efforts, seek to understand why PDAC has proven resistant to many targeted therapies, with single agent immunotherapy eliciting almost no response.[54-56] Similarly, vaccine or cellular based therapies in PDAC have demonstrated modest effects with no significant improvement in outcome

to date[57-59]. Early studies describing immune mediated tumor rejection and the ability of tumors to establish in immune compromised hosts revealed T-lymphocytes, or T cells, to be crucial effector cells in the body's fight against cancer. It is hypothesized that the aggressive nature of this disease and the failure of many therapies to affect tumor progression can be attributed to the broad T-cell suppressive activity within PDAC. Thus, much of the work describing immune suppression in PDAC focuses on the exclusion or suppression of lymphocyte activity within PDAC tumors.

While pursuing a deeper understanding of the PDAC tumor microenvironment, a firm grasp of the studies detailing T-cell biology provides necessary context to elicit the mechanisms of T-cell suppression in PDAC. Here, key studies in the field of immunology are outlined that led to our current understanding of lymphocytes and their relationship with inflammation. Humoral biologists first described phenotypic differences between T cells, whereby T cells could be separated based on their ability to bind Fc portions of IgM, IgG or neither[60]. Investigation into these T-cell subsets additionally revealed phenotypic differences that drove investigators to fully characterize different subsets of T cells by secretory profiles, effector function and phenotypic markers detected by flow cytometry[60-63]. With the emergence of flow cytometry, studies led by Stuart Schlossman utilized some of the first flow cytometry based antibodies to identify markers that could generally distinguish T cells from other blood cells, as well as antibodies that could identify subsets of T cells[62,63]. The first of these markers bound by the monoclonal antibody OKT3 not only identified all peripheral T cells, but also stimulated proliferation of peripheral T cells with activity similar to that of previously used mitogens[63]. Another monoclonal antibody, OKT4, bound just over 50% of peripheral T cells and seemed to specifically identify a subset of T cells that could provide "help" to B-cells in culture[63]. We now know these antibodies to bind cluster of differentiation-3 eta (CD3ε) and cluster of differentiation-4 (CD4) respectively. Subsequent studies revealed the presence of a cytotoxic subset

that could be identified by specific antisera[63]. Almost simultaneously with these aforementioned experiments, murine studies led to the identification of CD8 binding antibodies[64-66].

As $CD4^+$ and $CD8^+$ T cells were identified, the Schlossman group additionally characterized inherent phenotypes of these cells. While the existence of lymphocytes with distinct phenotypic properties had been observed and characterized by many groups[61-63,67,68]; however, no one had yet identified specific phenotypic markers to uniquely identify these cells by flow cytometry. T cells marked by $CD4^+$ were observed to provide "help" to B-cells through the production of various cytokines[69-73], while T cells expressing CD8 were identified by their ability to elicit cell death of infected cells[61,63-68]. These phenotypic differences led to the classification of $^{CD4+T\text{-}cells}$ as T-helper cells, while $CD8^+$ T cells became known as Cytotoxic T-lymphocytes (CTLs). Overtime it has become clear that these classifications generally hold true, but that subsets of $CD4^+$ and $CD8^+$ T cells have many overlapping functions. For example, some $CD4^+$ subsets exhibit cytolytic function while CD8 expressing T-cell subsets can secrete a heterogeneous array of chemokines and cytokines[74,75].

In general, T-helper cells can be identified by a distinct secretory profile of cytokines and growth factors as well as subtype specific transcription factors driving aspects of this secretory profile[60,61,71-73]. Interestingly, the differentiation of T-helper cells into unique subsets is also determined by particular cytokine and growth factor influences[76,77]. In the context of cancer, Th1, Th2, Th17 and regulatory T cells are the T-helper subsets that have been most thoroughly evaluated for their role in mediating tumor progression or anti-tumor immunity. More recently, the importance of Th9, Th22 and T Follicular Helper (Tfh) subsets have emerged and are gaining the attention of tumor immunologists. While these latter subsets are certainly important, little is known about the role for these helper subsets in PDAC. Therefore, the detailed background below will focus on Th1, Th2,

Th17 and T-regulatory subsets and the significance of these cells in the context of PDAC.

While differential activity of T-cell subsets had been previously described, Th1 and Th2 subsets were first defined by Mossman et al. in 1986[71]. Using recently developed antibodies, $CD4^+$ T-cell clones were generated and stimulated with Concanavalin-A (ConA) to promote cytokine and growth factor production[71]. Using innovative cellular based assays to define cytokine production, Mossman et al. revealed Th1 cells to produce IL-2 and IFN-γ while Th2 cells produce Il-4, IL-5, IL-6, and IL-10 among others[71]. This initial characterization of Th1 and Th2 still informs our approach to defining these cells through *in vivo* and *in vitro* investigation. Characterization of cytokine and growth factor production by these cell types certainly comprises the most thorough way to evaluate the phenotype of these cells *in vivo*, as Th1 and Th2 cells may only make a portion of these cytokines in certain inflammatory conditions.

However, about 15 years after Mossman et al. first published this work other studies emerged describing chemokine receptor profiles and transcription factors associated with Th1 and Th2 cells that could further distinguish these $CD4^+$ T-helper subsets[78-80]. For example, Th1, but not Th2 cells express C-X-C Chemokine receptor type 3 (CXCR3) which primarily responds to CXCL9 (MIG), CXCL10 (IP-10) and CXCL11(ITAC)[78-80] with IP-10 being the dominant chemokine for this receptor. On the other hand, Th2 cells express C-C chemokine receptor type 4 (CCR4) which binds and responds to CCL17 (TARC) and CCL22 (MDC)[78,80,81]. The differential expression of these chemokine receptors preferentially attracts one subset of T-helper cells as a result of the chemokine ligands generated by local or systemic inflammatory conditions[80]. Further, it was discovered that Th1 cells express the transcription factor T -box protein 21 expressed in T cells (TBET) which induces the expression of both IFN-γ and CXCR3 on Th1 cells[82,83]. In contrast, Th2 cells can be identified

by the expression of the transcription factor GATA binding protein-3 (GATA-3) which directly induces the transcription of many Th2 associated cytokines including IL-4, IL-6 and IL-10[84]. The balance of these transcription factors is regulated by many ectopic and intrinsic influences and as a result, controls the eventual phenotypic properties of T-helper cells associated with the Th1 and Th2 lineages.

Studies of autoimmunity in the context of Th1 cells revealed the Th1-derived interleukin-12 (IL-12) as a driver of inflammation[77]. For many years Th1 and Th2 cells were thought to be the major source of lymphocyte/cytokine related inflammation[61,71,73,76-78,84,85]. However, studies of autoimmune related inflammation of the joints and the brain revealed interleukin-23 (IL-23) to be another important cytokine mediator of inflammation[86-88]. This led researchers to probe for the existence of additional T-helper subsets since neither Th1 nor Th2 cells produce IL-23. Harrington et al. subsequently revealed a population of T-helper cells, distinct from Th1 and Th2 cells, to produce IL-17 and IL-23[89]. Thus, they deemed this population of T-helper cells "Th17"[89]. While IFN-γ signaling is a hallmark signature of Th1 cells, this soluble factor inhibited the development of Th17 cells by reducing the expression of IL-23 receptor in naïve $CD4^+$ T cells. A similar inhibition of Th17 development was evident when exogenous IL-4, used to polarize Th2 cells, was added to cultures of naïve $CD4^+$ T cells. Culturing naïve $CD4^+$ T cells with IL-12 and IL-27 induces a Th1 phenotype, while Th17 development relies on IL-23 stimulation and the neutralization of both IFN-γ and IL-4. Since these foundational studies of Th17 cells, our understanding of the cytokines and growth factors responsible for T-helper cell development have matured. While Th1 and Th2 cells rely on IL-12 and IL-4 respectively for their differentiation, as described above, Th17 cells are generally polarized by a combination of TGFβ, IL-21 and IL-6[90] (**Figure 1.5**). TGFβ and IL-6 lie at the crux of Th17 and T-regulatory cell development, the latter of which is expanded by TGFβ in the

absence of IL-6 signaling. A regulatory population of immune cells was first proposed by Gershon and Kondo in 1970[91]; however, the existence of such cells was largely written off for the next decade. In 1982, Sakaguchi et al. described broad auto-immune disease in some strains of mice following thymectomy that was strongly associated with the absence of $CD5^{hi}CD45RB/C^{lo}$ T cells[92]. As molecular technology such as flow cytometry advanced, a separate study by Sakaguchi et el. established that a $CD4^+$ population of thymocytes marked by high expression of CD25, the IL-2 receptor, exhibited both *in vivo* and *in vitro* regulatory phenotypes[93]. Unfortunately, the overlap of these markers with other thymocyte populations without regulatory capabilities prevented definitive conclusions related to existence of a specific T-regulatory population. It was not until the early 2000s that an onslaught of converging studies detailed a relationship between regulatory T cells and the expression of the transcription factor forkhead box protein P3 (FOXP3), also known as scurfin[94-101]. $CD4^+CD25^{hi}FOXP3^+$ cells are now widely accepted as T-regulatory cells (Tregs), which arise in the thymus and possess the ability to control and suppress effector T-cell responses in the periphery and in solid tissue[97,100,102,103]. generally polarized by a combination of TGFβ, IL-21 and IL-6[90] (**Figure 1.5**). TGFβ and IL-6 lie at the crux of Th17 and T-regulatory cell development, the latter of which is expanded by TGFβ in the absence of IL-6 signaling. A regulatory population of immune cells was first proposed by Gershon and Kondo in 1970[91]; however, the existence of such cells was largely written off for the next decade. In 1982, Sakaguchi et al. described broad auto-immune disease in some strains of mice following thymectomy that was strongly associated with the absence of $CD5^{hi}CD45RB/C^{lo}$ T cells[92]. As molecular technology such as flow cytometry advanced, a separate study by Sakaguchi et el. established that a $CD4^+$ population of thymocytes marked by high expression of CD25, the IL-2 receptor, both *in vivo* and *in vitro* regulatory phenotypes[93]. Unfortunately, the overlap of these markers with both *in vivo* and *in vitro* regulatory phenotypes[93]. Unfortunately, the overlap of these markers with other thymocyte populations without

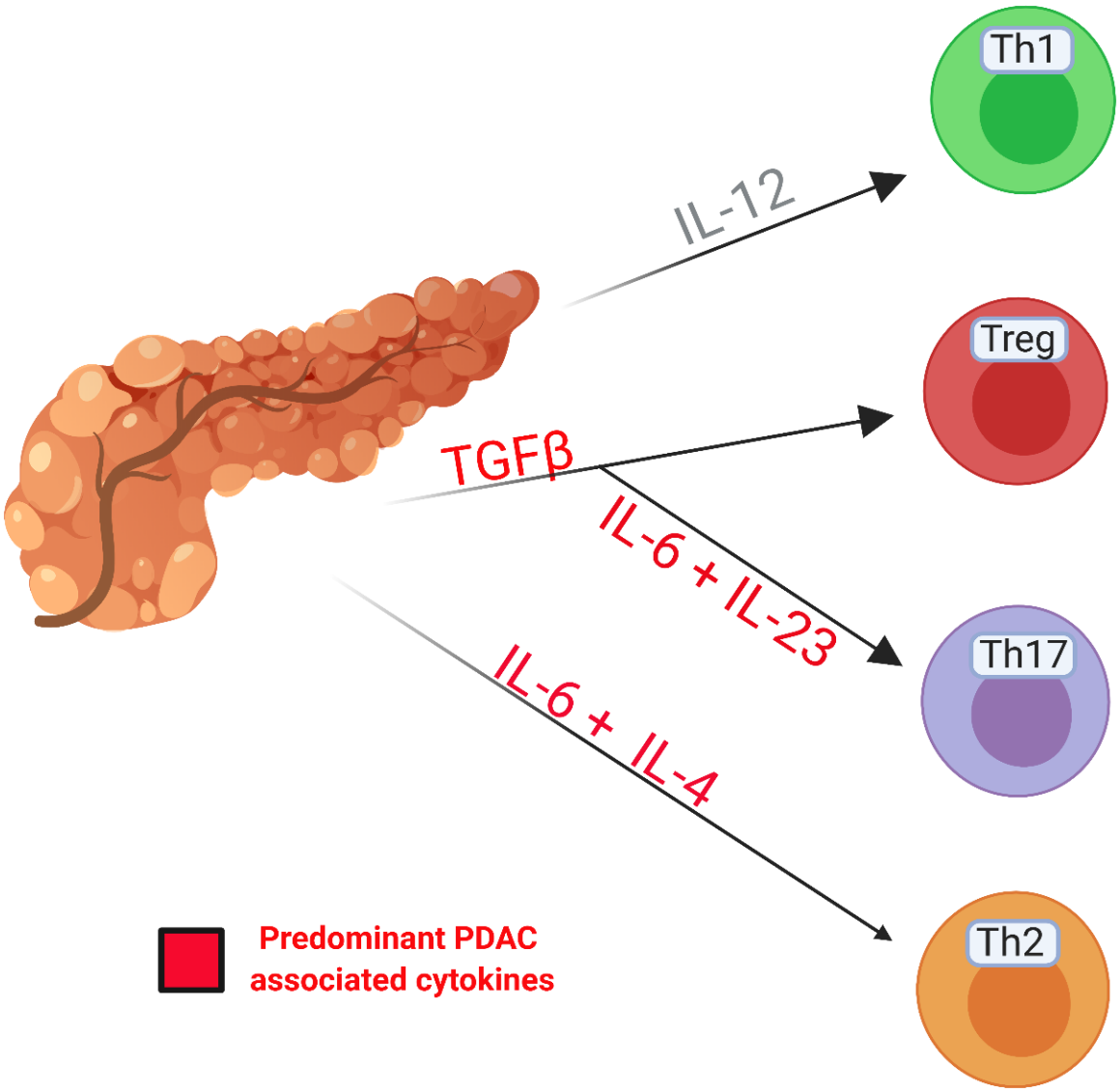


**Figure 1.5 T-helper polarization by PDAC associated cytokines.** Predominant PDAC associated cytokines such as Il-6, Il-4 and TGFβ induce expansion of T-helper cells with a Th2, Th17 or Treg phenotype. This not skews toward a higher prevalence of these T-helper populations, but also depletes the naïve pool of T-helper cells negatively impacting the frequency of Th1 cells that can be expanded in the pancreas. Figure made with Biorender.

regulatory capabilities prevented definitive conclusions related to existence of a specific T-regulatory population. It was not until the early 2000s that an onslaught of converging studies detailed a relationship between regulatory T cells and the expression of the transcription factor forkhead box protein P3 (FOXP3), also known as scurfin[94-101]. $CD4^+CD25^{hi}FOXP3^+$ cells are now widely accepted as T-regulatory cells (Tregs), which arise in the thymus and possess the ability to control and suppress effector T-cell responses in the periphery and in solid tissue[97,100,102,103].

Since these foundational studies, the field of tumor immunology has blossomed. Unsurprisingly, there exists dramatic heterogeneity between tumor types with respect to T-cell infiltration, activation and phenotypes. This heterogeneity has led to disagreement in the field with respect to $CD4^+$ T-helper cells concerning which subset is most effective at eliminating tumors and which are involved in tumor promoting inflammation. Recent studies in PDAC have shed light on which $CD4^+$ phenotypes are associated with tumor regression, and which promote immune suppression and tumor growth in PDAC.

**1.6 Inflammatory dynamics of T cells within the complex cytokine milieu of PDAC**

The highly immunomodulatory cytokine milieu conjured by tumor cell, fibroblast and immune secretions does not lend itself to the natural differentiation or expansion of Th1 cells or CTLs. We and others have reported systemic and intra-tumoral elevations of immunosuppressive cytokines and growth factors in PDAC such as Il-6, Il-10, TGFβ which promote skewing of infiltrating $CD4^+$ helper T cells towards a Th2, Th17 or Treg phenotype[42,50,104-112]. Due to intra-tumoral heterogeneity of cytokine production, this $CD4^+$ T-cell skewing effect may be regional, differing throughout portions of the tumor. Past literature in PDAC has almost uniformly tagged Tregs and Th17 cells as immune suppressive and tumor promoting[18,94,95,102,113-115]; however, this is not the case for all cancer

types[90,116]. In contrast, $CD4^+$ Th1 cells have an essential role in T-cell mediated anti-tumor immune responses across cancer types, including PDAC[50,117-119]. Pharmacologically counteracting this imbalance of cytokines within the tumor as well as within the host has generated promising results. Neutralization of IL-6 or blockade of its receptor synergizes quite well with ICI to induce potent anti-tumor responses. Concurrent with improved anti-tumor responses after dual blockade of IL-6 and PD-L1, Th1 cells increased systemically as well as within PDAC tumors in murine models[48,50,109]. Our knowledge of how Th1 cells might be best leveraged to induce anti-tumor immune responses to PDAC is still lacking, as many investigators focus their attention on $CD8^+$ CTLs rather than T-helper cells. This can be partially attributed to the $CD8^+$ T-cell dependence of PD-1/L1 blockade which has emerged as a promising ICI option for the treatment of cancer[50]. However, the mechanisms of action surrounding emerging immune based therapies have not been fully defined. Together, these data highlight a gap in our understanding of how therapeutic modulation of $CD4^+$ helper T cells could benefit patients with PDAC.

**1.7 Targeting dominant pathways in the tumor microenvironment.**

While the genomic landscape of pancreatic cancer does not lend itself to immediately targetable mutations, there are a myriad of pathways mediating crosstalk between the tumor, stroma and, the immune system that can be pharmacologically modulated. The majority of single agent therapies have failed in PDAC, including small molecule inhibitors, antibody based pharmacological agents, and immune based therapies. Below, the insight gained from these unsuccessful attempts at targeting pancreatic cancer are summarized. Given the high prevalence of CAFs within the TME, and their multifactorial role in controlling inflammation and disease progression, several attempts have been made to target these cells. It was hypothesized that targeting CAFs or their derivatives would restore the natural vasculature and allow for increased drug delivery to sites of cancer. Investigations of the

sonic hedgehog pathway revealed this ligand was elevated in pancreatic cancer due to its secretion by pancreatic cancer cells and other stromal populations[38]. This ligand signals to fibroblasts and stimulates their activation and secretion of ECM components that were theorized to prevent drug delivery and vascular growth, while promoting hypoxia in pancreatic tumors[120]. Targeting this pathway in mice with sonic hedgehog inhibitors indeed resulted in significant changes in vascular growth and fibrosis in pancreatic tumors[38], leading to a clinical trial (NCT01130142). This trial employed the sonic hedgehog inhibitor, saridegib alongside gemcitabine. The overall hypothesis was that saridegib would allow gemcitabine to access pancreatic cancer cells and regress tumors as observed in murine models[38]. Conversely, this inhibitor actually accelerated disease progression with increased metastatic spread of tumors in patients. While this trial was quickly halted, it substantiated the stroma was more complex of a pharmacologic target that originally thought.

Contrasting these results were positive indications from trials targeting hyaluronic acid, an ECM component with increased expression in pancreatic tumors[121-123]. This polysaccharide component of the ECM can be secreted by tumor cells and CAFs and is localized to fibrotic areas of pancreatic tumors[124]. Again, investigators hypothesized that targeting this molecule would relieve the protective effect of the fibrotic stroma and allow for more effective drug delivery to sites of pancreatic tumor cells. Clinical trials have employed a pegylated form of hyaluronidase, an enzyme which cleaves and digests hyaluronic acid. Only a subset of patients benefited from this approach with a survival of 9.2 months compared to 5.2 months in the control group[121,122]. Despite this marginal increase in survival, these two approaches together provide an important example that targeting the stroma in pancreatic cancer can be advantageous but must be approached with caution.

Rather than targeting the ECM, our group has chosen to leverage antibodies against IL-6. This cytokine is secreted at extremely high levels by pancreatic CAFs and elevated both systemically and

intratumorally in pancreatic cancer[48,109]. IL-6 works through either a soluble or membrane bound receptor to activate the transmembrane protein gp130 which signals downstream through STAT3 to activate proliferative and inflammatory pathways (**Figure 1.6**). The Jak2/STAT3 pathway is a dominant signaling pathway in pancreatic cancer which can be activated in immune populations and stromal cells in pancreatic cancer[109]. We hypothesized that this molecule could similarly impact immune cells in the TME by promoting the expansion of suppressive myeloid subsets and blunting cytotoxic T-lymphocyte (CTL) responses to pancreatic cancer. Indeed, several previously published manuscripts from our lab provided ample evidence to support this hypothesis[50]. Our current clinical trial (NCT04191421) at the Winship Cancer Institute of Emory University is testing the ability of IL-6 blockade to significantly enhance PD-1 blockade in pancreatic cancer. Similarly, investigators are working to target TGFβ, focal adhesion kinase (FAK), heat shock protein 90 (HSP90), CCR2, and CD40 among other targets in order to leverage imbalanced signaling pathways to improve immunotherapies in PDAC[37].

**1.8 Scope and Goals for this Project.**

Given the impact of the stroma in mediating pancreatic tumor growth and progression, my first goal for this project was to characterize the contributions of cancer associated fibroblasts to PDAC progression. Our previous work found these cells to secrete high Il-6 levels, which has a dramatic negative impact on immune responses to pancreatic cancer. Therefore, my second goal for this project was to explore therapeutic targeting of IL-6 as a method to enhance immune based therapy to mediate tumor regression. Here, I describe my efforts on these two closely related projects which demonstrate advancements in our understanding of pancreatic cancer and an ability to translate findings to therapeutic options for patients.

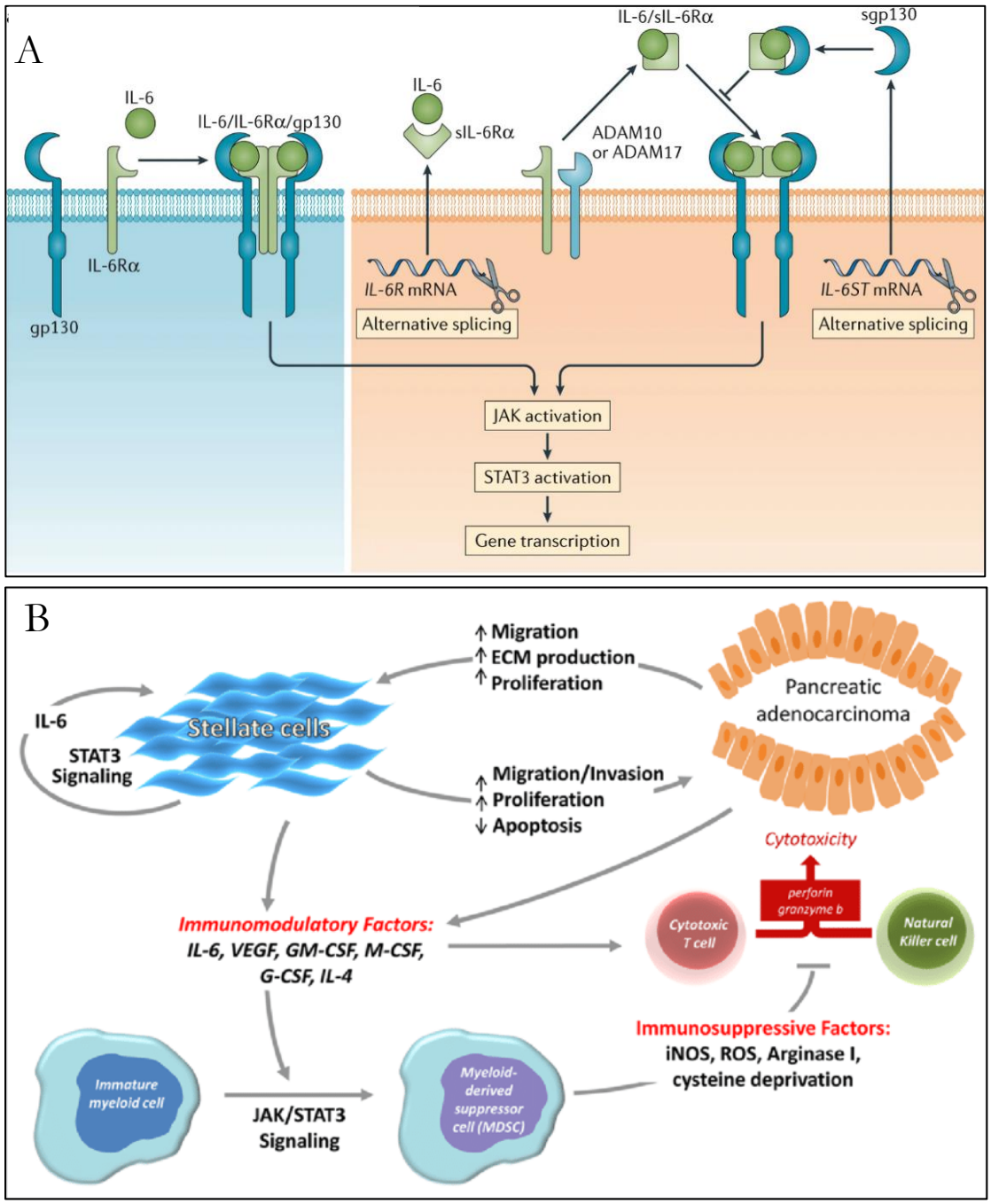


**Figure 1.6. Jak/STAT signaling induced by IL-6 is a central mediator of many processes in pancreatic cancer. (A)** IL-6 can bind to membrane bound IL-6R or soluble IL-6R that has been cleaved by the γ-secretase ADAM17. Ligation of IL-6 to its receptor, signaling through gp130 leads to JAK activation and subsequent phosphorylation of the transcription factor STAT3. Figure

adapted from Johnson et. al.[125] **(B)** IL-6 activation of STAT3 signaling can alter pancreatic stellate cells in the TME as well as numerous immunosuppressive populations, leading to tumor progression. Figure originally published by Mace et. al.[49]

## Chapter 2: Metastatic Spread of PDAC is Supported by Fibroblasts

### 2. 1 Introduction

Due to the silently progressing nature of pancreatic cancer, most PDAC patients present with advanced metastatic disease at first diagnosis. In 2019, only 10% of pancreatic cancer patients were reported to present with only local disease, and over 50% of patients with distal metastasis[1]. While patients with local disease often qualify for surgical resection, over 80% will recur, most often with distal metastasis[44]. The most common sites of metastasis for pancreatic cancer are the liver and the lungs (**Figure 2.1**), with a time from relapse to death (TRD) of 9 and 15 months, respectively[126]. Thus, the mechanisms by which pancreatic cancer metastasizes is an area in urgent need of investigation.

A prominent histopathological feature of PDAC is a dense fibrotic stroma intercalating throughout the tumor, surrounding cancerous lesions. This stroma is heterogeneous in nature, consisting of desmoplastic extracellular matrix components, immune cells, and activated CAFs that together are estimated to compose up to 90% of PDAC tumors by volume[127]. CAFs produce collagen, growth factors and other soluble factors that modulate the immune reaction to cancer. They also metabolically reprogram cancer cells, while promoting tumor growth and inhibiting drug delivery[128,129]. Surprisingly, in studies targeting this fibrotic stroma, as well as deletion of alpha-smooth muscle actin (α-SMA) positive fibroblasts from PDAC genetic models, more invasive tumors and increased incidence of metastatic lesions were evident. Paradoxically, the efficacy of immunotherapy with antibodies targeting the CTLA-4 immune checkpoint receptor was enhanced in these more aggressive tumors[40,41]. Within pancreatic tumors, there are a number of CAF populations which include; inflammatory CAFs that produce a multitude of inflammatory cytokines, chemokines and growth factors; myofibroblastic CAFs that produce ECM components, and

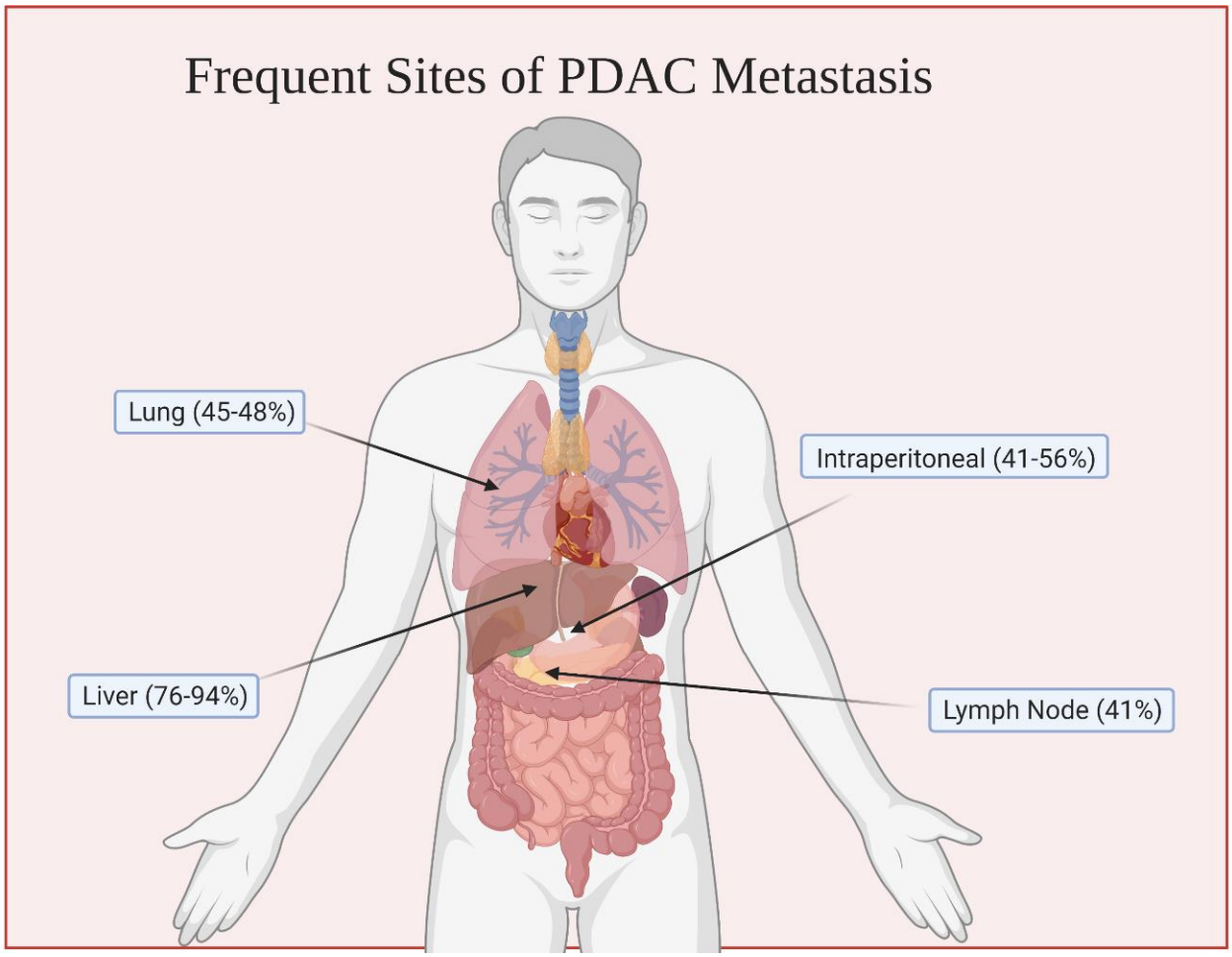


**Figure 2.1 Site frequency of PDAC metastasis in patients with advanced metastatic PDAC.** Here, the four most frequent sites of PDAC metastasis; the liver, lung, lymph node and peritoneum are indicated. Additionally, the percentage with which patients present with metastatic disease at these four sites is listed. Patients with multiple sites of metastasis were counted in multiple categories. Information from Le Large *et al*[5] and figure created with Biorender.

antigen-presenting CAFs that possess the intrinsic ability to interact with immune populations, such as T cells. However, the influence of individual CAF populations on metastasis and disease progression has not been investigated[35].

Our prior research defined a role for CAFs as mediators of immune suppression. Specifically, we have demonstrated CAFs are a source of interleukin-6 (IL-6), which promotes cancer cell proliferation and regulate expansion of myeloid-derived suppressor cells (MDSCs) in a STAT3-dependent manner[14,109]. Previous literature identified CAFs and immunosuppressive MDSCs at sites of metastasis in models of melanoma, and pancreatic cancer. However, there remain key gaps in our understanding of how PDAC cooperates with these populations to metastasize[130-132]. Furthermore, many of the studies performed in murine PDAC models were in nude mice, thus negating the ability to study how lymphocytes influence this process. Studies of metastasis in lung cancer have provided evidence of **novel** "collective invasion" mechanisms by which distinct phenotypes of cells work together to invade[133]. Additionally, recent research from the Beatty lab implicates hepatocytes in the secretion of many chemoattractant and soluble factors that could initiate this process[47]. Further, work by the Tuveson lab has described dynamic interactions between CAFs and cancer cells mediated by inflammatory soluble factors such as Interleukin 1- alpha, TGFβ and others[42]. Our published data on CAFs and IL-6, as well as current literature on metastasis, demonstrate a strong scientific premise to further characterize and investigate metastatic PDAC lesions and determine the role of CAFs in collective invasion and metastasis. In particular, we posit that collective invasion in PDAC may be prominently influenced by activation of stromal cell components and production of soluble factors such as IL-6 that are quite unique to this disease. I hypothesized that IL-6 secreting PSCs stimulate metastatic signaling in PDAC, and that collective invasion between PSC and pancreatic cancer cells represents a key mechanism by which metastasis occurs in this aggressive

disease. To probe this hypothesis, I utilized novel and innovative mouse models and *in vitro* methods which are described in detail below.

**2.2 Methods**

*Cell line and antibodies*

PSC5 cells (a kind gift from David Tuveson, Cold Spring Harbor Laboratory, New York) are a fibroblast line derived from a spontaneously arising KPC tumor and immortalized using SV40 large T antigen and were cultured in DMEM (Gibco) with 5% FBS, 10nM L-glutamine and antibiotics (GiminiBio). Murine KPC-luc ($Kras^{LSL\text{-}R270H}$, $p53^{-/-}$, Pdx1-cre) cells expressing an enhanced firefly luciferase construct (a gift from Dr. Craig Logsdon, MD Anderson Cancer Center) were cultured in DMEM with 10% FBS, 10nM L-glutamine and antibiotics. PSCmC cells were generated from a spontaneously arising KPC tumor and express both hTERT and mCherry. These cells were grown in DMEM with 10%FBS, 10nM L-glutamine and antibiotics. HPAC (an immortalized human PDAC line purchased from ATCC), and the immortalized human fibroblast lines, h-iPSC-PDAC-1 and hT137 (a gift from David Tuveson, Cold Spring Harbor Laboratory, New York) were grown in DMEM with 10% FMS, 10nM L-glutamine and antibiotics. Murine MT5 ($Kras^{LSL\text{-}G12D}$, $Trp53^{LSL\text{-}R270H}$, Pdx1-cre) pancreatic cancer cells were a gift from David Tuveson (Cold Spring Harbor Laboratory, Cold Spring Harbor, NY) and cultured in RPMI-1640 (Gibco) with 10% FBS, 10 mM L-glutamine, and antibiotics (GiminiBio). Murine KP2 ($Kras^{LSL\text{-}G12D}$, $Trp53^{LSL\text{-}R270H}$, Pdx1-cre) pancreatic cancer cells were a gift from David DeNardo (Washington University School of Medicine in St. Louis, Missouri) and cultured on collagen coated plates in DMEM/F-12 with 10% FBS and antibiotics. Panc02 murine pancreatic cancer cells were a gift from Shari-Pilon Thomas (H Lee Moffitt Cancer Center, Tampa, Florida) and cultured in RPMI (Gibco) with 10% FBS, with 10nM L-glutamine, and antibiotics.

*In vivo murine studies*

All animal studies were conducted under an approved institutional animal care and use committee (IACUC) at Emory University. For orthotopic *in vivo* studies, $2x10^5$, $5x10^5$ or $1x10^6$ MT5 tumor cells, KP2 tumor cells, or Panc02 tumor cells were orthotopically injected into the pancreas of 6-8 week old female C57BL/6 mice and allowed to grow until detectable by palpation. For co-culture murine studies, $2x10^5$ KPC-luc tumor cells, $2x10^5$ PSC5 fibroblasts, or $1x10^4$ KPC-luc tumor cells mixed with $9x10^4$ PSC5 fibroblasts were orthotopically injected into the pancreas of 6-8 week old female C57BL/6 mice. Tumors were permitted to grow for 7 days and presence of pancreatic tumors were confirmed by bioluminescent imaging as previously described [50]. Tumor growth was then monitored by abdominal palpation every other day and BLI on days 14, 21 and at end of study.

*Immunohistochemical staining of tumors and livers*

Tissues harvested from mice were formalin-fixed and paraffin-embedded (FFPE) and 5-7μm slices of tissue were then cut and mounted on slides. Mounted tissue was then stripped of paraffin and rehydrated, followed by antigen retrieval in either citrate buffer (pH 6) or EDTA buffer (pH 9). Cell lines were plated on fibronectin (ThermoFisher) coated 12mm-#1.5 coverslips for 24 hrs before being fixed in ice cold methanol. Autofluorescence was quenched with $NH_4Cl$ and slides were blocked in 3% donkey serum and 3% bovine serum albumin in PBS. Primary antibody against murine αSMA (Santa Cruz clone 1A4) was diluted 1:200 in blocking solution and incubated with fixed cells overnight at 4ºC. Slides were then incubated with secondary antibody (donkey anti-mouse 488, Abcam) diluted 1:1000 and DAPI diluted 1:5,000 in blocking solution. Coverslips were then washed and mounted using Vectashield hardset (Vector Labs). Slides were then imaged on a Leica SP8 confocal microscope.

*Flow cytometry*

To prepare cells grown *in vitro* for staining, enzyme free Cell Dissociation Media (ThermoFisher) was used to lift cells. Cells were then centrifuged, counted and washed twice in FACS wash (10% FBS with 5mM EDTA). Cells were then distributed into 5ml glass tubes at $1x10^5$-$1x10^6$ cells/tube. Cells were then stained with Ghost dye 780 (tonbo) at 1:5000, CD31 PE-Vio770 (Clone 390, Miltenyi), CD90.2 (Clone 30-H12, BioLegend), EpCAM (Clone G8.8, BioLegend), or PDGFRβ (Clone APA5, BioLegend) in FACS wash at a concentration of 1:100.

*3D invasion assays*

Cells were harvested by trypsinization and counted using a hemocytometer. In each well, 3,000 cells were then plated in a low-adherence round-bottom 96 well plate and centrifuged at 600 x g. After 72hr, 4-5 spheroids per condition were collected and embedded in a collagen matrix containing 3mg/ml rat tail collagen I (Corning). Z-stacks of each spheroid were collected at baseline and every 24hrs for 48hrs using a Leica SP8 confocal microscope.

*Proteome Profiler Array*

$2x10^5$ HPAC cancer cells were plated in each well of a 6 well plate. The next day, media was replaced with either DMEM containing 5% FBS, anti-anti, and L-glutamine, the same media with 10% conditioned media from SC36 primary pancreatic stellate cells, or the same media with 5% conditioned media from SC36. Additionally, DMEM containing 5% FBS, anti-anti, and L-glutamine with 10% conditioned media from SC36 was added to a well without cells to control for chemokines already contained within SC36 conditioned media. After a 48hr incubation, supernatant was collected and spun at 1000 x g to remove cellular contaminates. Supernatant was then analyzed using a Proteome Profiler Human Chemokine Array (R&D systems, Inc.) according to manufacturer's suggested protocol.

*Statistical analysis*

For all *in vitro* experiments, statistical significant was evaluated by one-way ANOVA followed by individual t-tests to compare changes with respect to negative controls. Statistical significance was defined as comparators with a p-value less than 0.05.

## 2.3 Results

*Establishing a 3D invasion model for pancreatic cancer*

While previous studies by our collaborators and others have employed a Matrigel-based matrix to study invasion and metastasis in 3D, here we found spheroids of human HPAC cancer cells preferentially invaded in a collagen based matrix. After 48hrs, HPAC spheroids grown in a Matrigel based matrix appeared to bleb at the spheroid edge rather than invade, while HPAC spheroids embedded in a collagen based matrix migrated through the matrix with ease (**Figure 2.2**). The tension and stiffness of a collagen-based matrix more closely models the fibrotic and collagen-rich microenvironment of pancreatic cancer. Based on these characteristics, collagen was chosen as the preferred medium for all other experiments moving forward. Notably, the utilization of collagen in an assay such as this is often referred to as a "collagen constriction assay", though I will solely refer to these assays as 3D invasion assays.

*CAF-derived soluble factors promote pancreatic cancer migration and invasion*

We hypothesized that pancreatic cancer associated fibroblasts could contribute to migration and

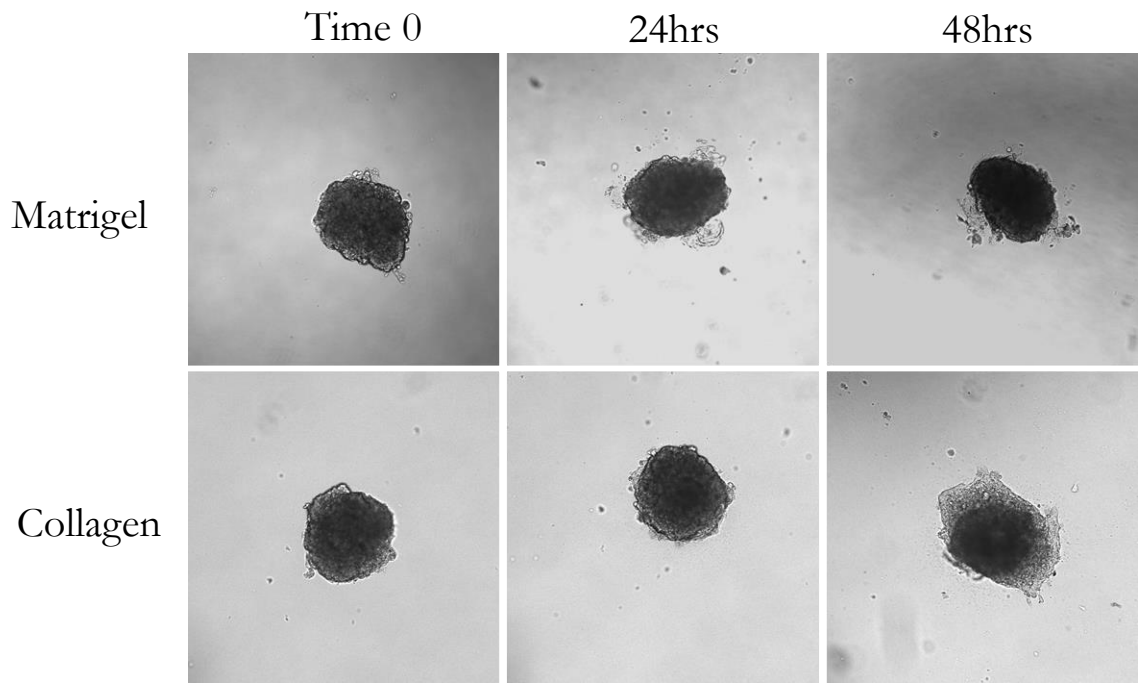


**Figure 2.2 Pancreatic cancer spheroids preferentially invade in a collagen based matrix.** HPAC spheroids were embedded in either 200ul matrigel or a collagen based matrix and observed over 48 hrs. Z-stacks were collected every 24 hrs starting at time 0. Images here are representative of 5 spheroids per condition.

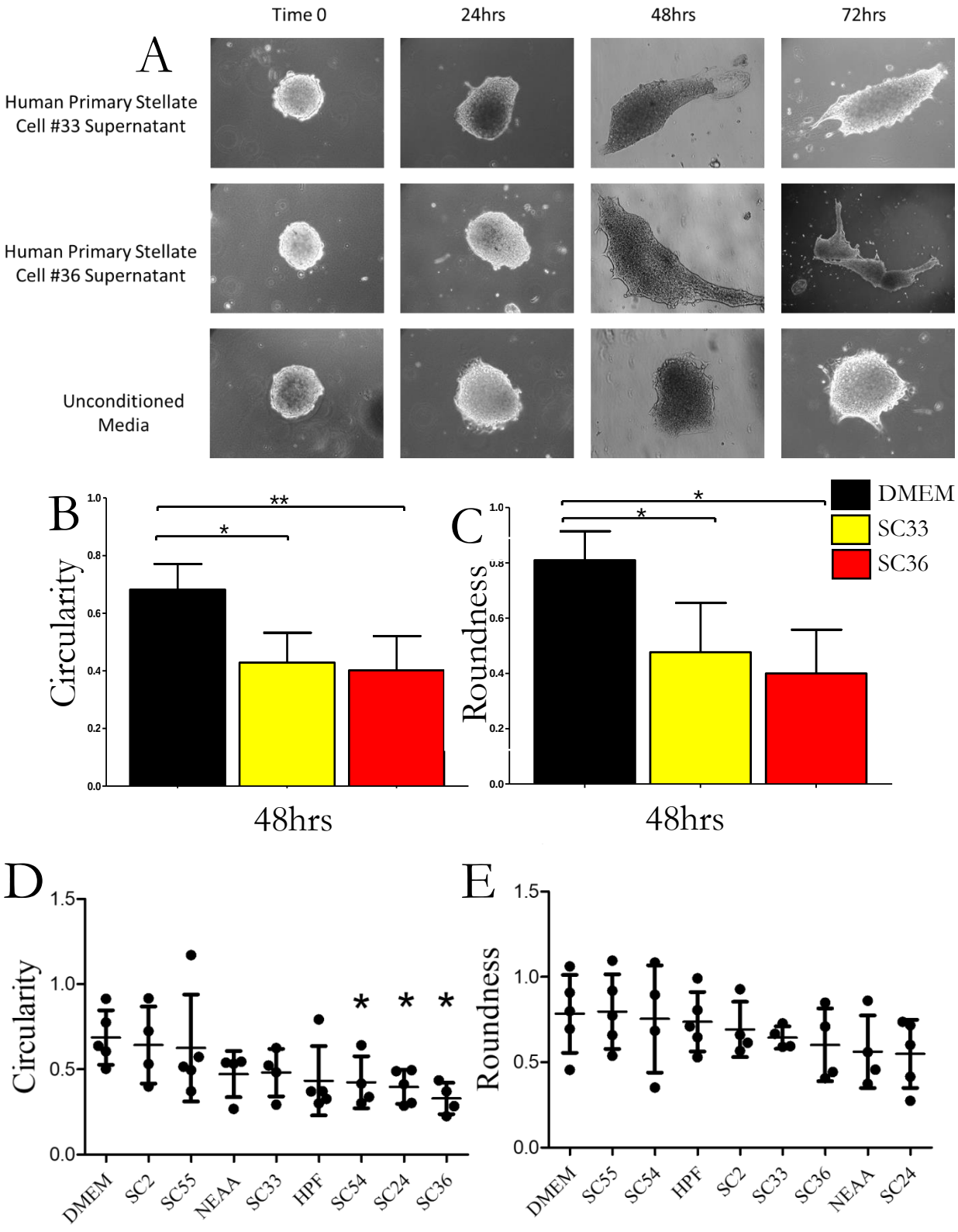
A
Time 0
24hrs
48hrs
72hrs
Human Primary Stellate Cell #33 Supernatant
Human Primary Stellate Cell #36 Supernatant
Unconditioned Media
B
Circularity
48hrs
C
Roundness
48hrs
DMEM
SC33
SC36
D
Circularity
DMEM
SC2
SC55
NEAA
SC33
HPF
SC54
SC24
SC36
E
Roundness
DMEM
SC55
SC54
HPF
SC2
SC33
SC36
NEAA
SC24

**Figure 2.3. Conditioned media from primary human CAFs derived from PDAC specimens elicit heterogeneous degrees of invasion by pancreatic cancer spheroids.** HPAC spheroids were embedded in a collagen matrix, which was then detached from the bottom of the plate and floated in DMEM or DMEM with 10% conditioned supernatants from cultures of primary human pancreatic stellate cells (PSCs) derived from resected PDAC specimens at Emory University under an IRB approved protocol. (A) Z-stacks were taken of each spheroid (~5 per condition) every 24 hrs for 72 hrs. Conditions included a media control vs spheroids exposed to 10% supernatants from cultures of PSCs derived from two separate patients. (B-C) Spheroids were outlined using FIJI (NIH) and both roundness and circularity were calculated based on the resulting shape. Lower roundness indicates elongation of the spheroid, while lower circularity indicates increased protrusions into the surrounding matrix. (D-E) HPAC spheroids were exposed to supernatants of primary Pan-CAFs from n-6 patients, DMEM alone, 1x NEAA or supernatant from normal fibroblasts (HPF) and images every 24hrs for 48 hrs. Spheroids were then outlined and the roundness and circularity of each spheroid was calculated with FIJI (NIH). Resulting averages of each condition are displayed sorted from least invasive to most invasive (Left to right). Statistics calculated in GraphPad using a One-Way ANOVA, asterisk indicated significance compared to DMEM alone ($p<0.05$).

invasion of pancreatic cancer cells by secretion of soluble factors or through contact dependent mechanisms. To address the first hypothesis, HPAC spheroids grown in normal media were compared to identical spheroids exposed to 90% normal media and 10% conditioned media from cultures of primary pancreatic cancer derived fibroblasts (Pan-CAF). These fibroblasts were derived from pancreatic tumor specimens collected from patients at Emory University under an IRB approved protocol. Fibroblasts were grown in 6 well plates until they reached 70% confluence, at which point supernatant was collected and spun at 1000*xg* for 5 min to remove any contaminant. Spheroids exposed to Pan-CAF conditioned media demonstrated dramatic invasion and migration compared to spheroids grown in DMEM alone after 48 hrs (**Figure 2.3)**. Surprisingly, we found that spheroids exposed to Pan-CAF conditioned media had migrated through the collagen matrix and physically contacted other spheroids in the matrix after 72hrs (**Figure 2.3**). Media derived from Pan-CAF isolated from different patients produced differing degrees of this effect but was reproducible between experimental replicates. Spheroids exposed to Pan-CAF conditioned media demonstrated significant decreases in both roundness (indicating elongation of the spheroid) and in circularity (indicating increased protrusions into the local matrix) compared to spheroids grown in normal media. This difference was evident at both 48hrs (**Figure 2.3**) and 72hrs (data not shown), although the merging of spheroids at 72hrs presented a technical challenge in the quantification of these features. Given these findings, we decided to screen Pan-CAF conditioned media from all patients which we had available materials (n=6). We observed heterogeneity between patients with some Pan-CAF samples eliciting no effect and others recapitulating our earlier observations by inducing significant invasion as measured by roundness and circularity (**Figure 2.3**).

*Pan-CAF conditioned media stimulates the 3D invasion of pancreatic cancer cells with distinct phenotypes*

We next used live cell imaging to gain further insight into the mechanisms mediating the migration

of spheroids towards one another. Using a Leica SP8 confocal microscope, Z-stacks of HPAC spheroids were collected every 10 minutes for 72hrs in the presence of SC37 or SC36 Pan-CAF conditioned media. The majority of cells migrating out the spheroid migrate collectively as a sheet 5-10 cells wide, while a few cells (10-25 per spheroid) move independently at the leading edge of the spheroid and seem to guide invasion of the sheet into the surrounding matrix (**Figure 2.4).** These latter cells move much more rapidly than those cells contained within the sheet and extend extremely long protrusions that occasionally make contact with cells in the sheet and with the surrounding matrix. The behavior of these rapidly moving cells at the invasive front is reminiscent of dogs herding sheep, thus we refer to these cells as "sheepdog cells".

*Pancreatic cancer cells and Pan-CAFs produce distinct profiles of chemokines*

I hypothesized that migration of spheroids towards one another was mediated by changes in chemokine production from HPAC cancer cells in response to stimulation with Pan-CAF conditioned media. To address this hypothesis, we conducted a pilot study to profile the expression of cytokines and chemokines produced by HPAC and Pan-CAF alone, as well as determine how Pan-CAF supernatants influence production of these factors from HPAC cells. Briefly, HPAC cells grown in a monolayer were stimulated with 10% or 5% conditioned media from SC37 Pan-CAFs for 48 hrs and supernatants were collected from tumor cell monolayers. As a control, HPAC cells were frown as a monolayer in normal media, while 10% conditioned SC37 Pan-CAF media was also plated in a well without cell to assess the baseline secretion of chemokines and cytokines from each cell type individually. The chemokine content of all four conditions were then evaluated using a Human Proteome Profiler Chemokine Array (R&D). No changes in chemokine production by HPAC cells were observed in the presence of 10% Pan-CAF conditioned media (Figure 2.5);

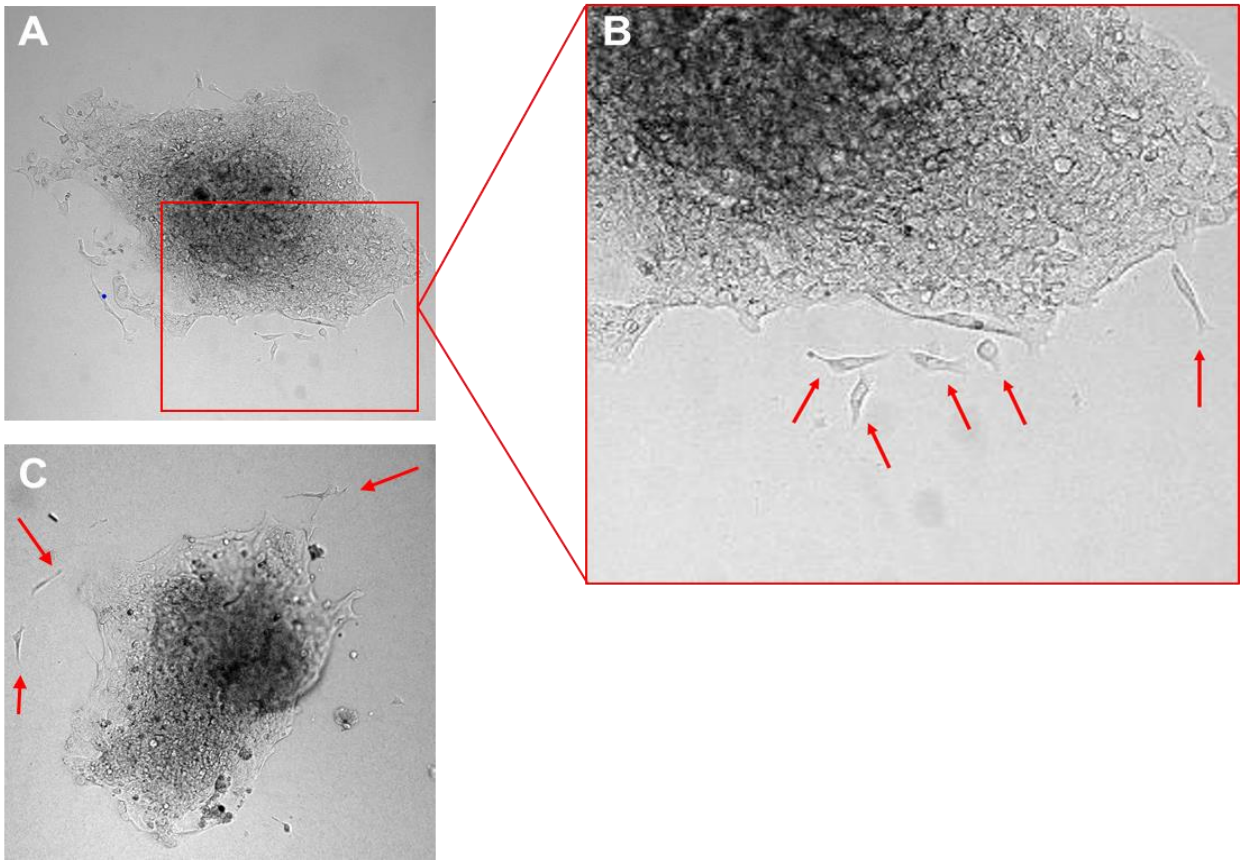


**Figure 2.4. Single "sheepdog" cells are highly active at the invasive front of HPAC spheroids.** HPAC spheroids were embedded in a collagen matrix in an Ibidi glass bottom chamber slide. Spheroids were exposed to conditioned media from primary Pan-CAFs. Z-stacks of each spheroid were collected every 10 minutes for 72 hrs. (A) A representative single 10x 2D image of an HPAC spheroid exposed to conditioned media from SC36 primary Pan-CAFs. (B) Digital magnification of the image in Figure 2.4(A) with red arrows indicating the single cells referred to as "sheepdog" cells at the leading invasive edge of the spheroid. (C) A single 10x 2D image of an HPAC spheroid exposed to SC33 primary Pan-CAF conditioned media with red arrows again indicating "sheepdog" cells.

HPAC cells in 10% SC36 Supernatant

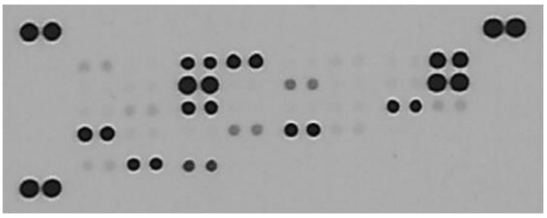

HPAC cells in 5% SC36 Supernatant

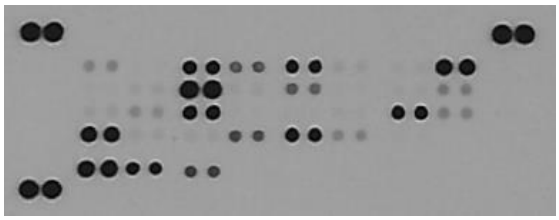

HPAC cells in DMEM

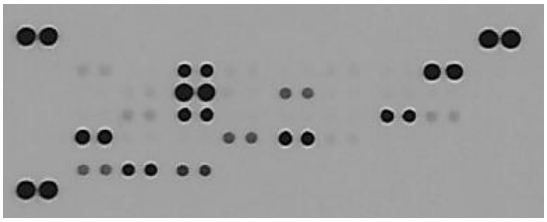

No Cells + 10% SC36 Supernatant

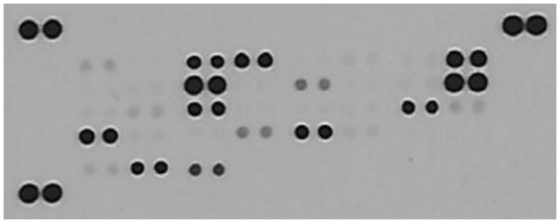

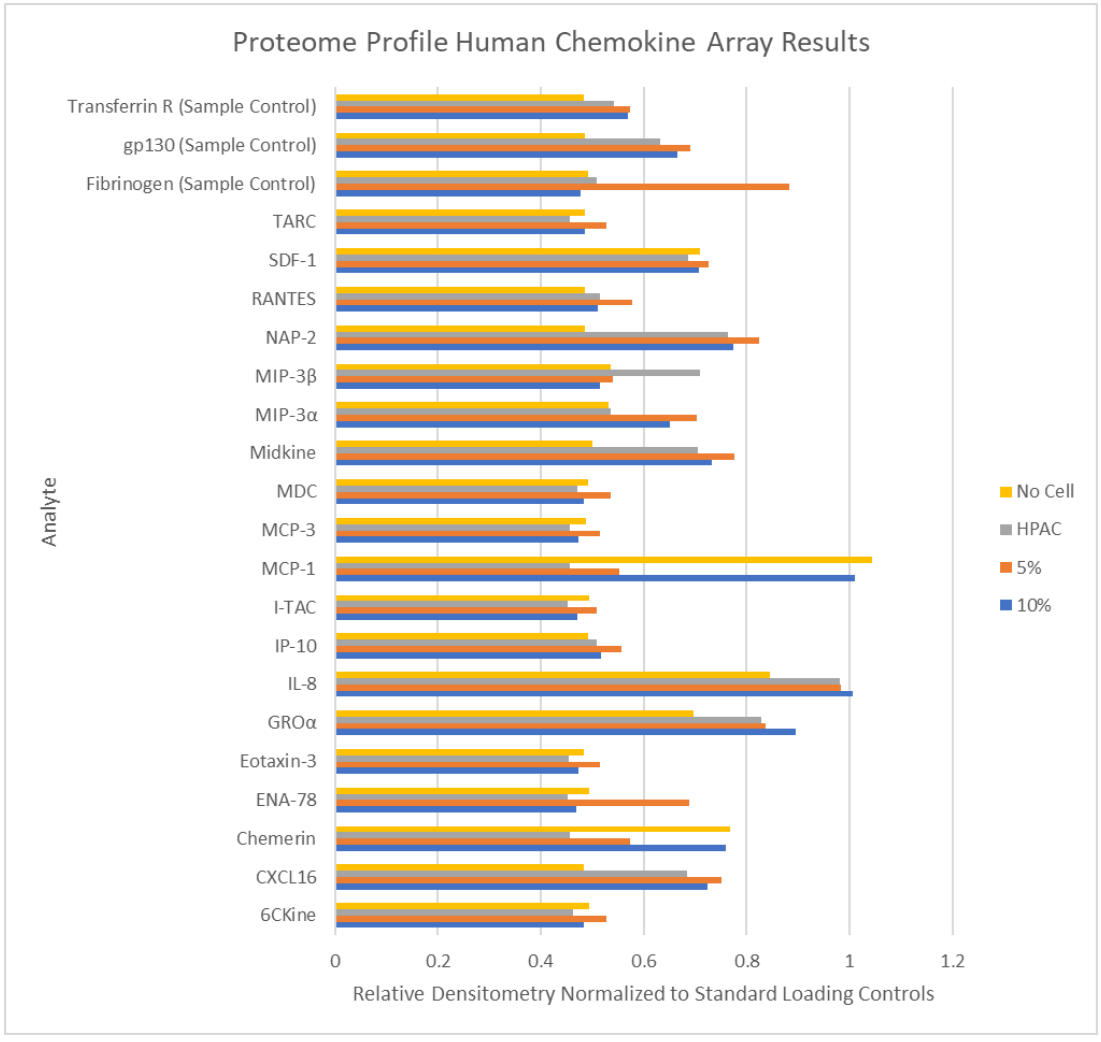

**Figure 2.5 Pan-CAF conditioned media alters chemokine secretion of pancreatic cancer cells.** HPAC cancer cells were exposed to 10% or 5% conditioned media from SC36 Pan-CAFs, or grown in normal medium for 48 hrs. A Proteome Profiler Human Chemokine Array from R&D was then used to assess the presence of chemokines within media from these conditions, as well as in SC36 Pan-CAF conditioned media diluted with DMEM. (A) Images of the membranes demonstrating the presence or absence of chemokines within each condition. (B) Densitometry of each chemokine for each condition normalized to loading controls for each membrane.

however, HPAC cells grown in 5% conditioned media produced much higher levels of ENA-78 (CXCL5) (**Figure 2.5**). Distinct profiles of chemokine production were observed in SC37 Pan-CAFs and HPAC cancer cells, when considered individually. For example, HPAC cells secreted detectable CXCL16, Midkine, CCL20, CXCL7, and gp130 while Pan-CAF supernatant contained higher levels of TIG-2 and MCP-1(**Figure 2.5**). Both HPAC and Pan-CAF supernatants contained moderate levels of IL-8 and CXCL12 (**Figure 2.5**).

*Non-essential amino acids and exogenous IL-6 can recapitulate invasive phenotypes in HPAC spheroids*

Given these results, we questioned whether the induction of invasion by Pan-CAF conditioned media was the result of a proteinaceous factor or perhaps a metabolite or other molecular secretion. A review of the literature reveals significant contributions of both Pan-CAF derived metabolites, growth factors, cytokines and chemokines to pancreatic cancer progression. The differential and complementary metabolic states of Pan-CAFs and pancreatic cancer cells has become a recent area of interest with relevant findings to our studies. Specifically, two independent studies reported Pan-CAFs to secrete non-essential amino acids (NEAA) which could modulate pancreatic cancer growth and progression[134,135]. We therefore tested the ability of NEAA to recapitulate our findings above by exposing HPAC spheroids to 1x NEAA (**Figure 2.5A**). HPAC spheroids exposed to NEAA demonstrated significant invasion with changes in both roundness and circularity that phenocopied our data from Pan-CAF conditioned media (**Figure 2.2**). To determine whether metabolites such as NEAA present in Pan-CAF conditioned media contributed to invasion, we repeated 3D invasion assays with SC54 conditioned media as before, or after boiling it for 15 minutes to denature proteinaceous factors with heat susceptible structure. Under these conditions, metabolites should be unaffected and retain their activity. Boiling of SC54 supernatant indeed reversed the effects of the conditioned media and significantly protected against induction of metastasis(**Figure 2.5B**). Thus,

metabolites such as NEAA present in Pan-CAF media may act in trans as mediators or cross-talk to promote invasive phenotypes of pancreatic cancer cells. These data support the idea that heat susceptible factors with tertiary or quaternary protein structure likely mediates the invasive phenotypes observed in response to Pan-CAF conditioned media. Our previously published data have demonstrated Pan-CAFs secrete extremely high levels of multiple cytokines, including IL-6. This factor is well characterized in its ability to promote suppressive myeloid cell expansion and tumor progression[109]. Additionally, previous studies of cancer metastasis report IL-6 to promote metastasis and invasion[108,136,137]. In Figure 2.4 we found HPAC cells secreted detectable levels of soluble gp130, the common transmembrane signal transduction moity for the IL-6 receptor. Together, these data suggested a potential role for IL-6 signaling in mediating increased invasion of of HPAC spheroids into the surrounding matrix when exposed to Pan-CAF supernatants (**Figure 2.3**). We therefore exposed HPAC spheroid to 10ng/ml recombinant IL-6, imaging and analyzing spheroids as before (**Figure 2.5C-D**). Spheroids exposed to recombinant IL-6 demonstrated significant changes in circularity, invading into the surrounding matrix, but no change in roundness. We also performed ELISA quantification of IL-6 in patient supernatants screened in **Figure 2.3** to evaluate whether there was any correlation between Il-6 secretion and the invasive response of spheroids to the same supernatants (**Figure 2.5E**). No correlation between IL-6 concentration in Pan-CAF supernatants and induction of invasion in HPAC spheroids was observed. Thus, IL-6 may be a contributing factor to this process but there are likely other more dominant factors responsible for driving the invasive process observed in HPAC spheroids.

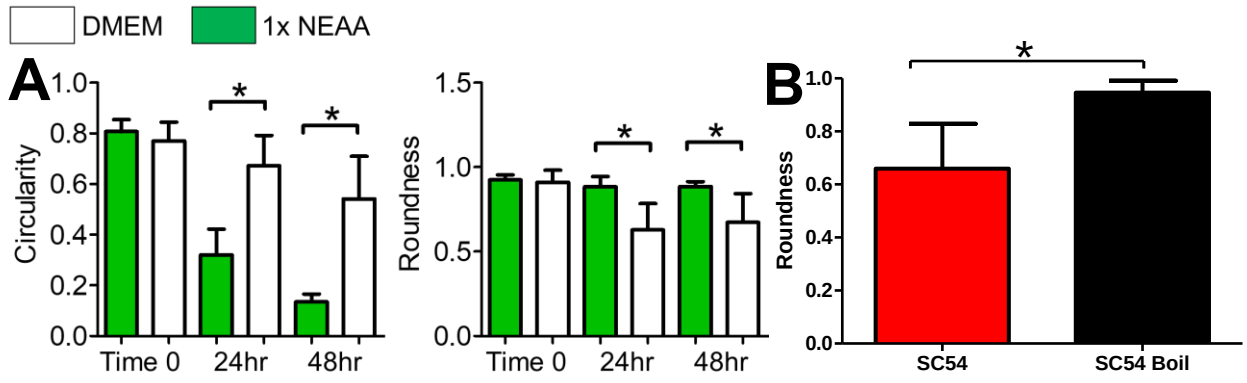
DMEM
1x NEAA
A
Circularity
1.0
0.8
0.6
0.4
0.2
0.0
Time 0
24hr
48hr
*
*
Roundness
1.5
1.0
0.5
0.0
Time 0
24hr
48hr
*
*
B
Roundness
1.0
0.8
0.6
0.4
0.2
0.0
SC54
SC54 Boil
*

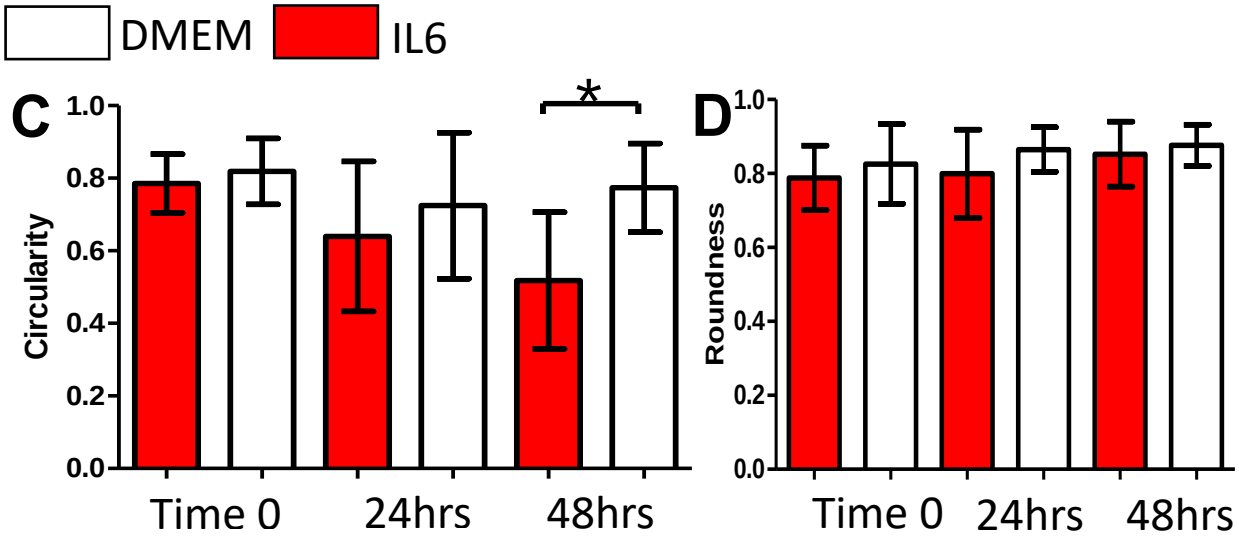
DMEM
IL6
C
Circularity
1.0
0.8
0.6
0.4
0.2
0.0
Time 0
24hrs
48hrs
*
D
Roundness
1.0
0.8
0.6
0.4
0.2
0.0
Time 0
24hrs
48hrs

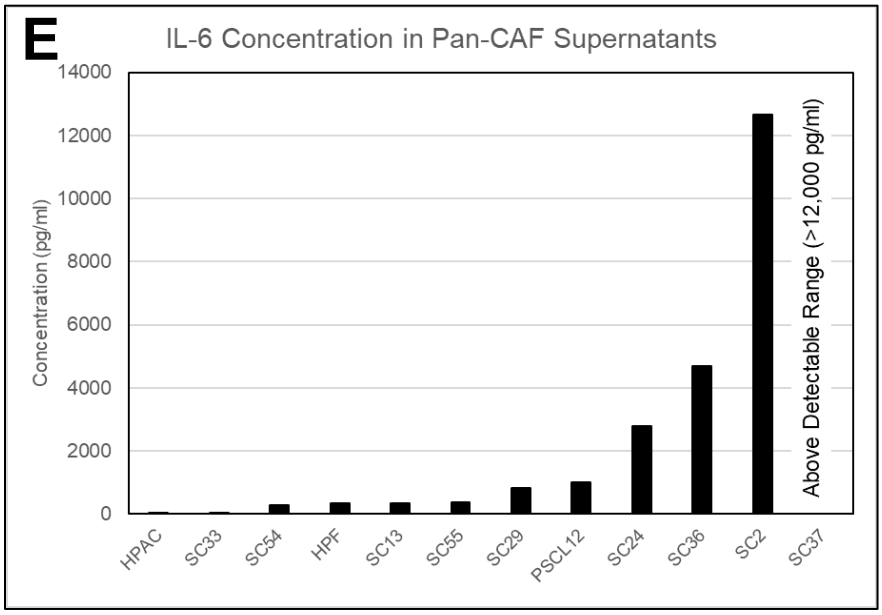
E
IL-6 Concentration in Pan-CAF Supernatants
Concentration (pg/ml)
14000
12000
10000
8000
6000
4000
2000
0
Above Detectable Range (>12,000 pg/ml)
HPAC
SC33
SC54
HPF
SC13
SC55
SC29
PSCL12
SC24
SC36
SC2
SC37

**Figure 2.6 NEAA and IL-6 recapitulate the invasive phenotype induced by Pan-CAF supernatants in HPAC 3D spheroids.** (A) NEAA induce significant invasion of HPAC spheroids and recapitulate the phenotypic invasion induced by Pan-CAF spheroids. (B) Boiling of Pan-CAF supernatants derived from SC54 primary CAF line ablated the invasion promoting effects of the conditioned media. (C) 10ng/ml recombinant human IL-6 induces significant increases in the invasion of HPAC spheroids. (D) but no changes in the roundness or elongation of the same spheroids. (E) Supernatants from HPAC cancer cells, HPF normal fibroblasts, PSCL12 immortalized fibroblasts and primary Pan-CAF lines were evaluated for IL-6 protein expression by ELISA. All samples were run in duplicate. * indicates significance for each comparison ($p<0.05$).

*Pan-CAF influence invasive phenotypes of HPAC cancer cells in 3D co-cultured spheroids*

The spatial relationship between Pan-CAFs and cancer cells can heavily influence the phenotype of Pan-CAFs, including their distinct cytokine and growth factor secretion profile. We therefore hypothesized that introduction of Pan-CAFs into 3D HPAC spheroids would distinctly influence the phenotype of Pan-CAFs and subsequent invasion of cancer cells. To address this hypothesis we first utilized immortalized Pan-CAF lines, h-iPSC-PDAC-1(PSCL12) and hT1. HPAC cells and PSCL12 cells were first co-cultured together for 24 hrs in a monolayer, harvested and then used to form spheroids. Ratios of 9:1, 4:1, 1:1, 1:4 and 1:9 HPAC cells to PSCL12 cells were used to simulate heterogeneous stromal content observed between patients (Figure 2.4A). In contrast to the phenotype observed when HPAC spheroids were exposed to Pan-CAF conditioned media **(Figure 2.3),** co-culture spheroids exhibited dramatic and significant changes in circularity with no significant alteration in roundness **(Figure 2.7 B-E)**. Additionally, there was no indication that co-culture spheroids were shifting position and moving through the collagen matrix as we observed with HPAC spheroids exposed to Pan-CAF conditioned media **(Figure 2.3).** Interestingly, spheroids containing less PSCL12 cells than cancer cells exhibited significantly lower circularity compared to spheroids containing only cancer cells (**Figure 2.6 B-C**), indicating that PSCL12 cells were indeed promoting local invasion. Spheroids containing more Pan-CAF cells than cancer cells exhibit an opposite effect, trending toward increased circularity compared to cancer spheroids alone **(Figure 2.7 D-E)**. This latter effect was not significantly different between any of the conditions.

Given these results, we next sought to visually evaluate the interactions between Pan-CAFs and HPAC cells in 3D spheroids. The hT1 Pan-CAF cell line expresses an mCherry construct, thereby allowing hT1 Pan-CAF cells to be distinguished from HPAC cells in 3D co-culture. In co-culture spheroids with high ratios of cancer cells to Pan-CAFs we did not observe CAFs to be present in

the invasive sheet of cells protruding outward from the spheroid. Instead the Pan-CAFs remained within the main body of the spheroid. However, in co-culture spheroids with higher ratios of Pan-CAFs to cancer cells, we observed fibroblasts to migrate outward from the spheroid into the surrounding matrix as single cells or as small packs of cells with tumor cells detached from the body of the spheroid.

*Establishing a orthotopic co-injection model of pancreatic cancer cells and cancer associated fibroblasts in immune competent C57BL/6 mice.* These *in vitro* studies demonstrate a strong scientific premise to further investigate our hypothesis that CAFs promote PDAC migration and move alongside cancer cells to sites of metastasis *in vivo.* As of yet, no markers have been discovered that reliably distinguish cancer associated fibroblasts originating from the pancreas rather than the liver, lymph nodes or other tissues. Interestingly, CAFs express the thymic marker CD90, also known as CD90.2 in wild-type C57BL/6 mice. Thus, these cells can be injected into a $CD90.1^{+}$ mouse and be readily distinguished from host CAFs.

We established several of our own lines and additionally received the CAF line PSC5 which was established in a similar manner. Briefly, KPC mice 18-25 weeks of age bearing pancreatic tumors were euthanized and tumors were collected into DMEM with 1%FBS. Half of the tumor was FFPE and analyzed by H&E to confirm the presence of cancer. The remaining sample was minced and then digested using a combination of collagenase and liberase for over an hour. The resulting material was filtered and grown out under puromycin. This strategy takes advantage of the puromycin resistance construct built into the lox-stop-lox cassette of the stop sequence preceding mutant *KRAS* in KPC mice. Cells with activated mutant *KRAS* will lack puromycin resistance which is retained by wild-type cells. Thus, we are able to purify out cancer cells and expand only wild-type

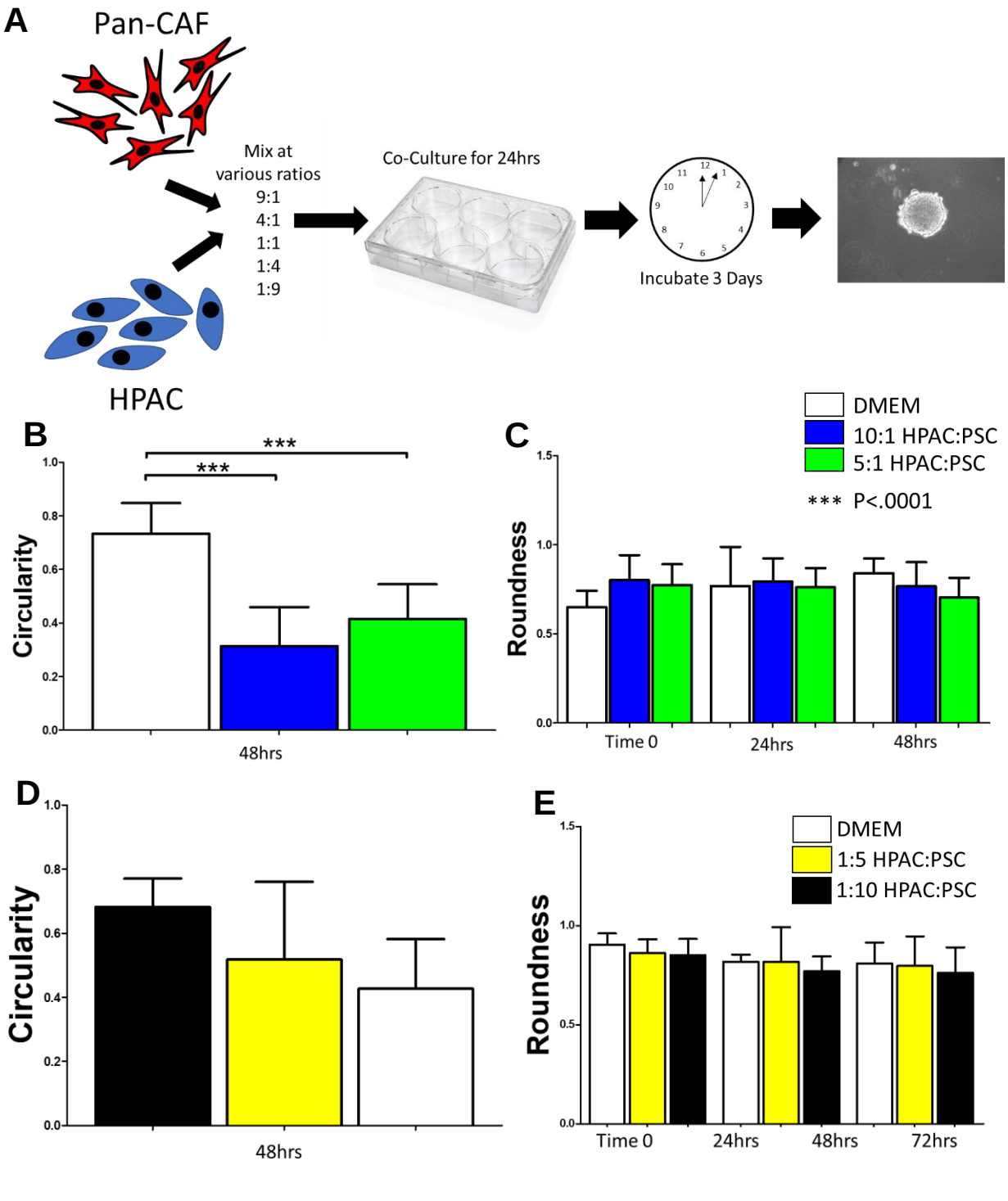
A
Pan-CAF
HPAC
Mix at
various ratios
9:1
4:1
1:1
1:4
1:9
Co-Culture for 24hrs
Incubate 3 Days
B
***
***
Circularity
1.0
0.8
0.6
0.4
0.2
0.0
48hrs
C
DMEM
10:1 HPAC:PSC
5:1 HPAC:PSC
*** P<.0001
Roundness
1.5
1.0
0.5
0.0
Time 0
24hrs
48hrs
D
Circularity
1.0
0.8
0.6
0.4
0.2
0.0
48hrs
E
DMEM
1:5 HPAC:PSC
1:10 HPAC:PSC
Roundness
1.5
1.0
0.5
0.0
Time 0
24hrs
48hrs
72hrs

**Figure 2.7 Pan-CAF shift the invasive phenotype of pancreatic cancer cells in 3D co-culture.** (A) Immortalized Pan-CAF cells and HPAC cancer cells were co-cultured at various ratios for 24 hrs in 2D and then harvested and counted. 3,000 cells per well were utilized to form 3D spheroids which were embedded in a collagen matrix after 3 days. (B-E) Z-stacks of each spheroid were collected at baseline and then at 24 and 48 hrs. Images were outlined in FIJI and the circularity and roundness of each spheroid was measured. The average for all spheroids in a given experimental group was evaluated using a one-way ANOVA. ***=$p<.0001$

cells. After at least 3 passages, limiting dilution was performed on resultant cultures to generate clonal cell lines. A combination of immunofluorescent staining for αSMA and flow cytometric staining for CD31 confirmed the phenotype of these cells. Additionally, PCR to detect genomic alterations to *KRAS* was performed to confirm purity of wild-type cells.

After confirming PSC5 express the thymic marker CD90.2 (**Figure 2.9A**) by flow cytometry. We then co-cultured KPC-luc cells and PSC5 cells at ratios of 9:1, 1:1, and 1:9 and injected 100k cells in 40ul of Matrigel into the pancreas of CD90.1$^{+}$ C57BL/6 mice. For this pilot study only 1 mouse per condition was injected, as a control PSC5 or KPC-luc cells were injected alone. Tumors established quickly (1 week) and mice were euthanized 3 weeks after surgery due to overgrowth of tumors. No mouse showed visible signs of metastasis to the liver and PSC5 cells on their own failed to lead to tumor development. While we have previously detected metastasis in this model we believe the primary tumor growth is too fast for accurate detection of metastasis in this model. We therefore decided to test the kinetics of 3 other tumor cell lines (MT5, KP2 and Panc02), in comparison to KPC-luc cells in order to develop a model with slower primary tumor growth. As demonstrated in **Figure 2.8C**, MT5 tumors were not palpable until 4 -5 weeks after surgery and demonstrated the slowest primary tumor growth of all the murine pancreatic cancer cell lines available to us. Going forward, we will utilize co-injections of MT5 and murine CAF lines to optimize a co-injection model of PDAC and test the ability of CAFs to metastasize with PDAC cells.

**2.4 Discussion**

The majority of patients with pancreatic cancer present with local or distal metastatic disease, precluding them from surgical resection. Despite this fact, development of PDAC specific therapies has primarily focused on targeting primary tumor growth. Therefore, my research pursued a

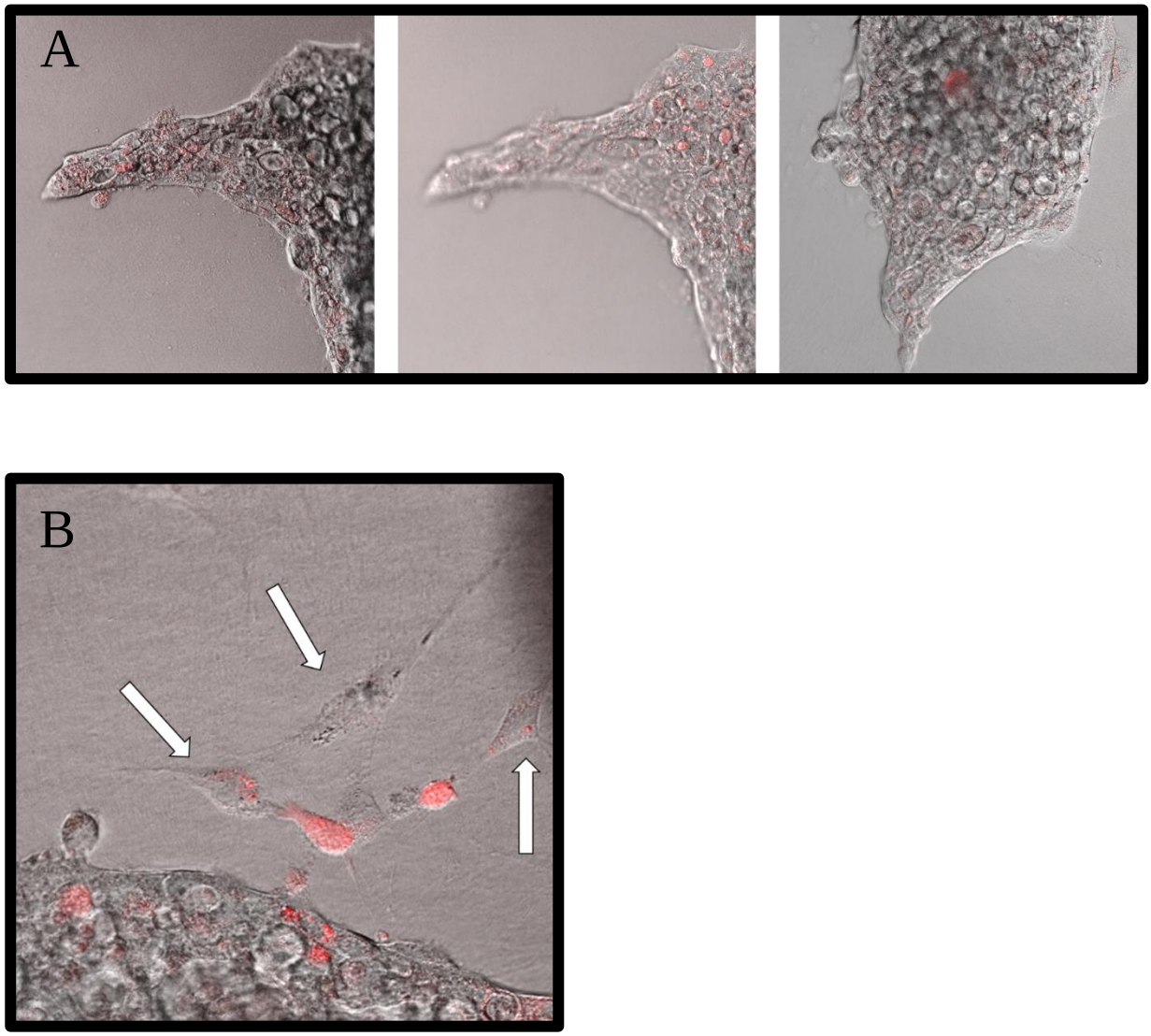


**Figure 2.8 CAFs migrate out of co-culture spheroids ahead of HPAC cells and position themselves distally in the surrounding matrix.** The mCherry labeled immortalized Pna-CAF line hT1 was co-culture in 2D with HPAC cancer cells. Co-cultures of cells were then used to form 3D spheroids and spheroids were imaged at 48hrs by differential interference contrast and fluorescence on a Leica SP8 confocal microscope. (A) Representative images of a co-culture spheroid at a HPAC:Pan-CAF ratio of 9:1 with Pan-CAF cells labeled with mCherry (red). (B) Representative images of a co-culture spheroid at a Pan-CAF:HPAC ratio of 4:1 with Pan-CAFs cells labeled with

mCherry and mCherry negative tumor cells indicated with white arrows. This phenotype was not observed in spheroids containing higher ratios of Pan-CAFs (data not shown).

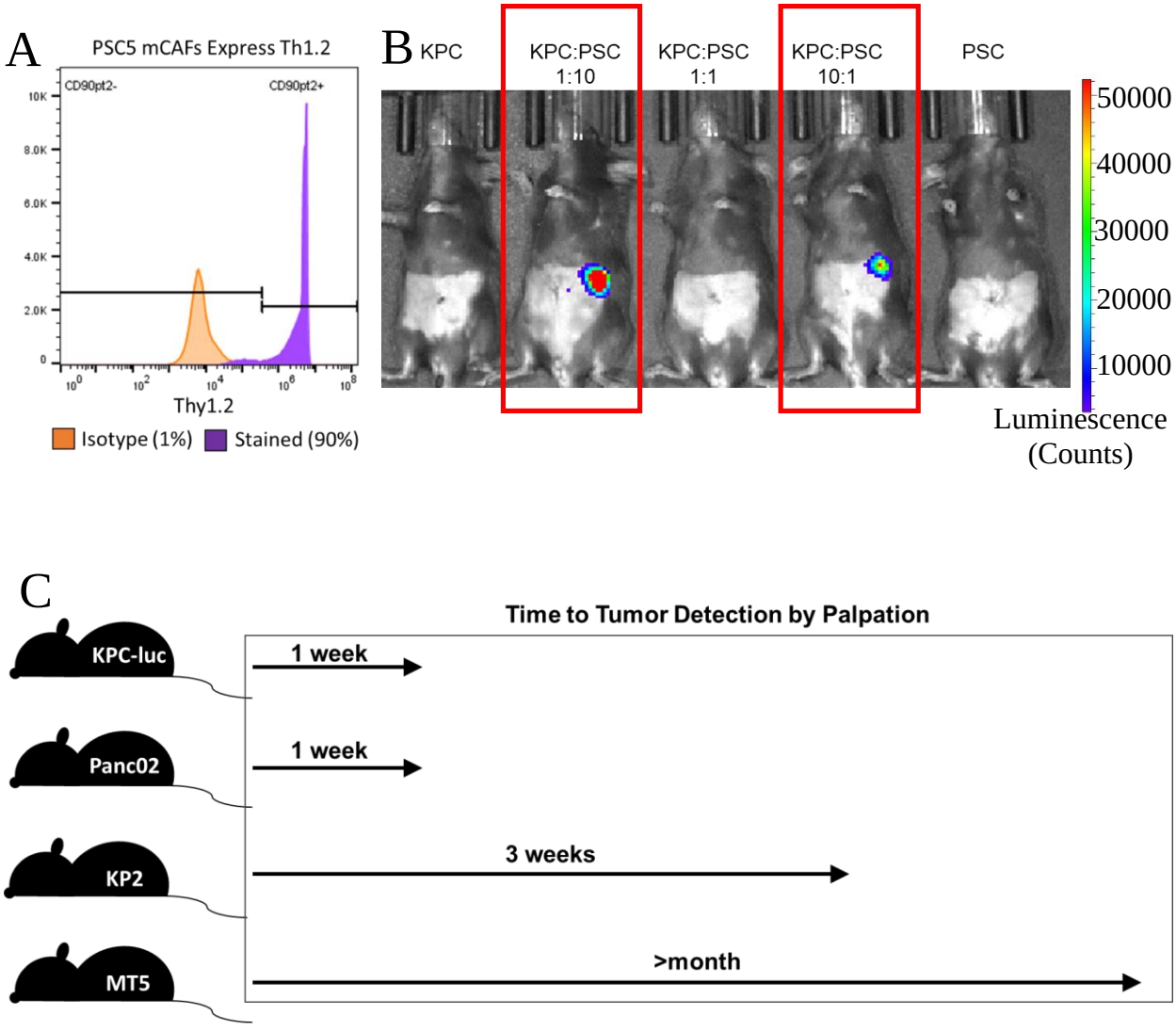


**Figure 2.9 Developing tools for an immune competent murine orthotopic co-injection model of PDAC with CAFs and pancreatic cancer cells. (A)** PSC5 CAFs isolated from the primary tumor of a KPC mouse were stained for Thy1.2 (CD90.2) or isotype controls. 90% of the PSC5 CAFs were positive for CD90.2 **(B)** KPC-luc cells alone, together with PSC5 CAFs or PSC5 CAFs alone were orthotopically implanted in the pancreata of CD90.1 C57BL/6 mice. After 1 week bioluminescent imaging was used to detect tumor growth. Red boxes highlight mice in which tumors were detected at this timepoint, though all mice injected with tumor cells had visible primary tumors at endpoint. The mouse injected with PSC5 cells alone had no tumor

growth detected. **(C)** A graph visually demonstrating the time at which various murine tumor cell line lines orthotopically implanted in C57BL/6 mice are detected by palpation (n=3 mice per group).

determined line of investigation to reveal multicellular mechanisms of PDAC metastasis. I hypothesized that CAFs within primary PDAC tumors promote the metastasis of pancreatic cancer cells and travel with cancer cells to sites of metastasis in the liver. Utilizing Pan-CAF derived supernatants and innovative 3D invasion assays, I demonstrate the ability of PDAC associated CAFs to stimulate pancreatic cancer cell migration and invasion by secreting potent soluble factors that are protein in nature. Our *in vitro* investigations using human HPAC spheroids describe unique phenotypic characteristics of invasion by PDAC cells. Namely, we have identified the presence of single, hyperactive cells (sheepdog cells) which quickly move about the invasive front and interact with masses of cells invading out of tumor spheroids. While the exact molecular mechanisms mediating these effects remain to be defined, these data have elicited provocative hypothesis based on this novel data and generated significant observations to drive future studies. I observed differing phenotypes of invasion in co-culture spheroids that were actually more dramatic when CAFs were present in low quantities. While the data concerning co-culture of these cells is not definitive, evidence suggests distinct mechanisms by which Pan-CAFs induce metastasis in co-culture. Further, the techniques I established and the findings reported here have the potential to spur highly impactful studies of metastasis in PDAC moving forward.

Studies of metastasis across cancer types has raised the "seed and soil" hypothesis proposing that cancer cells metastasize to sites "prepared" for them by other cells. Realistically, this hypothesis simply proposes that cancer cells will follow the least restrictive path to escape immune destruction and acquire new sources of nutrition as the tumor evolves and develops. While we desire an understanding of the immune landscape in metastatic PDAC lesions, there are numerous non-immune related cell types with the potential to impact this process. In order for metastatic tumor cells to arrive at sites of metastasis unscathed, they must avoid immune destruction as they move

about in circulation. MDSCs not only provide an ideal "metastatic niche" in the liver for PDAC cells, but they are also expanded by IL-6 derived from CAFs and are expanded in patients with PDAC[109,113,130,137-145]. Additionally, suppressive T-cell and B-cell subsets have ethe potential to respond to CAF derive cytokines and mediate immune suppression in multiple organs to facilitate PDAC progression[37,113,146-150]. In fact, CAFs themselves have the ability to directly quell anti-tumor T-cell responses throughout multiple mechanisms[37,151,152]. In recent years, much attention has been given to the unique populations of fibroblasts positioned throughout primary pancreatic tumors. These cells are alternatively referred to as pancreatic stellate cells, and share many characteristics with hepatic stellate cells, which were actually recognized before their pancreatic counterparts[153]. While we hypothesized that Pan-CAFs might be necessary soil to seed metastatic PDAC lesions in the liver, two notable studies by Ozdimir *et. al.* and Rhim *et. al* have described the tumor promoting effects of depleting or targeting fibroblasts from mice bearing pancreatic tumors. These studies were limited in that all fibroblasts were depleted without bias for subtype: however, the prevailing view in the field that fibroblasts were unilaterally tumor promoting was altered. Multiple studies approaching fibroblasts in PDAC as a singular, homogeneous populations of cells had reported conflicting evidence about the pro- or anti-tumorigenic potential of these cells[41,154]. Given the inherent heterogeneity of CAF populations within the TME of PDAC, consideration of fibroblasts as a singular population proved to be an extremely oversimplified approach. Rather, further investigation needs to pinpoint contributions of individual fibroblasts populations to PDAC progression. Detailed genomic approaches demonstrated similar abilities to detect multiple fibroblast populations in PDAC[36,43]. Thus, investigative pursuit of the TME in PDAC must now elucidate the contributions of individual fibroblast populations to tumor growth, immune suppression, TME development and metastasis. My data demonstrates dynamic changes in the metastatic potential of CAFs and PDAC cells in co-culture when the relative ratios of these cells is altered. Going forward, we should seek to

understand how individual CAF populations contribute to the metastatic process. My observations can potentially be explained by differences in the types of CAFs that were isolated using our protocols. Pursuing this hypothesis has the potential to elicit provocative and actionable discoveries to inform pharmacological targeting of the stroma in metastatic disease.

Overall, these studies of tumor-CAF interactions demonstrate heterogeneous effects of fibroblasts from different patients on the invasive phenotype of pancreatic cancer cells. Moving forward, our research will interrogate the frequency and genetic features of populations such as iCAFs, myCAFs and apCAFs in cultures of patient fibroblasts to correlate these populations with the invasiveness of spheroids exposed to Pan-CAF conditioned media. Due to the detailed genomic profiling of fibroblasts populations by the Tuveson and Turley labs, this approach will provide us with insight on the soluble factors that could mediate the effects observed here.

The initial potentiation of migration and metastasis of pancreatic cancer cells by Pan-CAF conditioned media has still yet to be elicited. In my initial hypothesis that fibroblasts could initiate pancreatic cancer cell metastasis through the secretion of soluble factors, I hypothesized that this factor would be a secreted protein such as a cytokine or growth factors. Indeed, boiling of Pan-CAF conditioned media completely ablates the metastasis promoting effects of SC54 conditioned media on HPAC spheroids indicating that a factor susceptible to heat, such as a protein with tertiary or quaternary structure, is responsible for driving the effects observed here. We detected TIG-2 and MCP-1 to be uniquely detectable in Pan-CAF, but not HPAC, supernatants. TIG-2, also known as chemerin, should be further investigated for its role in promoting invasion and migration as it promotes downstream angiogenesis and chemotaxis. Interestingly, collective invasion of lung cancer cells relies heavily on angiogenic signaling to facilitate communication and collective migration in 3D

spheroids. Additionally, our previous data transcriptionally profiling PDAC derived CAFs provides numerous targets which should be investigated in this system including CCL11, SAA1 and CCL2 among many others[50].

Supporting these data, addition of non-essential amino acids to the media promotes significant invasion and metastasis of HPAC cells. Previous literature has reported significant contributions of metabolites and amino acids on pancreatic cancer growth. Further, the metabolic profiles of fibroblasts and cancer cells are strikingly different and complementary. These observations have provoked research into how therapeutic modulation of metabolism in PDAC could disrupt the tumor promoting cycle between fibroblasts and tumor cells. Here, boiling of supernatant from CAFs ablated the metastasis promoting effects seen in 3D invasion assays. Boiling supernatants should denature proteins and stop enzymatic activity while leaving metabolites unaffected. No metabolite in CAF conditioned media was able to overcome the boiling of conditioned media. Given that the previous literature demonstrated alterations in amino acid metabolism in pancreatic cancer, future investigations addressing the influence of proteinaceous factors in CAF supernatants may be informative. Similarly, our observation that IL-6 can elicit significant invasion and migration of PDAC cells sheds further light on this process. Of note, there may be a dynamic of several signaling factors which either overlap or synergize to impact this process. Thus, the potential for several overlapping influences should be considered in future investigations.

To fully characterize the interactions mediating the phenotypes observed here, innovative techniques will need to be employed. Foremost, employing a novel murine model with which metastasis of these cells can be observed is being optimized by our group. As a starting point for this process, my preliminary data demonstrates the utility of using a congenic murine system whereby orthotopic

injection of both CD90.2$^{+}$ CAFs and murine tumor cells into immune competent CD90.1$^{+}$ mice. Further, this system is adaptable across multiple murine cancer cell lines (MT5, KPC-luc, Panc02 and KP2) which exhibit vastly different growth kinetics, and may be relevant to different incubation times required for establishment of metastasis. Both KP2 and MT5 murine pancreatic cancer cell lines grow much more slowly than KPC-luc cells or Panc02 cells, making them promising candidates to employ in an orthotopic model of metastasis. Developing these tools will not only allow for highly impactful *in vivo* studies of metastasis, but will also more accurately mimic the stromal presence observed in patients and increase the relevance of our therapeutic studies.

Together, these data provide strong scientific premise to spur future studies of CAFs in the metastasis of pancreatic cancer. These data also provide novel evidence that CAFs derived from human primary pancreatic tumors elicit potent invasive phenotypes in pancreatic cancer spheroids. The novelty of targeting CAFs to control invasive or metastatic spread of PDAC carries the potential to be highly impactful in the field of pancreatic cancer treatment. Considering the overwhelming portion of PDAC patients presenting with metastatic disease and the failure to therapeutically target the growth of metastatic tumor burden, there is an urgency to advance this research. Certainly, gaining a better understanding of the tumor microenvironment in the metastases of pancreatic cancer patients will benefit the field moving forward.

# Chapter 3: Dual blockade of IL-6 and CTLA-4 regresses pancreatic tumors in a CD4$^+$ T-cell-dependent manner.

## 3.1. Author's Contribution and Acknowledgement of Reproduction.

This chapter is reproduced with minor edits from Michael Brandon Ware[1], Christopher McQuinn[2], Mohammad Y. Zaidi[3], Hannah Knochelmann[4], Thomas A. Mace[5], Zhengjia Chen[6], Chao Zhang[6], Matthew R. Farren[1], Amanda N. Ruggieri[1], Jacob Bowers[4], Reena Shakya[7], A. Brad Farris[8], Gregory Young[9], William E. Carson, III[2], Bassel El-Rayes[1], Chrystal M. Paulos[4] and Gregory B. Lesinski[1]. *Dual blockade of IL-6 and CTLA-4 regresses pancreatic tumors in a CD4$^+$ T-cell-dependent manner*. In Revision to Gut, 2020.

MB Ware, C McQuinn, MY Zaidi, H Knochelmann, TA Mace, MR Farren, AN Ruggieri, and J Bowers performed the experiments. G Young, Z Chen and C Zhang performed the statistical analysis. R Shakya, MB Ware, C McQuinn, H Knochelmann, TA Mace, AB Farris, WE Carson III, B El-Rayes, CM Paulos and GB Lesinski collaborated to design experiments and approach. MB Ware, C McQuinn, and GB Lesinski wrote the manuscript with feedback from all authors.

Affiliations:

[1]Department of Hematology and Medical Oncology, Winship Cancer Institute of Emory University; [2]Division of Surgical Oncology, Department of Surgery, Department of Internal Medicine, The Ohio State University; [3]Department of Surgery, Winship Cancer Institute of Emory University, [4]Department of Microbiology and Immunology, Hollings Cancer Center, Medical University of South Carolina, [5]Division of Gastroenterology Hepatology and Nutrition, Department of Internal Medicine, The Ohio State University; [6]Department of Biostatistics, Emory University, [7]Comprehensive Cancer

Center, The Ohio State University, [8]Department of Pathology, Winship Cancer Institute of Emory University, [9]Center for Biostatistics, The Ohio State University.

**3.2 Abstract.**

Objective: This study aimed to enhance anti-tumor immune responses to pancreatic cancer via antibody-based blockade of interleukin-6 (IL-6) and cytotoxic T-lymphocyte-associated protein 4 (CTLA-4).

Design: Mice bearing subcutaneous MT5 or orthotopic KPC-luc pancreatic tumors were treated with antibodies to IL-6, CTLA-4, or the combination. In mice bearing orthotopically implanted pancreatic tumors, we evaluated the efficacy of this combination in the presence of $CD4^+$ or $CD8^+$ T-cell depletion or CXCR3 blockade. *In vitro* evaluation of IL-6 and CTLA-4 dual blockade therapy utilized T cells from a TRP-1 transgenic mouse as an antigen-specific model system. Chemokine production by pancreatic tumor cells was analyzed by proteome array and ELISA.

Results: Dual blockade of IL-6 and CTLA-4 in tumor bearing mice significantly inhibited tumor growth, accompanied by overwhelming T-cell infiltration and changes in $CD4^+$ T-cell subsets. T-cell depletion studies unveiled a unique dependence on $CD4^+$ T cells for anti-tumor activity of this combination therapy. Dual blockade therapy elicited increased IFN-γ production by activated $CD4^+$ T cells *in vitro*. *In vitro* stimulation of pancreatic tumor cells with IFN-γ profoundly increased tumor cell production of CXCR3 specific chemokines. *In vivo* blockade of CXCR3 prevented orthotopic tumor regression in the presence of the combination treatment, demonstrating a dependence on the CXCR3 axis for anti-tumor efficacy.

Conclusion: These data represent the first report of IL-6 and CTLA-4 blockade as a means to regress pancreatic tumors with defined operative mechanisms of efficacy. Given these results, this therapeutic combination has potential for immediate clinical translation.

**3.3 Introduction.**

Antibodies targeting immune checkpoint receptors and their ligands have gained regulatory approval and demonstrated efficacy in patients. The most notable examples include blockade of cytotoxic T-lymphocyte protein-4 (CTLA-4) and programmed cell death protein 1 (PD-1). Despite encouraging data in patients with various malignancies, there remain a number of key challenges with this approach [155]. Many patients still do not gain benefit from immune checkpoint inhibition (ICI), while resistance is common in those who do initially respond to therapy [155]. Most tumors arising in the pancreas are also inherently resistant to ICI [156]. Overcoming the limitations for individuals unresponsive to these emerging therapies is a priority area of research, as it could advance treatment outcomes across multiple tumor types.

The highly desmoplastic stroma unique to PDAC is a dynamic, immune suppressive component contributing to the poor impact of immune therapy in this malignancy. Our laboratory and others have recently demonstrated that the PDAC stroma and stromal-derived cytokines restrain host immunity [32,151,152,157]. Although dysregulated cytokines represent rational therapeutic targets, there are limited data to help prioritize them in patients for immediate translation. In a cohort of seventy-two treatment naïve patients with metastatic PDAC, circulating IL-6 independently correlated with reduced overall survival [48]. These data were intriguing as IL-6 can regulate phenotypic and functional properties of a smattering of various lymphocyte and myeloid cell populations [144,158]. Detailed immune phenotyping of peripheral blood mononuclear cells from the same cohort of patients revealed additional observations of interest. Notably, a similar relationship between reduced overall

survival and elevated circulating T-cells expressing CTLA-4 was observed [48]. These data encourage strategic combination therapies incorporating CTLA-4 targeting antibodies in PDAC.

Based on these data, we hypothesized that IL-6 blockade would enhance the efficacy of CTLA-4 blockade therapy. Herein, we report that combined blockade of IL-6 and CTLA-4 inhibits pancreatic tumor growth by potentiating infiltration of T cells into tumors. Notably, this therapy is reliant on $CD4^+$ T cells for its efficacy. *In vitro,* this therapy promotes IFN-γ production by activated antigen-specific $CD4^+$ T cells. In turn, we demonstrate IFN-γ promotes the production of lymphocyte-attracting chemokines by tumor cells, including high levels of the CXCR3-associated chemokine CXCL10. Further, this treatment regimen induced systemic shifts in $CD4^+$ T-helper subsets and was dependent upon CXCR3 for efficacy. Together our new findings suggest that combined blockade of IL-6 and CTLA-4 can regress pancreatic tumors via a unique mechanism by imparting $CD4^+$ T-cell-mediated anti-tumor immune responses.

**3.4 Results.**

*Combined blockade of IL-6 and CTLA-4 augments antitumor efficacy in murine PDAC models.*

We first sought to determine the efficacy of dual IL-6 and CTLA-4 blockade in mice bearing subcutaneous MT5 tumors. The MT5 cell line originated from a KPC tumor, harboring G12D mutated *Kras* and R172H mutated *Trp53* [159]. Tumor growth was significantly reduced in mice treated with combined IL-6 and CTLA-4 blocking antibodies compared to mice treated with isotype control antibodies ($p=0.0001$) (**Figure 3.1A**). Although single agent anti-CTLA-4 inhibited tumor growth to a greater extent than mice treated with an isotype control ($p<0.0004$), blockade of IL-6 alone did not delay tumor growth. Notably, mice receiving antibodies to IL-6 and CTLA-4 together experienced more impressive tumor growth inhibition compared to mice receiving single agent CTLA-4

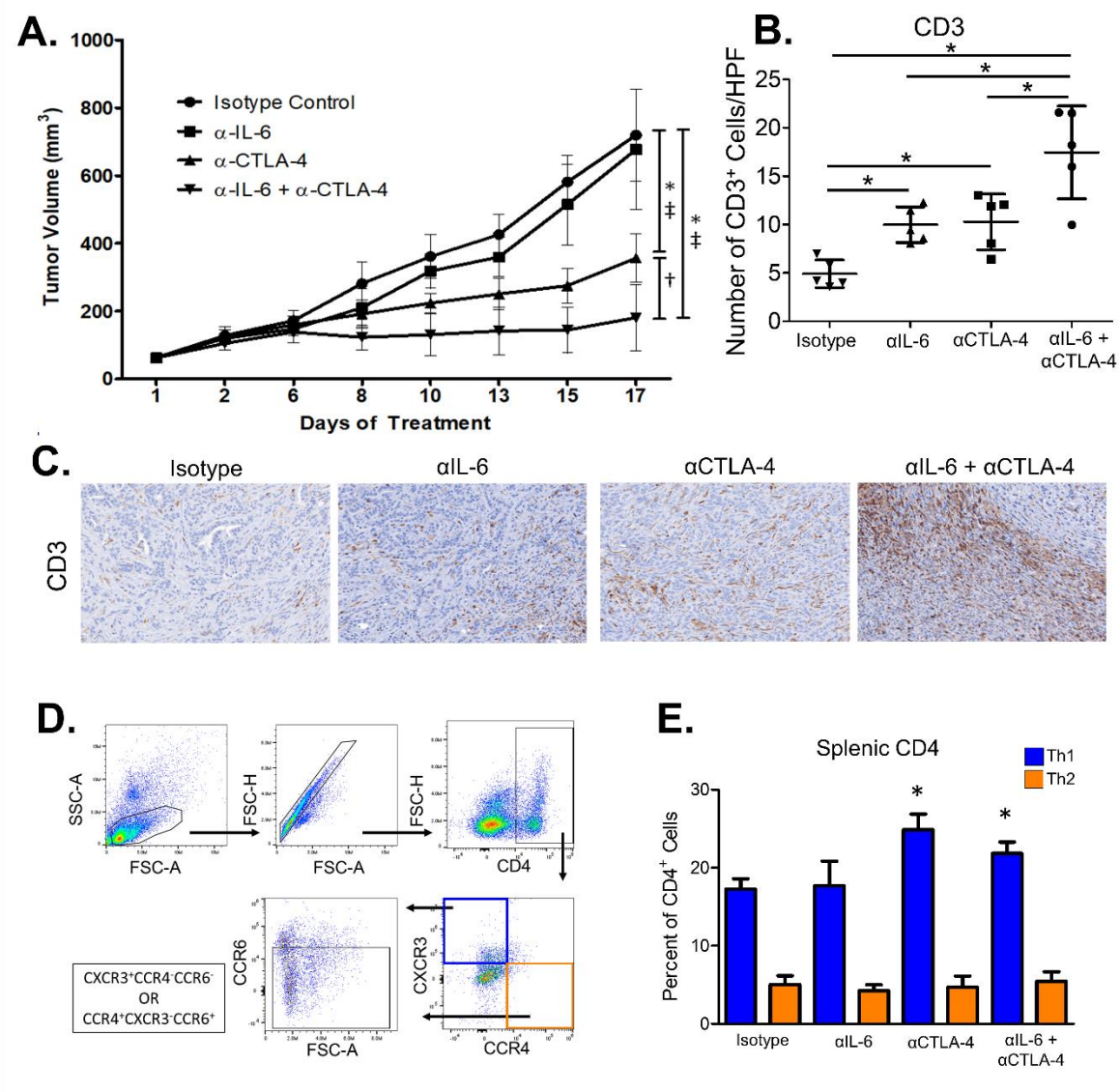


**Figure 3.1. Combined blockade of IL-6 and CTLA-4 significantly inhibits tumor growth and promotes CD8⁺ T-cell infiltration of tumors in a subcutaneous murine model of pancreatic cancer.** MT5 murine pancreatic tumor cells were subcutaneously injected into C57BL/6 mice with treatment beginning when tumors reached 50-100mm$^3$. Mice were treated with 200mg (intraperitoneal injection 3 times/week) of isotype control, cytokine blockade (anti-IL-6) and/or anti-CTLA-4 antibodies (n=5 mice/group) until mice met pre-specified IACUC-approved early removal criteria. **(A)** Changes in tumor volume as determined by caliper measurement throughout the course of antibody treatment. Mean ± SD; * P<0.05 vs. Isotype Control, ‡ P<0.05 vs. Anti-IL-6, † P<0.05 vs. Anti-CTLA-4. **(B)** Representative 20x images of IHC staining for CD3 in FFPE tumor tissue slices from mice in the different treatment groups.

**(C)** Mean ± SD for percent of cells expressing $CD3^+$ in subcutaneous tumors per high-powered field. Symbols represent individual mice; * indicates significance compared to isotype control treated mice ($P<0.05$). **(D)** Splenocytes were isolated from the mice receiving treatment as stated in figure 1A. Flow cytometry was performed with antibodies against CD4, CCR6, CXCR3, CCR4, and RORγt. $CD4^+CCR6^-CXCR3^+CCR4^-$ were identified as suggestive of a Th1 phenotype and $CD4^+CCR6^-CXCR3^-CCR4^+$ as a Th2 phenotype. **(E)** Graph of mean percentages of $CD4^+$ T cells that have a Th1 or Th2 phenotype. Data shown as Mean ± SD; * indicates significance compared to isotype control treated mice.

(p=0.0207) or IL-6 (p=0.0002) blockade. This impact on tumor growth was encouraging, however the mechanism of action was unknown.

*Combined blockade of IL-6 and CTLA-4 mediates increased T cells in pancreatic tumors.*

In light of previous research investigating the influence of IL-6 and CTLA-4 on T-cell populations [50,160], we hypothesized this combined blockade could impact T-cell infiltration into pancreatic tumors. Immunohistochemical staining of tumors from mice treated with this therapy indicated an altered presence of T cells in the tumor microenvironment (**Figure 3.1B)**. Further quantification revealed that both single agent blockade of IL-6 (p=0.0038) or CTLA-4 (p=0.0035) increased infiltration of $CD3^+$ T cells as compared to tumors from isotype control-treated mice (**Figure 3.1C**). Mice given combined therapy had more T cells infiltrating the tumor compared to mice treated with either single agent blockade of IL-6 (p=0.035), CTLA-4 (p=0.038) or isotype controls (p<0.0001) **(Figure 3.1C).**

*Systemic changes in Th1 immunity occur following combined IL-6 and CTLA-4 blockade.*

IL-6 plays a role in regulating differentiation and activation of T-cell subsets [85,117,161]. Therefore, we evaluated the impact of this combination treatment regimen on splenic-derived T cells as a surrogate of systemic immune response. Treatment with anti-CTLA-4 alone or combined with IL-6 blockade increased circulating cells with a Th1 phenotype ($CD4^+CCR6^-CXCR3^+CCR4^-$) as compared to mice treated with isotype control (p<0.05) or anti-IL-6 alone (p<0.05) (**Figure 3.1D-E).** No change was observed in cells with a Th2 ($CD4^+CCR6^-CXCR3^-CCR4^+$) or Th17 ($CD4^+ROR\gamma t^+$) phenotype **(Figure 3.1D-E and Figure 3.2A-B, respectively).** Unexpectedly, the proportion of splenocytes expressing T-regulatory cell (Treg) phenotypic markers ($CD4^+CD25^+FoxP3^+$) was

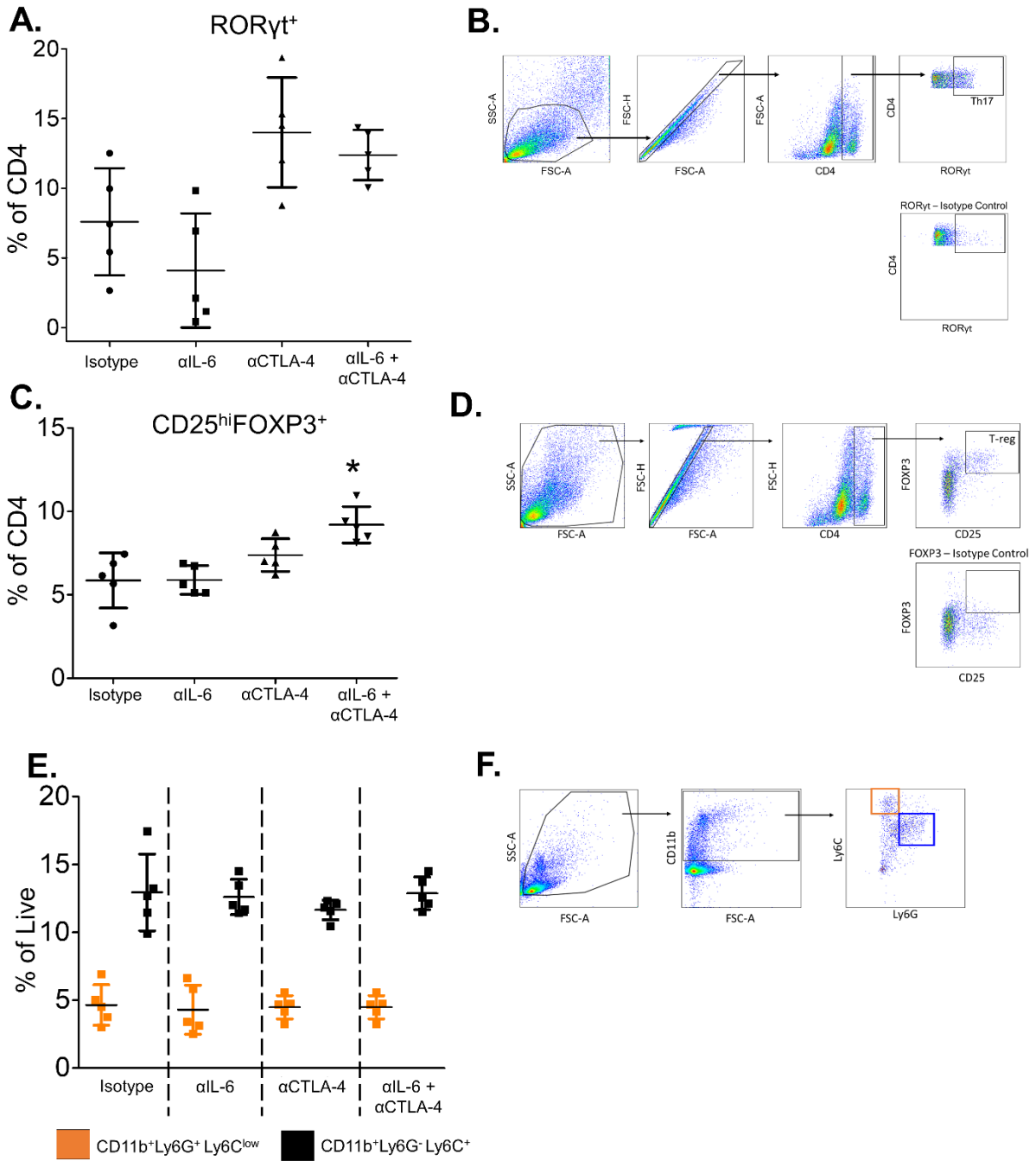


**Figure 3.2. Analysis of Th17, T-reg and MDSC populations in splenocytes from mice treated with single agent, combination, or isotype control antibodies to IL-6 and CTLA-4.**

Splenocytes were isolated from the spleens of mice from the subcutaneous therapeutic study

described in **Figure 1. (A)** Splenocytes were stained with antibodies to CD4, CD25 and FOXP3 and analyzed by flow cytometry. The percentage of $CD4^+$ cells that were $CD25^{hi}FOXP3^+$ were graphed as mean ± SD. * indicates significance ($P<.05$) compared to isotype control treated animals. **(B)** Gating strategy for the identification of Tregs ($CD4^+CD25^{hi}FOXP3^+$) **(C)** Splenocytes were stained with antibodies to CD4 and RORγt and analyzed by flow cytometry. The percentage of $CD4^+$ cells that were $ROR\gamma t^+$ were graphed as mean ± SD. **(D)** Gating strategy for the identification of Th17 cells ($CD4^+ROR\gamma t^+$) **(E)** Splenocytes were stained with antibodies to CD11b, Ly6C and Ly6G as well as and analyzed by flow cytometry. The percentage of $CD4^+$ cells that were $ROR\gamma t^+$ were graphed as mean ± SD. **(F)** Gating strategy for the identification of monocytic-MDSCs ($CD11b^+Ly6G^-Ly6C^+$) and polymorphonuclear-MDSCs ($CD11b^+Ly6G^+Ly6C^{lo}$).

higher in the combination treatment group in comparison to both isotype control ($p<0.05$) and anti-IL-6 ($p<0.05$) (**Figure 3.2C-D**). Because IL-6 also regulates expansion of myeloid-derived suppressor cells in PDAC [109], phenotypic properties of these cells were assessed. No significant change in frequency of either monocytic ($CD11b^+Ly6G^-Ly6C^+$) or granulocytic ($CD11b^+Ly6G^+Ly6C^{low}$) populations were observed across individual groups (**Figure 3.2E-F**). These data indicate a dual role for combined IL-6 and CTLA-4 blockade in driving T-cell infiltration and phenotype.

*$CD4^+$ and $CD8^+$ cells contribute to efficacy of combined IL-6 and CTLA-4 blockade.*

Given the increased infiltration of $CD3^+$ T cells into subcutaneous tumors and systemic alteration of $CD4^+$ T cells, we questioned whether this therapy might be $CD4^+$ or $CD8^+$ T-cell-dependent. For these studies, we orthotopically implanted luciferase-expressing KPC-luc cancer cells into the pancreas of immune competent mice. These cells express enhanced firefly luciferase that allows longitudinal bioluminescent imaging (BLI) of tumors. For these experiments, $CD4^+$ or $CD8^+$ T cells were depleted in mice bearing orthotopic KPC-luc tumors prior to treatment with isotype control antibodies, or combined IL-6 and CTLA-4 blockade (**Figure 3.3A**). Confirmation of $CD4^+$ or $CD8^+$ T-cell depletion was accomplished by flow cytometric analysis of cells isolated from the spleens at the endpoint (**Figure 3.3B**). Longitudinal BLI data indicated efficacy of combined IL-6 and CTLA-4 blockade was $CD4^+$ T-cell-dependent, as mice depleted of $CD4^+$ T cells receiving these therapeutic antibodies had accelerated tumor progression compared to mice receiving only combination therapy (**Figure 3.3C-D**). Tumor progression in some animals was striking, and faster than that of mice receiving isotype control antibodies. $CD8^+$ T-cell depletion also impacted tumor growth, albeit not to the magnitude of $CD4^+$ T-cell depletion, nor to a significant degree compared to combination

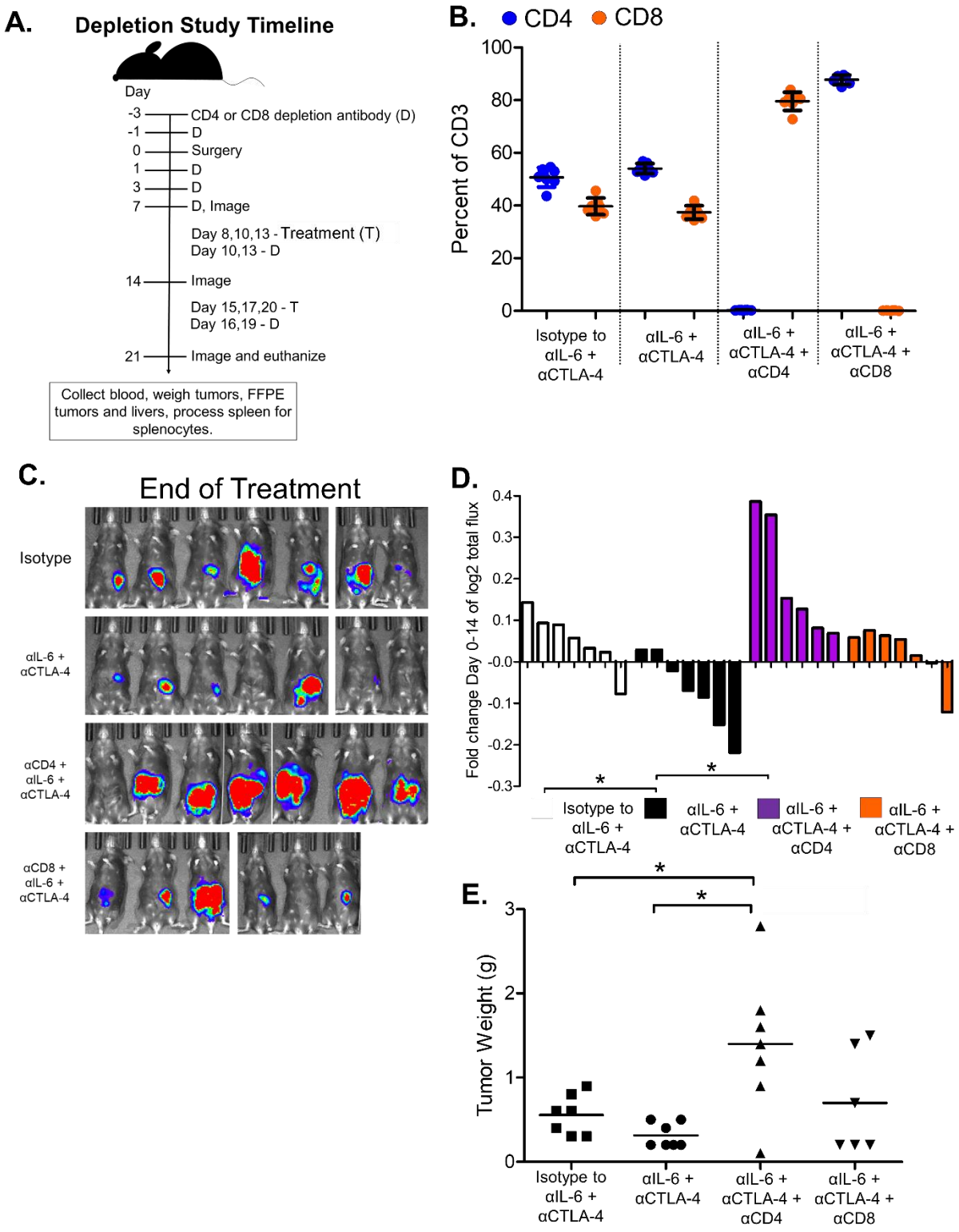


**Figure 3.3. Both CD4$^+$ and CD8$^+$ T cells are required for anti-tumor responses to orthotopic pancreatic tumors in mice treated with combined IL-6 and CTLA-4 blockade.** Female

C57BL/6 mice, 6-8 weeks of age were orthotopically injected with $2x10^5$ KPC-luc cancer cells and imaged 1 week later by bioluminescent imaging (BLI) to confirm tumor establishment. **(A)** Timeline for the administration of $CD4^+$ or $CD8^+$ T-cell depleting antibodies relative to orthotopic injection and subsequent administration of IL-6 and CTLA-4 blocking antibodies or isotype control antibodies. **(B)** At the study endpoint, mice were euthanized and spleens were collected and processed for isolation of splenocytes. Splenocytes were then stained for CD3, CD4 and CD8 markers. The graph demonstrates the percentage of $CD3^+$ cells in splenocytes from each group that expressed the markers CD4 (blue) or CD8 (orange). **(C)** EOT Bioluminescent images for the each mouse in the study outlined in Figure 3.3A are displayed. **(D)** Tumor growth for each mouse from the study outline in Figure 3.3A was measured over time by BLI and the fold change in $Log^2$ of total flux for each mouse was graphed as a bar. **(E)** At the study endpoint (see outline in Figure 3.3A), mice were euthanized and the weight of each tumor was measured and graphed with symbols representing individual mice and mean displayed for each treatment group.

treated mice (**Figure 3.3C-D**). To complement the trends observed with BLI data, the total pancreas and tumor weight was also measured post-mortem (**Figure 3.3E**). All mice were found with primary tumor burden localized to the tail of the pancreas, while mice with advanced disease presented with small metastatic extensions into the local peritoneum. 1 mouse receiving dual IL-6/CTLA-4 blockade presented with no visible tumor burden but the weight of the pancreas was recorded. These data confirmed consistent efficacy of the combination and highlighted a unique coupled mechanism of action requiring $CD4^+$ T cells.

*Combined IL-6 and CTLA-4 blockade supports Th1 cytokines that cross-talk to facilitate chemokine production from tumor cells.*

We posited that combined blockade of IL-6 and CTLA-4 would promote generation of $CD4^+$ T cells with a Th1 cytokine profile. To test this idea, we assayed how modulation of IL-6 and CTLA-4 impacted the biology of transgenic TRP-1 $CD4^+$ T cells bearing a TCR that recognizes tyrosinase-related protein (TRP-1) as a means to model recognition of endogenous tumor antigen. Consistent with our findings in the MT5 model, we found that expanding TRP-1 $CD4^+$ T cells in the presence of IL-6 and CTLA-4 blocking antibodies fostered their capacity to secrete IFN-γ when re-stimulated with cognate antigen (**Figure 3.4A-B)**. This work suggests dual blockade therapy imparts a direct effect on T cells, which in turn drives production of Th1-associated cytokines by $CD4^+$ T cells.

We next surveyed chemokine production from murine MT5 or KPC-Luc tumor cells following *in vitro* stimulation with IFNγ, IL-6 or both cytokines together. Stimulation with IFN-γ resulted in canonical upregulation of chemokines from tumor cells, as detected by chemokine array

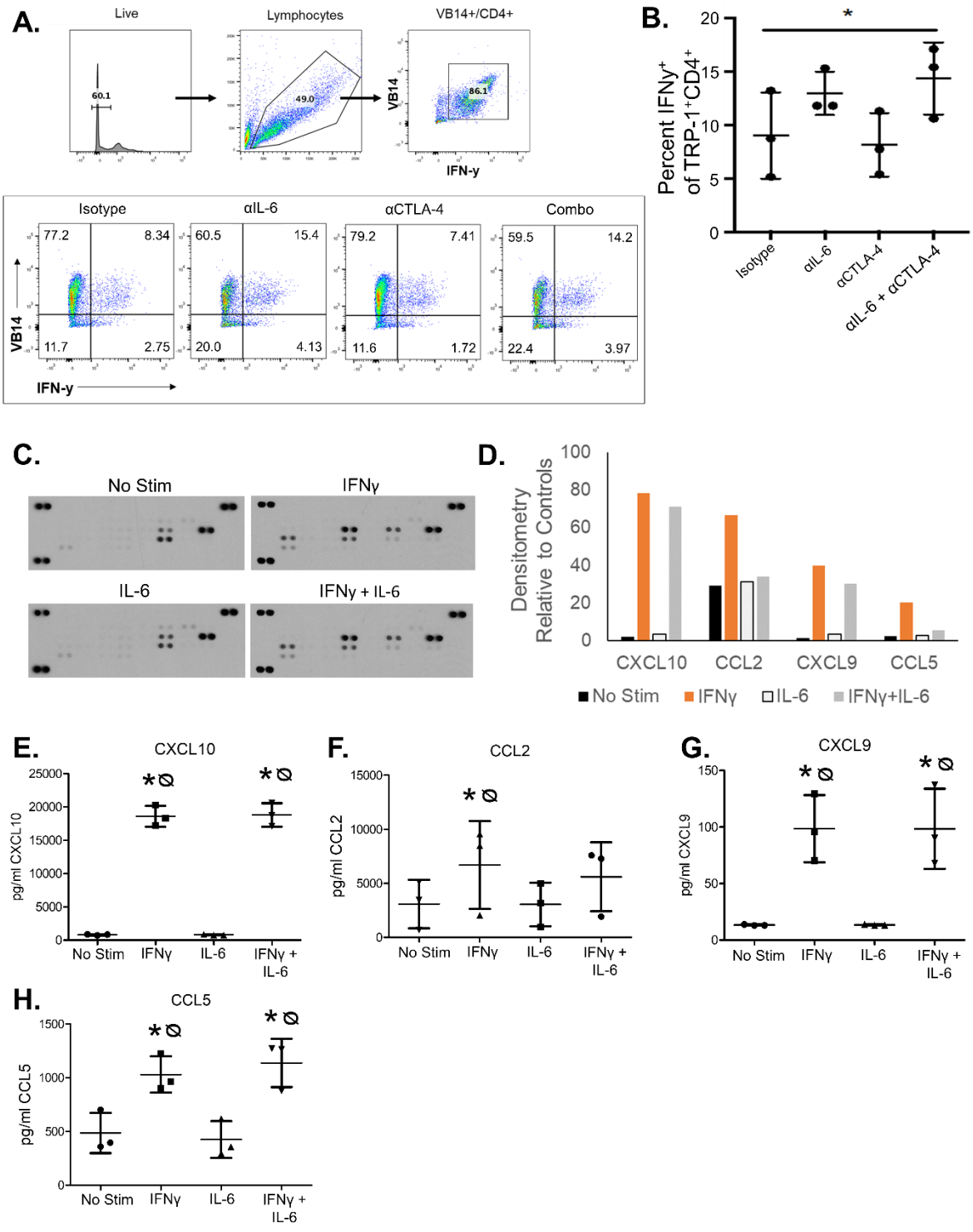


**Figure 3.4. Combined blockade of IL-6 and CTLA-4 promotes IFN-γ production by antigen-activated CD4$^+$ T cells, which can elicit changes in chemokine production by**

**pancreatic tumor cells. (A)** Trp-1 specific $CD4^+$ T cells were stimulated in the presence of antibodies to IL-6, CTLA-4, the combination of both or isotype control antibodies. The percentage of cells expressing Vβ14 and IFN-γ were quantified by flow cytometry. **(B)** Graph shows percentages of $CD4^+$ T cells expressing IFN-γ for each mouse with mean ±SD. $CD4^+$ T cells expressed more IFN-γ in the presence of dual CTLA-4 and IL-6 blockade compared to isotype control antibodies ($p=0.0217$) **(C)** KPC-luc cells were plated at $2x10^5$ cells per well in 6 well plates and then stimulated with 1μg/ml IFNy, 10ng/ml IL-6, both or vehicle control for 24 hrs. Resulting supernatants were collected and analyzed using the Proteome Profiler Mouse Chemokine Array Kit. Shown are resulting images of a chemokine membrane exposed to supernatants of KPC-luc cells from each treatment condition. **(D)** The relative densitometry to loading controls for CXCL10, CCL2, CXCL9, CCL5 as detected by the chemokine array are graphed for each treatment condition. Repetitions of the experiment described in Figure 3.4C were quantified by ELISA and the resulting concentrations were graphed for **(E)** CXCL10 **(F)** CCL2 **(G)** CXCL9 and **(H)** CCL5. Data are shown with symbols marking individual experiments and mean ± SD for each group.

(**Figure 3.5A**) including elevated CXCL10 and CXCL9, which ligate the CXCR3 receptor (**Figure 3.4C-D)** [162-165]. CCL2 and CCL5 were also upregulated upon IFN-γ stimulation (**Figure 3.4C-D**). When tumor cells were concurrently stimulated with IL-6 and IFN-γ, we found that CCL2 and CCL5 production by tumor cells was dramatically decreased (**Figure 3.4C-D**). These results only represented n=1 experimental result, so we repeated these experiments with KPC-luc (**Figure 3.4E-H**) and MT5 cells (**Figure 3.5B-E**) using ELISA to confirm significant upregulation of CXCL10, CXCL9, CCL2 and CCL5 by treatment with IFN-γ. Using ELISA however, revealed to change in chemokine production after treatment of cells with IL-6 alone, nor did combined stimulation with IL-6 and IFN-γ differ significantly from IFN-γ stimulation alone as quantified by ELISA (**Figure 3.4 E-H**).

*CXCR3 is required for the efficacy of combined IL-6 and CTLA-4 blockade.*

Given these *in vitro* results, we hypothesized that improved Th1 cell trafficking into the PDAC tumor microenvironment via CXCR3 is a key mechanism that contributes to the efficacy of combined IL-6 and CTLA-4 blockade. To determine if CXCR3 receptor interactions were essential mediators of the observed T-cell response, we employed CXCR3 blocking antibodies in mice receiving combination therapy. All mice receiving combined IL-6 and CTLA-4 blockade experienced tumor regression as detected by BLI (**Figure 3.6A-B**). Mice receiving combination therapy demonstrated significant decreases in BLI signal compared to mice receiving isotype control antibodies, or blockade of IL-6 or CTLA-4 alone. Concurrent CXCR3 blockade significantly inhibited the efficacy of the combination therapy, leading to results similar to that seen when mice were treated with isotype controls (**Figure 3.6A-B**). No significant change in tumor growth was detected by BLI when comparing isotype control mice to those receiving single agent therapy.

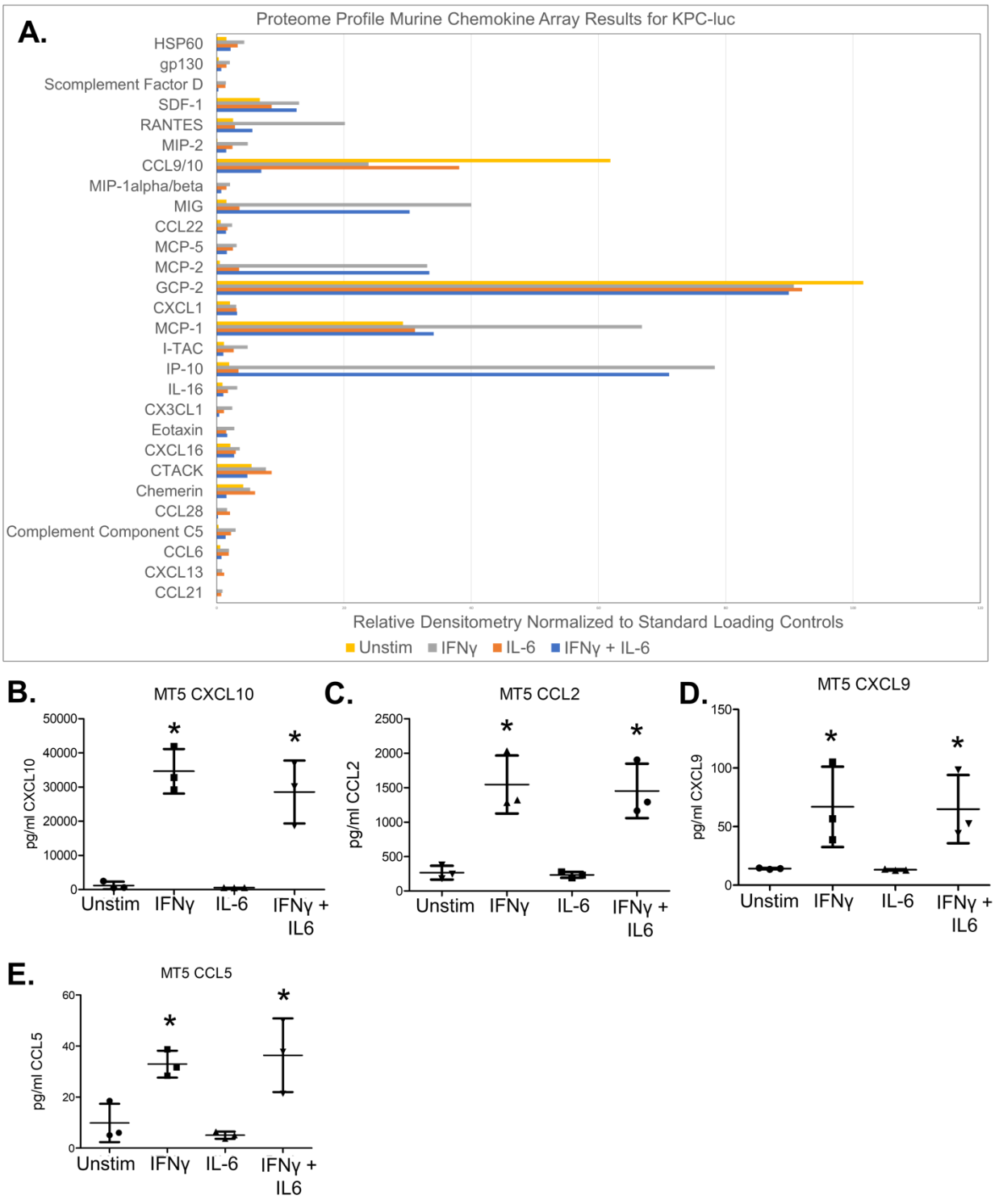


**Figure 3.5. Chemokine array analysis of supernatants from IFNγ and IL-6 stimulation of murine cancer cell lines. (A)** Relative densitometry for each chemokine produced by KPC-luc cells unstimulated (yellow), or treated with 1μg/ml IFNγ (grey), 10ng/ml IL-6 (Orange), or the

combination of IFNγ and IL-6 (Blue). ELISA quantification of **(B)** CXCL10 **(C)** CCL2 **(D)** CXCL9 and (E) CCL5 production by MT5 pancreatic cancer cells unstimulated or treated with 1μg/ml IFNγ, 10ng/ml IL-6, or the combination of both IFNγ and IL-6. Data is graphed as mean of 3 replicates ± SD. * indicates significance ($p<.05$) compared to unstimulated cells or cells treated with IL-6.

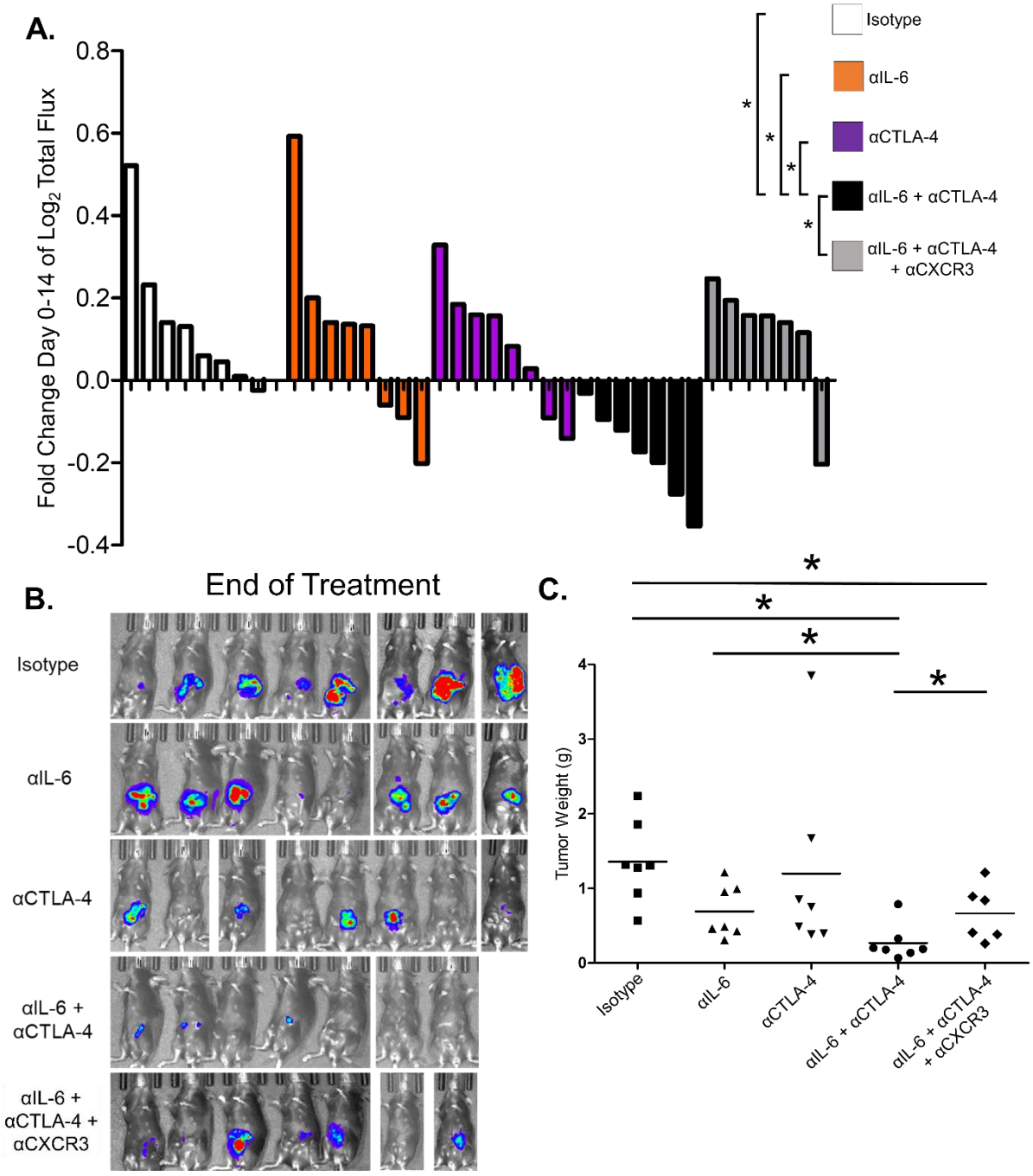


**Figure 3.6. Treatment of murine orthotopic pancreatic tumors with antibodies to IL-6 and CTLA-4 results in significant tumor regression and increased intra-tumoral $CD4^+$ and $CD8^+$ T cells in a CXCR3 dependent manner.** Female C57BL/6 mice, 6-8 weeks of age were orthotopically injected with $2x10^5$ KPC-luc cancer cells and imaged 1 week later by bioluminescent imaging (BLI) to confirm tumor establishment. Mice were then treated 3 times a week for 2 weeks

with antibodies to IL-6, CTLA-4, the combination of both, the combination and antibodies to CXCR3 or isotype control antibodies. **(A)** Tumor growth was measured over time by BLI and the $Log^2$ fold change in total flux for each mouse was graphed as a bar. * indicates significance ($p<0.05$) to mice receiving dual blockade of IL-6 and CTLA-4. **(B)** Resulting bioluminescent images for each mouse at the end of treatment demonstrates the anti-tumor efficacy measured by BLI. **(C)** After two weeks of treatment, mice were euthanized and the total weight of each tumor was collected and graphed as mean for each treatment group. Symbols represent individual mice. * indicates significance ($p<0.05$) for each comparison.

Analysis of post-mortem pancreas/tumor weight at the study endpoint confirmed growth inhibitory effects of the combination were significant, as compared to treatment with either CTLA-4 blockade or isotype control antibodies ($p<0.05$; **Figure 3.6C**). All mice were found with primary tumor burden localized to the tail of the pancreas, while mice with advanced disease presented with small metastatic extensions into the local peritoneum. 4 mice receiving the combination therapy presented with no visible tumor burden but the weight of the pancreas was recorded.

*Dual blockade therapy alters T-cell infiltration of tumors in a murine orthotopic PDAC model.*

Histologic analysis was utilized to survey changes in the tumor microenvironment that may explain the efficacy of this treatment combination. Although prior observations from our group show IL-6 is largely derived from fibroblasts in the PDAC microenvironment [50,109], no difference in alpha smooth muscle actin (α-SMA) staining was observed in tumors between treatment groups (**Figure 3.7A-B**). A trend toward increased $CD8^+$ T cells in tumors from mice receiving dual blockade was seen, but did not reach significance (**Figure 3.8A-B**). Although no differences in $CD4^+FoxP3^+$ T cells emerged (**Figure 3.7C**), a profound increase in $CD4^+$ T cells lacking FOXP3 expression was observed in tumors from mice receiving combined IL-6 and CTLA-4 blockade compared to control mice ($p=0.0297$) or to mice receiving IL-6 single agent blockade ($p=0.0439$) (**Figure 3.8C-D**).

*Dual blockade therapy expands systemic $TBET^+$ and $GATA3^+CD4^+$ T-cell populations in a murine orthotopic PDAC model.*

We next investigated the effects of this treatment on systemic T-cell phenotypes. Flow cytometry analysis (**Figure 3.9A**) recapitulated observations of Th1 immunity, consistent with our splenocyte data in the subcutaneous model (**Figure 3.1D-E**). Robust expansion of $CD3^+CD4^+TBET^+$ (Th1) T-

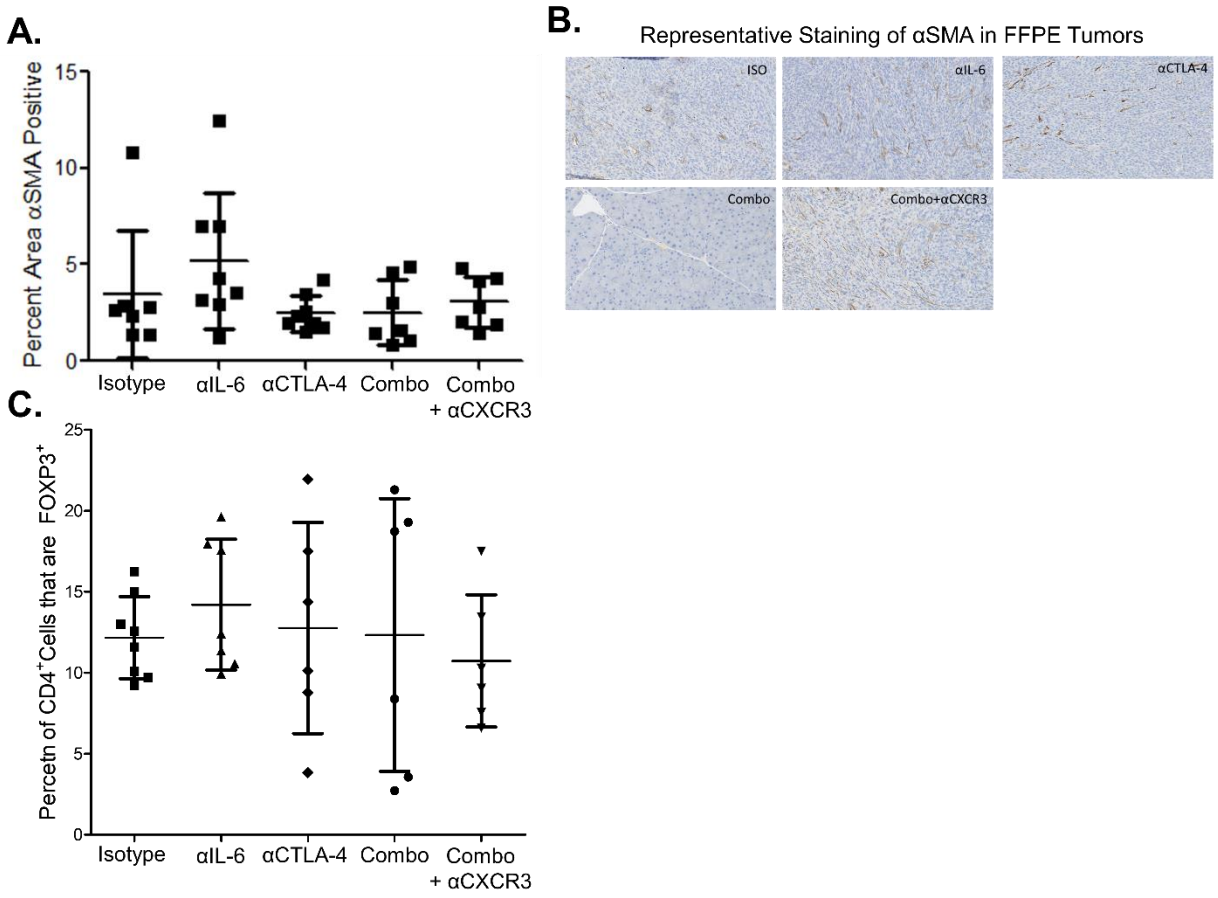


**Figure 3.7. IHC staining of murine tumors for αΣMA and T-regulatory cells.** Tissue slices of FFPE tumors from mice in the orthotopic study outlined in Figure 4 were stained for alpha-smooth muscle actin (αSMA) or CD4, FOXP3 and DAPI. **(A)** Each tissue slice stained for αSMA was sampled based on total tissue area and the resulting 20x images were analyzed using FIJI to determine the percent area positive for αSMA. The mean ± SD was then graphed for each treatment group. **(B)** Representative 20x images of αSMA staining of tumors from each treatment group. **(C)** Immunofluorescent whole slide scans were collected on the Vectra Polaris Slide Scanner and analyzed using the Qupath to determine the percentage of $CD4^+$ cells expressing FOXP3. The mean ± SD for each group was graphed. No significance was detected across groups for either measurement.

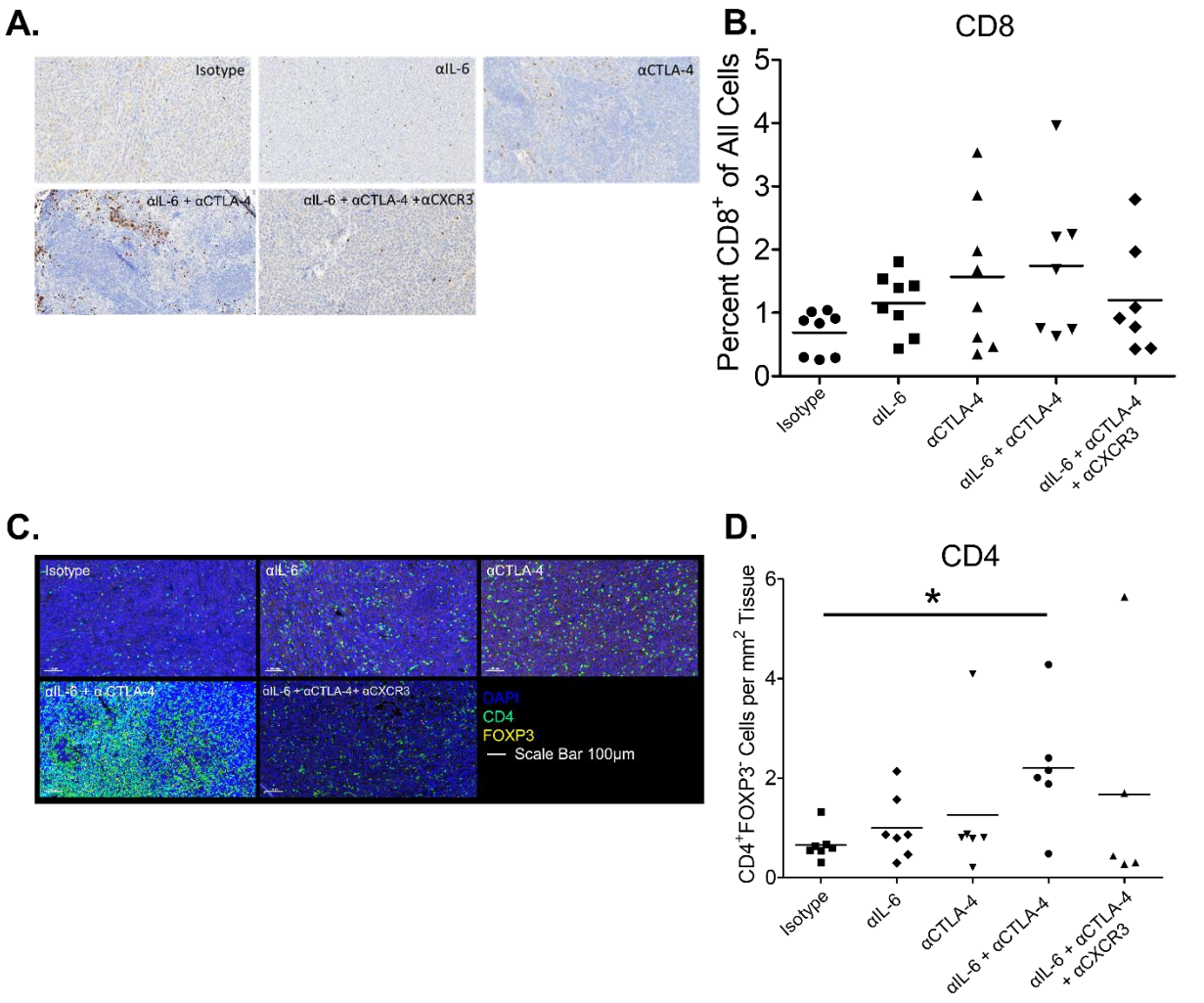


**Figure 3.8. T-cell infiltration of pancreatic tumors in altered in the presence of combined IL-6 and CTLA-4 blockade. (A)** FFPE tissue slices of tumors from mice described in Figure 4 were stained for CD8 by IHC, quantified using Qupath and graphed as the percentage of cells expressing CD8. Results are displayed as mean for each treatment group. Symbols represent individual mice. **(B)** Representative images of IHC staining for CD8 in tumors from mice described in Figure 4A. **(C)** Slices from these tumors were also stained for CD4 and FOXP3 with DAPI counterstain followed by primary antibody-detection with Opal-conjugated antibodies. After scanning slides using a Perkin Elmer Vectra Polaris fluorescent slide scanner, the percentage of cells positive for CD4 but negative for FOXP3 were quantified with Qupath and graphed as mean for each treatment

group. * indicates significant difference between isotype treated mice and mice receiving dual IL-6 and CTLA-4 blockade (P=0.0297). **(D)** Representative images are displayed with CD4 staining in green, FOXP3 staining in red and DAPI staining in blue. Scale bars are 100μm.

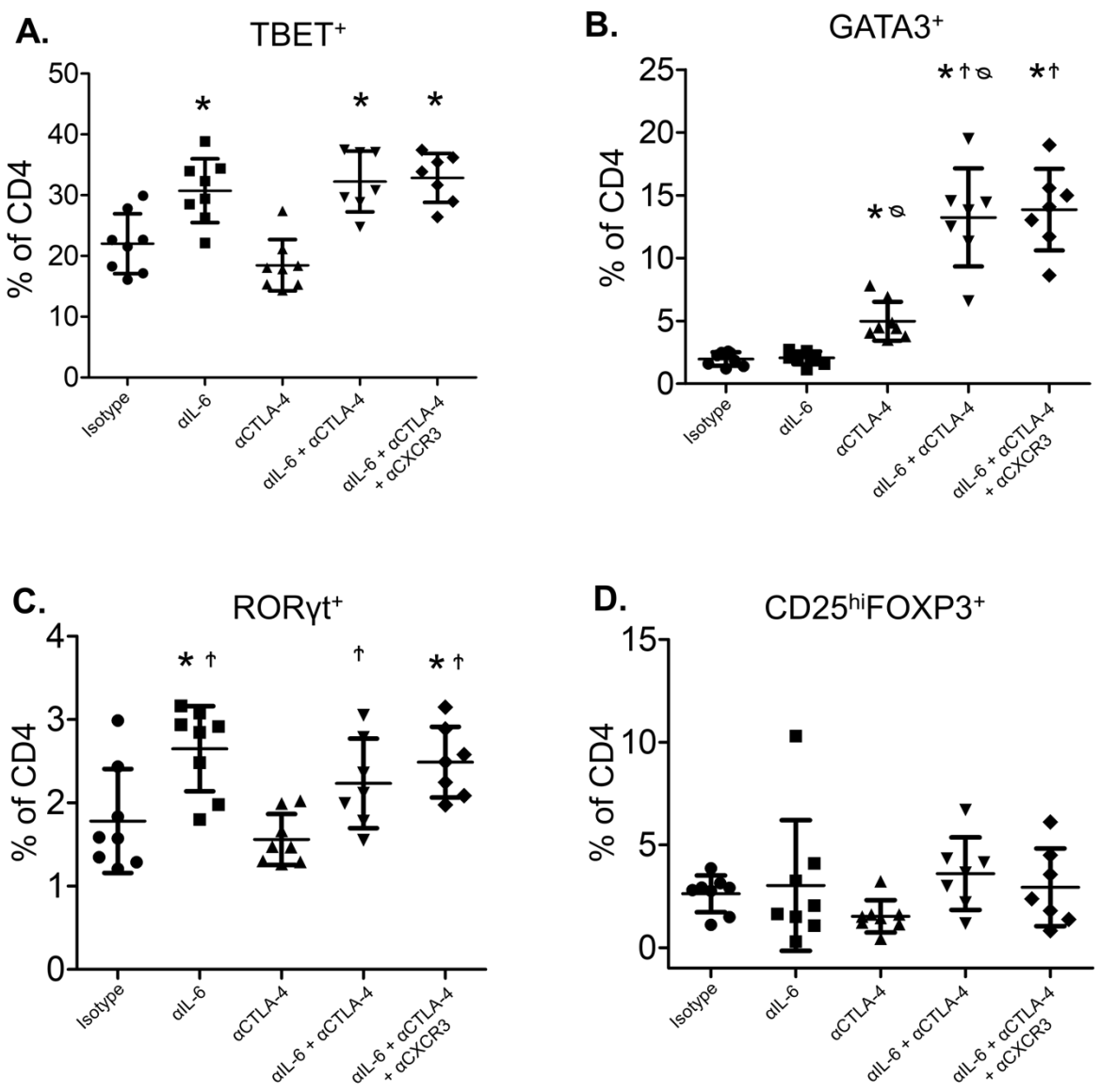


**Figure 3.9. Combined blockade of IL-6 and CTLA-4 in mice bearing orthotopic pancreatic tumors results in systemic changes in CD4$^+$-helper T cells.** Splenocytes were isolated from the mice receiving treatment as stated in Figure 4. Cells were stained for CD3, CD4, and CD8 surface markers with Ghost 780 viability stain to mark dead cells. After fixation and permeabilization, cells were stained for the transcription factors TBET, GATA3, FOXP3, and RORyt. The percentage of CD4$^+$ T cells that were **(A)** TBET$^+$ **(B)** GATA3$^+$ **(C)** RORγt$^+$ or **(D)** CD25$^{hi}$FOXP3$^+$ were graphed

as mean ± SD with symbols indicating significance ($p<0.05$) compared to * isotype control mice, † αCTLA-4 treated mice, or ⍉ αIL-6 treated mice.

cells was observed in splenocytes from mice receiving combined IL-6 and CTLA-4 blockade ($p=0.0015$) or anti-IL-6 alone ($p=0.0041$) versus isotype treated mice (**Figure 3.9A**). We also observed a significantly higher frequency of splenic $CD3^+CD4^+GATA3^+$ (Th2) T cells in mice treated with the combination compared to isotype-treated mice ($p=0.0003$; **Figure 3.9B**). Of note, $CD3^+CD4^+GATA3^+$ T cells were more abundant in mice receiving combination blockade, as compared to those treated with anti-CTLA-4 alone ($p=.0012$; **Figure 3.9B**). We also observed no difference in the frequency of T-regulatory cells, defined phenotypically as $CD3^+CD4^+CD25^{hi}FOXP3^+$, or in $CD3^+CD4^+ROR\gamma t^+$ cells from mice receiving combined IL-6 and CTLA-4 blockade as compared to isotype control-treated mice (**Figure 3.9C**). There were no differences in these systemic biomarkers between mice receiving only the combination or the combination together with CXCR3-targeted antibodies (**Figure 3.9A-D**).

We observed a higher percentage of $CD4^+$ T cells positive for PD-1 in splenocytes from mice treated with anti-IL-6 alone or combined with CTLA-4 blockade as compared to isotype control or single agent anti-CTLA-4 **(Figure 3.10A).** Contrasting data for $CD4^+$ T-cell subsets, few changes were observed in the composition of $CD8^+$ T cells within spleens of mice treated with single agent or combination therapy. However, mice receiving combined IL-6 and CTLA-4 blockade demonstrated significantly more $CD8^+PD\text{-}1^+$ T cells as compared to mice receiving isotype control or anti-IL-6 antibodies (**Figure 3.10B**). Immunologically, this strategy dramatically impacted $CD4^+$ T cells, driving increases in both Th1 and Th2 immunity, with more limited systemic changes in $CD8^+$ T cells.

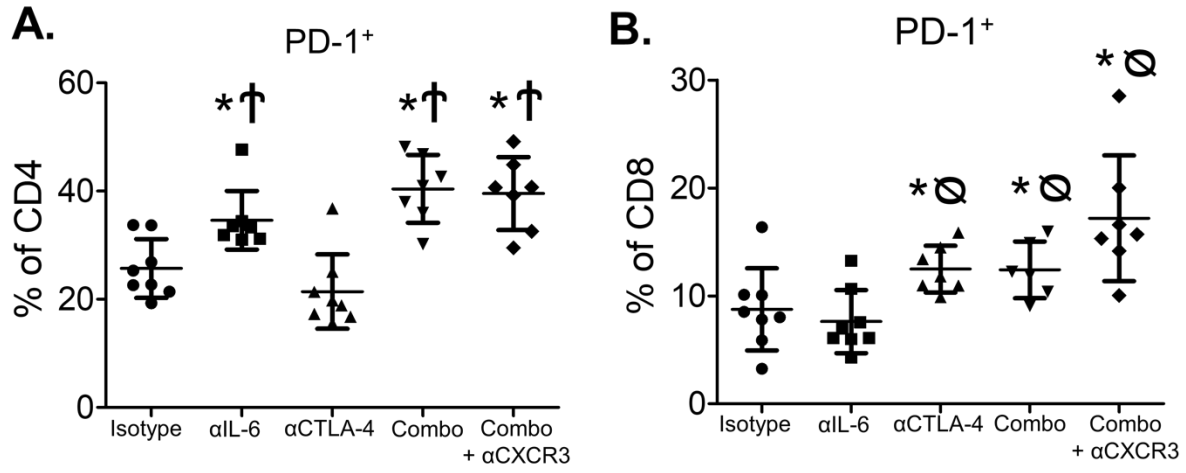


**Figure 3.10**. **Combination IL-6 and CTLA-4 blockade increases PD-1 expression on $CD4^+$ and $CD8^+$ T -cells.** Splenocytes isolated from mice treated in the orthotopic study described in Figure 3.6 were stained and the percentage of (A) $CD8^+$ T cells expressing PD-1 or (B) $CD4^+$ T cells expressing PD-1 were determined by flow cytometry analysis. Graphs show mean ± SD for each treatment group. * indicates significance ($p<.05$) to isotype control treated mice, ⌀ indicates significance ($p<.05$) to mice treated with IL-6 antibody, and † indicates significance ($p<.05$) to CTLA-4 antibody treated mice.

**3.5 Discussion.**

Antibodies that neutralize IL-6 have not been effective as single agents in patients with PDAC [166]. Moreover, blockade of CTLA-4 has limited efficacy as a single agent drug in this aggressive disease [55,167]. Here, we demonstrate that combined blockade of these targets elicits potent and long-lasting anti-tumor activity. The efficacy of concurrently targeting IL-6 and immune checkpoints was first established by our group[50]. In these studies, blockade of IL-6 and PD-L1 in MT5 and Panc02 murine PDAC models significantly inhibited tumor growth while promoting effector T-cell infiltration of tumors[50]. Strikingly, this effect has since been reproduced in multiple murine solid tumor models including glioblastoma, colorectal cancer and melanoma [168-170]. The data from this current report are particularly important in lending flexibility to clinical translation whereby multiple immune checkpoint antibodies may have efficacy via non-overlapping mechanisms. Importantly, this study highlights novel immune responses observed upon neutralizing IL6 alongside CTLA-4 blockade rather than PD-1/PD-L1 blockade, drawing attention to unique mechanisms of action for different ICI modalities.

Results from this study indicate a unique mechanism of action when compared to combined IL-6 and PD-1/PD-L1 blockade, with several evident differences. Previously, the anti-tumor efficacy resulting from combined blockade of IL-6 and PD-1/PD-L1 was determined to be dependent on the action of $CD8^+$ but not $CD4^+$ T cells. Here, in mice treated with the combination therapy, $CD8^+$ T-cell depletion resulted in significant restoration of tumor growth, while $CD4^+$ depletion resulted in even more pronounced and significantly greater tumor growth. Furthermore, in vivo CXCR3 blockade revealed IL-6/CTLA-4 combination therapy to be reliant on this chemokine-receptor. Additionally, combined blockade of IL-6 and PD-1/PD-L1 reduced stromal content, while CTLA-4 and IL-6 blockade revealed no such changes as determined by histological staining of

murine tumors for the activated fibroblast marker alpha-smooth muscle actin (αSMA) [50]. This possible discrepancy may be due to differential effects on various subsets of fibroblasts that could be affected by therapy, one of which produces high levels of IL-6 [35,42]. Additionally,

Previous studies investigating T-cell responses to PDAC have proposed differing results with respect to the effect of CTLA-4 on $CD4^+$ or $CD8^+$ T cells [114,160]. Here we observed a heavy dependence on $CD4^+$ T cells to mediate the anti-tumor effects of combined IL-6 and CTLA-4 blockade. $CD4^+$ T-helper support of $CD8^+$ T-cell responses in the PDAC microenvironment may provide heterogeneous T-cell responses that effectively kill neoplastic cells and mediate regression. Recent evidence from the Schreiber group describes the need for $CD4^+$ and $CD8^+$ T-cell activation for effective anti-tumor responses [171]. In particular, the response of the host to immune-based therapies requires $CD4^+$ T-cell responses to mediate effective T-cell-based rejection of tumors. This study reinforces the importance of $CD4^+$ T cells in mediating efficacy of immune therapies. As immunotherapy combination approaches move into clinic, it will be important to grasp how these therapies impact the various T-cell subsets present in the tumor microenvironment.

We hypothesized that the efficacy of IL-6 and CTLA-4 blockade may be mediated in part by stimulating tumor cells to increase the production of chemokines that enhance lymphocyte tracking into the tumor microenvironment. Studies of single agent CTLA-4 blockade in murine models of PDAC have reported CTLA-4 blockade to mediate $CD4^+$ T-cell infiltration from lymph nodes into tumors [160]. Our in vitro studies demonstrate combined blockade of IL-6 and CTLA-4 to elicit increases in the number of IFNγ producing $CD4^+$ T cells in the context of antigen specific activation[119,172]. While we observed this effect to be driven by blockade of IL-6, previous studies in

prostate cancer have observed elevated numbers of IFNγ producing $CD4^+$ T cells upon administration of CTLA-4 blocking antibodies. IFNγ has emerged as a multifaceted soluble factor capable of directly inhibiting tumor cell growth, driving potent immune activation, and stimulating the production of many interferon response genes by tumor cells[173-176]. One group has demonstrated the activation of interferon response genes in cancer cells to be a crucial requirement for the anti-tumor efficacy of CTLA-4 blockade, such that CTLA-4 blockade fails in patients with defects in these genes[177]. While MT5 and KPC-luc murine cancer lines used in this present study secrete high levels of the CXCR3 specific chemokines CXCL10 and MIG, it is possible that patients with defects in these pathways would not benefit from dual blockade of IL-6 and CTLA-4. Indeed, recent reports support the importance of the CXCR3 chemokine axis for mediating tumor responses to ICI [178], supporting our observations here. Furthermore, IL-6 has previously been shown to regulate the percentage of lymphocytes expressing receptors such as CXCR3 that are associated with $CD8^+$ T-cell and Th1 recruitment to sites of inflammation [179]. The requirement for this particular pathway is supported by the tumor protective effects of CXCR3 blockade observed in this report, which also suggests that infiltrating Th1-helper cells and $CD8^+$ T cells are important for tumor regression in the context of this combination therapy.

While this combination therapy elicits potent anti-tumor activity, clinical application of ICI has potential for toxicity in patients. Attempts to ameliorate the autoimmune toxicities of ICI including anti-CTLA-4 and anti-PD-1/PD-L1-targeted antibodies revealed the IL-6R blocking antibody tocilizumab is effective in patients refractory to steroids [180,181]. A recent report demonstrated tocilizumab alongside pembrolizumab in advanced melanoma not only prevented exacerbation of Crohn's disease, but also allowed for durable anti-tumor immune responses [180]. Similarly, a recent case report showed tocilizumab in a patient with stage IV pulmonary adenocarcinoma completely

resolved immune-related toxicities to nivolumab including oropharyngeal mucositis and esophagitis with severe esophageal stenosis [182]. Finally, the use of IL-6R-blocking antibodies with chimeric antigen receptor T cell (CART) therapy produced encouraging results while actually enhancing patient safety [181]. This emerging use of IL-6/IL-6R blockade to limit ICI-associated toxicities has led to clinical trials exploring the use of IL-6 blockade specifically for improved safety of these therapeutic options (NCT03601611).

Despite these encouraging results, efforts to apply IL-6 or IL-6R blockade prospectively with therapeutic intent in clinical trials have lagged behind the pre-clinical data, possibly due to resistance to repurpose these drugs from autoimmunity into the oncology setting. To date, only a single clinical trial from our group (NCT04191421) is exploring combining IL-6 blockade therapy with ICI for treatment of any oncology indication (pancreatic cancer). Continued clinical experience with IL-6 and ICI combinations across solid tumors will inform the field regarding both efficacy and ability to limit autoimmune sequelae.

**3.6 Materials and Methods.**

*Cell lines and antibodies*

Murine MT5 ($Kras^{LSL\text{-}G12D}$, $Trp53^{LSL\text{-}R270H}$, Pdx1-cre) pancreatic cells were a gift from David Tuveson (Cold Spring Harbor Laboratory, Cold Spring Harbor, NY) and cultured in RPMI-1640 (Gibco) with 10% FBS, 10 mM L-glutamine, and antibiotics (GiminiBio). Murine KPC-luc ($Kras^{LSL\text{-}R270H}$, $p53^{-/-}$, Pdx1-cre) cells expressing an enhanced firefly luciferase construct (a gift from Dr. Craig Logsdon, MD Anderson Cancer Center) were cultured in DMEM (Gibco) with 10% FBS, 10nM L-glutamine and antibiotics. Murine antibodies to IL-6 (Clone MP5-20F3), CTLA-4 (Clone 9D9), CXCR3 (Clone CXCR3-173) or isotype controls (Clones LTF-2 for subcutaneous or HRPN for orthotopic studies, MCP-11 and polyclonal Armenian hamster IgG, respectively) were purchased from BioXcell (West Lebanon, NH). Additionally, anti-mouse CD8a (Clone 2.43) and anti-mouse CD4 (Clone GK1.5) depleting antibodies were purchased from BioXcell.

*In vivo murine efficacy studies*

Animal studies were conducted under institutional animal care and use committee (IACUC) approval at The Ohio State University or Emory University. For efficacy studies, $1x10^6$ MT5 tumor cells were injected subcutaneously in the flank of female C57BL/6 mice. Once tumors reached 50 – 100 $mm^3$ (typically 7-10 days), antibody treatment was initiated. Subcutaneous studies were ended once tumors in mice receiving control antibodies reached a volume that met IACUC-mandated early removal criteria. For orthotopic efficacy studies, $2x10^5$ KPC-luc tumor cells were injected into the pancreas of 6-8 weeks old female C57BL/6 mice. Tumors grew for 7 days prior to randomization into treatment group and pancreatic tumors were confirmed by bioluminescent imaging as described [50]. Treatment details are in online supplementary material.

*Antibodies for flow cytometry and immunohistochemical staining*

All antibodies, with clone names, used for flow cytometry and immunohistochemistry can be found in Table 3.1.

*Flow cytometry*

At the completion of subcutaneous efficacy studies, tissues were harvested for immunophenotypic analyses of splenocytes and single cell suspensions from tumors were assessed by flow cytometry as described [50]. Flow cytometric analysis was performed on a LSRII flow cytometer (BD Biosciences). Splenocytes from mice bearing orthotopic tumors were stained with Ghost 780 dye to detect live cells and stained with antibodies to evaluate $CD4^+$ and $CD8^+$ T-cell phenotypes. For all studies, intracellular staining was performed using the eBioscience Foxp3/Transcription Factor Staining Buffer Set per manufacturer's protocol. Samples were run on a Cytek Aurora cytometer (Cytek). Full descriptions of myeloid and lymphocyte subsets from both studies are in online supplementary materials.

*Immunohistochemical analysis*

Formalin fixed paraffin-embedded (FFPE) tumors from subcutaneous experiments underwent IHC analysis following staining with Ab against CD3 (Catalog A0452; Dako). 40x magnification images of tumors (10 images per mouse tumor) were captured using PerkinElmer's Vectra multispectral slide analysis system. inForm software tools quantified CD3-positive cells (Fast Red chromogen) within each image. Additional tissue slices were stained for CD8, and αSMA and scanned with an Olympus Nanozoomer whole slide scanner and analyzed using Qupath (CD8) or FIJI (NIH) for αSMA. Tumors from mice bearing orthotopic tumors were also FFPE. Dual stains for DAPI (Perkin Elmer) with CD4 and FOXP3 were performed using a Roche autostainer and detected with Opal 520 and Opal

| Table 3.1 Antibodies used for flow cytometry and immunohistochemical staining of tissues | | | |
|---|---|---|---|
| Antibody | Fluorophore | Clone | Source |
| CD11b | APC | M1/70 | BD Biosciences |
| Ly6G | FITC | 1A8 | BD Biosciences |
| Ly6C | PE | AL-21 | BD Biosciences |
| CD4 | PE-Cy7 | RM4-5 | BD Biosciences |
| CD8 | PE-Cy7 | 53-6.7 | BD Biosciences |
| CD62L | PE | MEL-14 | BD Biosciences |
| CD44 | FITC | IM7 | BioLegend |
| CXCR3 | PE-Cy7 | CXCR13-173 | BioLegend |
| CCR4 | PE | 2G12 | BioLegend |
| CCR6 | APC | CK4-L3 | BD Biosciences |
| RORγt | FITC | AFKJs-9 | eBiosceince |
| CD3 | Brilliant Violet 650 | 17A2 | BioLegend |
| CD4 | Brilliant Violet 711 | GK1.5 | BioLegend |
| CD8 | Brilliant Violet 480 | 53-6.7 | BD Biosciences |
| ICOS | Brilliant Violet 510 | C398.4A | BioLegend |
| PD1 | Brilliant Violet 421 | RMP1-30 | BioLegend |
| CD25 | Alexa Fluor 488 | PC61 | BioLegend |
| CXCR3 | PerCP/Cy5.5 | CXCR3-173 | BioLegend |
| CCR4 | PE/Cy7 | 2G12 | BioLegend |
| GATA3 | PE-CF594 | L50-823 | BD Biosciences |
| RORγt | PE | Q31-378 | BD Biosciences |
| CCR6 | Alexa Fluor 647 | 29-2L17 | BioLegend |
| FOXP3 | Alexa Fluor 700 | FJK-16s | ThermoFisher |
| TBET | APC | 4B10 | BioLegend |
| CTLA4 | BV605 | UC10-4B9 | BioLegend |
| CD44 | FITC | IM7 | BioLegend |
| TCF1/7 | PE | 7F11A10 | BioLegend |
| TIM3 | PECy7 | RMT3-23 | BioLegend |
| CD69 | PerCP/Cy5.5 | H1.2F3 | BioLegend |
| CD39 | Aleca Fluor 647 | Duha59 | BioLegend |
| CD11b | BV510 | M1/70 | BioLegend |
| I-A/I-E | BV650 | M5/114.15.2 | BioLegend |
| CD206 | BV711 | C068C2 | BioLegend |
| CD24 | BV605 | M1/69 | BioLegend |
| B7-1 | BV421 | 16-10A1 | BioLegend |
| Ly6G | FITC | 1A8 | BioLegend |
| CD11c | Alexa Fluor 532 | N418 | ThermoFisher |
| Ly6C | PE-Cy7 | Al-21 | BD Biosciences |
| F4/80 | PE | BM8 | BioLegend |
| B7-2 | PerCp/Cy5.5 | GL-1 | BioLegend |
| CD103 | APC | 2E7 | BioLegend |
| CD64 | Alexa Fluor 647 | X54-5/7.1 | BioLegend |
| VB14 | FITC | 14-2 | BD Biosciences |
| CD4 | PE | RM4-5 | BD Biosciences |
| IFN-γ | BV450 | XMG1.2 | BioLegend |
| Live/Dead | | Zombie Aqua Fixable Viability Kit | BioLegend |
| Rat IgG2b, k Isotype Ctrl Antibody | BV421 | RTK4530 | BioLegend |
| Mouse IgG1, k Isotype Control | PE-CF594 | X40 | BD Biosciences |
| Rat IgG2a Kappa Isotype Control | Alexa Fluor 700 | eBR2a | ThermoFisher |
| Mouse IgG1, k Isotype Ctrl Antibody | APC | MOPC-21 | BioLegend |
| Rat IgM, k Isotype Control | PE-Cy7 | R4-22 | BD Biosciences |
| Rat IgG2a, k Isotype Ctrl Antibody | PerCP/Cy5.5 | RTK2758 | BioLegend |
| CD4 | Unconjugated | EPR19514 | abcam |
| CD8 | Unconjugated | Catalog Number ab203035 - polyclonal | abcam |
| FOXP3 | Unconjugated | Catalog Number NB100-39002 - polyclonal | Novus |
| CD3 | Unconjugated | Catalog Number A0452 - polyclonal | Dako |

630-conjugated secondary (Perkin Elmer), respectively. Slides were imaged using the Vectra Multispectral Imaging System version 2 (Perkin Elmer). Filter cubes used for imaging were DAPI (440–680 nm), FITC (520 nm-680 nm), Cy3 (570–690 nm), Texas Red (580–700 nm) and Cy5 (670–720 nm). Multispectral images were analyzed with Qupath [183].

*TRP-1 transgenic CD4$^+$ T-cell activation*

CD4$^+$ TRP-1 transgenic T cells [116] were activated with TRP-1106-130 peptide (SGHNCGTCRPGWRGAACNQKILTVR) loaded at 1μM concentration onto irradiated B6 splenocytes (10Gy) at a 2:1 TRP-1:feeder cell ratio. TRP-1 cells were cultured with monoclonal antibodies targeting CTLA-4 (10μg/mL, clone 9D9), IL-6 (10μg/mL, clone MP5-20F3) or isotype controls (10μg/mL, IgG2b or HRPN) with IL-2 (100IU/mL). Cells were assessed three days after activation for cytokine production post PMA/Ionomycin stimulation. Briefly, cells were activated in PMA (30nM) and Ionomycin (20nM) (Sigma) with Monensin (2μM) and Brefeldin A (5μg/mL) (Biolegend) for 4 hours, followed by fixation and permeabilization for cytokine staining per protocol (BioLegend).

*In vitro evaluation of chemokine production*

KPC-luc or MT5 cells were plated at 2x10$^5$ cells per well in 6 well plates. Media was supplemented with 10ng/ml IL-6 (peprotech), 1μg/ml IFNy (peprotech), both cytokines combined, or vehicle for 24 hours. Supernatant was collected and spun at 1000 *x g* then transferred to a new tube to limit cellular contamination. Supernatants were analyzed using the Proteome Profiler Mouse Chemokine Array Kit (ARY020, R&D Systems). Results were confirmed using DuoSet ELISA kits (R&D Systems) for CXCL10, CXCL9, CCL2, and CCL5.

*Statistical Analysis*

Data from subcutaneous studies obtained by flow cytometry, IHC and tumor volumes were log-transformed prior to analysis to meet model assumptions of normality and homoscedasticity. Tumor volume was modeled over time using mixed-effects regression with fixed effects for group, time and interaction of the two. Random intercepts and slopes by mouse were included with an unstructured covariance matrix for random effects. Other outcomes were compared using ANOVA. P-values of >0.05 were significant.

For numeric covariates, mean and standard deviation were calculated and presented. One-way ANOVA was performed for IHC and splenocyte data with univariate analysis. Least significant difference method (LSD) was used for pairwise multiple comparisons. Natural log transformation of bioluminescent imaging data was performed to achieve approximately normal distribution of data. For log transformed data, linear mixed models tested for significant change over time of each outcome and to detect any significant difference of each outcome among treatments. Significance was set at 0.05. For *in vitro* data, natural log transformation was performed to normally distribute data. We then performed one-way ANOVA and LSD to detect whether means significantly differed among treatment groups. All analyses were conducted in SAS v9.4 (SAS Institute, Cary, NC).

# Chapter 4: Conclusions and Closing Remarks

## 4.1 Future Studies

The field of cancer biology has evolved overtime to appreciate how influential the TME is on tumor progression and disease outcome. While many therapeutics are specifically designed to target mutated proteins, ectopically expressed receptors or deregulated processes within tumor cells, new and emerging strategies have turned to leverage the stroma, immune system and other components of the TME. Given their high prevalence and activated state, our work has characterized novel contributions of CAFs to PDAC. We have confirmed prior data that these CAFs are inflammatory and produce extremely high levels of the cytokine IL-6[50,109]. This pleiotropic cytokine has the ability to promote tumor cell proliferation, expand suppressive myeloid cells, exacerbate stromal fibrosis, and sway anti-tumor immune responses by directly influencing T cells.

Our previous work has adapted novel immunotherapy combinations against PDAC in pre-clinical models. In one key study, dual blockade of IL-6 and PD-L1 leads to $CD8^+$ T-cell dependent tumor regression in murine models of PDAC. IL-6 blockade not only enhanced $CD8^+$ T-cell infiltration but also reduced stromal content. Here, my data demonstrates dual blockade of IL-6 and CTLA-4 as a novel therapeutic combination that stimulates a unique $CD4^+$ T-cell dependent response and mediates PDAC regression in multiple murine models. Further, mechanistic studies revealed this combination therapy elicited efficacy in a CXCR3 dependent many, accompanied by systemic expansion of both Th1 and Th2 cells. In both cases, the effects of these successful therapeutics on myeloid cells or on specific CAF subsets was not explored. This is especially relevant since IL-6 influences dendritic cells[184] and myeloid derived suppressor cells[109] in PDAC. However, the influence of blocking IL-6 in combination with CTLA-4 or PD-L1 targeted antibodies on myeloid cells has

not been explored. Investigating the influence of these combination therapies on myeloid cells has the potential to uncover exploitable mechanisms of T-cell suppression or activation in PDAC.

My data has demonstrated dynamic interplay between CAFs and pancreatic cancer cells *in vitro*. Namely, CAFs promote pancreatic cancer migration and an invasive phenotype through secretion of soluble factors and in co-culture with pancreatic cancer cells. Utilization of supernatants from a selection of patient-derived CAFs allowed for analysis of impact on the invasion of the pancreatic cancer cell line HPAC. Interestingly, conditioned media from an immortalized CAF line, h-iPSC-PDAC-1(PSCL12), did not elicit significant invasion of HPAC cells into the surrounding collagen matrix in which they were buried. This difference may be explained by the lack of diverse fibroblast populations in the immortalized PSCL12 cell line. Primary CAF cultures from patients are freshly isolated from PDAC resection specimens, and these cultures likely contain similar CAF heterogeneity to the tumors from which they were isolated. While I would hypothesize that PSCL12 are more myofibroblastic and that the primary cultures are more inflammatory, ELISA and immunofluoresent imaging of PSCL12 reveals these cells concurrently express high amounts of IL-6 with dim expression of αSMA. Exposure of HPAC spheroids to high concentrations of IL-6 (10ng/ml) induced significant invasion into the surrounding matrix. Notably, this concentration is much higher than that measured in PSCL12 conditioned media, which does not induce significant invasion of these spheroids. Additionally, conditioned media from some primary human CAFs induced significant invasion and migration of HPAC spheroids but demonstrate variable expression of IL-6 which does not correlate with their impact on invasion. In fact, these lines also express moderate levels of several chemokines and cytokines including IL-10, SDF1α and Eotaxin, all of which have been implicated in cancer metastasis in other malignancies. Thus, it appears that IL-6 is capable of inducing pancreatic cancer cell migration but that this factor is not the singular, dominant soluble factor responsible for CAF induced changes in invasiveness of HPAC spheroids.

The inherent plasticity of CAF enable a spectrum of phenotypes to coexist in any one fibroblast culture at any given point in time. These phenotypes exist on a spectrum between the subsets so often highlighted in the literature[36,43]. This is evident in the single-cell sequencing data seen in multiple reports[36,43] and may be reflected here in my investigation where I see a spectrum of responses from HPAC spheroids in response to conditioned media from different primary CAFs.

While my data are intriguing and provocative, there are several limitations to these studies I preent here. Due to the scarcity of patient samples, it was challenging to obtain a significant amount of data with primary CAF lines on the collective migration of pancreatic cancer cells and CAFs. For this reason, most collective invasion data obtained here utilized two separate human CAF lines that had been immortalized (PSCL12 and hT1 which is labeled with mCherry). It is likely that immortalization and clonal generation of these lines detract greatly from the heterogeneity of a primary Pan-CAF line. Additionally, in this model system it is hard to decipher which cells are actually leading invasion and migration in co-culture or if "migrating" Pan-CAFs are simply reverting to *in vivo* conditions, whereby cells with a more inflammatory phenotype develop away from cancer cells. If the latter is true I would argue that these CAFs are still heavily influencing the movement of pancreatic cancer cells as they could produce soluble factors, lay down ECM components or remodel collagen to promote tumor cell migration. Another disadvantage to this in vitro system is that the many environmental cures such as hypoxia, the presence of immune cells and established matrices of diverse ECM components, cytokine and growth factors are absent. While we attempt to capture the soluble factors from Pan-CAFs in their natural state, their time in culture may shift their profile from that seen *in vivo.* Finally, HPAC cells are the only PDAC cell line we have been able to utilize for the generation of spheroids. These observations should not only be expanded to other cell lines, if possible, but should ultimately be confirmed *in vivo.*

Future studies of different CAF subsets in co-culture spheroids will utilize innovative approaches and techniques. To determine the possible conversion of PSCL12s to different CAF subsets in this 3D co-culture system, I have transduced the PSCL12 cell line to express photoconvertible Dendra2. Using this PSCL12-Dendra2 cell line will allow for co-culture of spheroids containing PSCL12-Dendra2 cells and HPAC cells to selectively profile CAFs with different invasive phenotypes. Using confocal microscopy and laser selection, we will select PSCL12-Dendra2 cells located at the invasive edge, within the spheroid body, or in distal areas of the surrounding collagen matrix. Using FACS we will then collect these cells and profile them by RNA sequencing to evaluate their respective phenotype. Information gleaned from this approach will help us better understand how CAFs interact with cancer cells in a 3D environment and affect metastasis and invasion of pancreatic cancer cells. In a reciprocal view, we also plan to generate HPAC cells expressing Dendra2. Generating these cells will allow us to similarly select, isolate and phenotypically profile the "sheepdog" cells that were identified and described in chapter 2.

Our previous analysis of CAFs in pancreatic cancer identified some of the most highly elevated factors secreted by these cells. While the immunological effects of these secreted factors in pancreatic cancer have been the topic of intensive investigation, the implications for these factors as potential drug targets in metastasis have not been considered. Previous literature provides conflicting reports about CAFs constraining or promoting pancreatic cancer progression. Here my data suggests the effects of CAFs isolated from individual patients on an invasive phenotype of PDAC cells are quite heterogeneous. Not surprisingly, my data also point to differential impacts of CAFs on the invasive phenotype in cancer cells depending upon their proximity to neoplastic cells. We have fortunately developed a suite of novel techniques and animal models that can examine how co-implantation of CAFs and PDAC cells impacts the metastatic process. Our future investigations

will seek to answer questions related to the relationship between CAFs and presence of metastasis in patients through clinical studies.

Over the past decade, there has been a concerted effort to advance our understanding of host immune responses to cancer. In particular, uncovering distinct checkpoint ligand/receptor interactions responsible for mediating immune exhaustion and tumor escape has provided a key leverage point for the application of anti-cancer therapeutics. Certainly the use of antibody based blockade of PD-1/PD-L1 has been the most popularized of these targets; however, many patients still fail to respond or develop resistance to this particular strategy. This is particularly true in pancreatic cancer where immune therapy has benefitted only a small subset of patients with microsatellite instable cancer. Thus, our research has sought to understand why the host immune response to pancreatic cancer fails in order to develop combination therapy strategies and improve immune based therapies in PDAC.

This current study, along with previous data from our group, demonstrates IL-6 neutralization to enhance multiple immune checkpoint blockade therapies, giving hope that his strategy could be expanded to additional immune therapies not previously explored. Utilizing neutralization of IL-6, a strategy previously developed by our lab, I demonstrate significantly enhanced anti-tumor efficacy of blocking the checkpoint receptor CTLA-4. This strategy elicited a potent anti-tumor response with a myriad of mechanistic differences delineating this strategy from our previous approach of dual IL-6 and PD-L1 blockade therapy. Perhaps the most striking difference between the two approaches is the relative dependence of the therapies on different T-cell populations. Namely, while dual blockade of IL-6 and PD-L1 is reliant upon $CD8^+$ T cells for efficacy, combined IL-6 and CTLA-4 blockade significantly enhanced $CD4^+FOXP3^-$ T-cell infiltration into pancreatic tumors and was dependent upon $CD4^+$ T cells. Notably, depleting $CD8^+$ T cells from mice receiving anti-IL-

6/CTLA-4 combination therapy provided only a modest inhibition of anti-tumor efficacy. Evaluation of the literature reveals mixed reports as to the $CD4^+$ or $CD8^+$ T-cell dependence of CTLA-4 blockade. Though my data demonstrates a heavy dependence on $CD4^+$ T cells for the efficacy of this particular combination therapy, $CD8^+$ T cells cannot be deemed uninvolved or unnecessary. Rather, both $CD4^+$ and $CD8^+$ T cells seem to mediate the effects of this therapy.

Other mechanistic studies revealed the importance of CXCR3 interactions as mediators of efficacy from combined blockade of Il-6 and CTLA-4. While CXCR3 blocking antibodies indeed prevented tumor regression, it should be noted that the infiltration of $CD4^+$and $CD8^+$ cells was only modestly and insignificantly inhibited. Further, mice receiving the combination therapy with or without CXCR3 blocking antibodies exhibited no differences in systemic frequencies of T-helper subsets. Thus, CXCR3 is not necessary for generating systemic immune responses to this therapy and is only partially responsible for the increased numbers of T cells present within the tumors of mice treated with the combination therapy. Perhaps, CXCR3 and its related chemokines have a role in the movement of cells, not only to the tumor, but also through the tumor itself or into and out of tertiary lymphoid structures. Future research should specifically interrogate the role of both tumor resident and infiltrating T cells in mediating the anti-tumor efficacy of this combination strategy as well as the role of CXCR3 in the activity of these T cells. A sophisticated *in vivo* approach could address this question. Fist, KPC-luc cells should be orthotopically implanted into immune competent C57BL/6 mice and allowed to establish for 1 week. To determine the role of T-cell trafficking from the lymph node, we could utilize the sphingosine 1-phosphate receptor (S1PR) agonist FTY720 prevents T cells from migrating out of lymph nodes into the lymphatic system and into tissues or tumors. These studies will allow us to determine whether T-cell trafficking from the lymph node is required for tumor regression mediated by our approach.

$CD4^+$ and $CD8^+$ T cells clearly mediate strong anti-tumor immune responses as a result of combined IL-6 and CTLA-4 blockade in multiple models of pancreatic cancer. The distinctive contributions of many myeloid cells or B-lymphocytes in this anti-tumor response is less clear. Of particular relevance is the expansion of $GATA3^+$ $CD4^+$ T cells observed in the presence of the combination therapy. Published literature supports multiple mechanisms of anti-tumor responses driven by Th2 cells including activation of eosinophil degranulation or induction of B cell class switching and subsequent complement activation[185-187]. While not explored here, understanding the involvement of other immune cells and molecules is extremely pertinent and essential to fully harnessing the potential of this combination therapy. Further, if these other immune responses are necessary for anti-tumor immunity in response to this therapy, the state of these immune components in patients should be evaluated before clinical application of this strategy.

Most importantly, my work reveals that checkpoint blockade therapies (PD-1/PD-L1 blockade and CTLA-4 blockade) can generate effective anti-tumor responses and tumor regression when combined with IL-6 neutralization in models of PDAC. This information is crucial to the future development of immune based therapies in PDAC, as it demonstrates that strategic timing and application of combination immune based therapies has the potential to elicit multi-phenotypic immune responses to pancreatic cancer. Recently, targeting of other checkpoint molecules such as LAG3, Galectin-9 and BTLA in other cancers has demonstrated significant promise to expand our arsenal of immune based therapeutic options. The mechanisms underlying the antitumor responses generated by these therapies rapidly becoming evident. As we gain understanding of mechanism by which these therapies affect immune responses in PDAC, this may impact our ability to strategically translate their use into the clinic. Going forward, significant effort should be made to determine if

utilizing blockade of IL-6, CTLA-4 and PD-1 can improve the already impressive results seen by blockade of IL-6 with either checkpoint receptor alone. This approach should be done strategically, as the different mechanisms mediated by the blockade of these two checkpoint receptors has the potential to be temporally controlled for an optimal anti-tumor immune response. Given the potent impact of CTLA-4 blockade therapy on T-helper cells, one logical application could be delivery of IL-6 and CTLA-4 blockade first, followed by the addition of PD-1 blockade to this regimen. These studies should be prioritized moving forward, as the tools and methods are readily available and established to test this hypothesis.

### 4.2 Concluding Remarks

These studies have made substantial efforts to understand the influence of the TME on PDAC progression and metastasis, there are still many questions left unanswered. First and foremost, the comparative differences between PDAC metastases and primary tumors should be addressed. Given the temperamental nature of the stroma in pancreatic tumors, developing therapeutics against CAFs or other stromal populations in the primary tumor may elicit unwanted responses in metastatic lesions. This may be have potentially occurred in trials with the sonic hedgehog inhibitor saridegib, which were discussed in section **1.7**. Thus, careful examination and comparison of the stroma in tumors and metastatic tumors is necessary to ensure safety of patients and efficient targeting of stromal elements that are associated with all stages of disease. On the other hand, our efforts to develop therapeutics and find novel treatment strategies for this devastating disease must push forward. It is possible that pre-clinical experience targeting IL-6 and CTLA-4 in combination will eventually make its way to the clinic to benefit patients, as with our previous study of IL-6 and PD--1. We must continue to explore potential mechanisms by which the immune response to PDAC can be manipulated therapeutically, while also seeking to understand the mechanisms underlying the

poor responses to early stages of this disease. I feel confident that the efforts I made will contribute to this understanding and the advancement of our fight against PDAC.

## References


1 Society, A. C. Cancer Facts & Figures. *Atlanta: American Cancer Society* (2020).

2 Siegel, R. L., Miller, K. D. & Jemal, A. Cancer statistics, 2020. *CA Cancer J Clin* **70**, 7-30, doi:10.3322/caac.21590 (2020).

3 Rahib, L. *et al.* Projecting cancer incidence and deaths to 2030: the unexpected burden of thyroid, liver, and pancreas cancers in the United States. *Cancer Res* **74**, 2913-2921, doi:10.1158/0008-5472.CAN-14-0155 (2014).

4 Al-Hajeili, M., Azmi, A. S. & Choi, M. Nab-paclitaxel: potential for the treatment of advanced pancreatic cancer. *OncoTargets and therapy* **7**, 187-192, doi:10.2147/OTT.S40705 (2014).

5 Alexandrov, L. B., Nik-Zainal, S., Wedge, D. C., Campbell, P. J. & Stratton, M. R. Deciphering signatures of mutational processes operative in human cancer. *Cell Rep* **3**, 246-259, doi:10.1016/j.celrep.2012.12.008 (2013).

6 Young, K., Hughes, D. J., Cunningham, D. & Starling, N. Immunotherapy and pancreatic cancer: unique challenges and potential opportunities. *Ther Adv Med Oncol* **10**, 1758835918816281, doi:10.1177/1758835918816281 (2018).

7 Hu, Z. I. *et al.* Evaluating Mismatch Repair Deficiency in Pancreatic Adenocarcinoma: Challenges and Recommendations. *Clin Cancer Res*, doi:10.1158/1078-0432.CCR-17-3099 (2018).

8 Cancer Genome Atlas Research Network. Electronic address, a. a. d. h. e. & Cancer Genome Atlas Research, N. Integrated Genomic Characterization of Pancreatic Ductal Adenocarcinoma. *Cancer Cell* **32**, 185-203 e113, doi:10.1016/j.ccell.2017.07.007 (2017).

9 Goess, R. & Friess, H. A look at the progress of treating pancreatic cancer over the past 20 years. *Expert Rev Anticancer Ther* **18**, 295-304, doi:10.1080/14737140.2018.1428093 (2018).

10 Mueller, S. *et al.* Evolutionary routes and KRAS dosage define pancreatic cancer phenotypes. *Nature* **554**, 62-68, doi:10.1038/nature25459 (2018).

11 Bryant, K. L., Mancias, J. D., Kimmelman, A. C. & Der, C. J. KRAS: feeding pancreatic cancer proliferation. *Trends Biochem Sci* **39**, 91-100, doi:10.1016/j.tibs.2013.12.004 (2014).

12 Kent, O. A. Increased mutant KRAS gene dosage drives pancreatic cancer progression: evidence for wild-type KRAS as a tumor suppressor? *Hepatobiliary Surg Nutr* **7**, 403-405, doi:10.21037/hbsn.2018.07.03 (2018).

13 Waters, A. M. & Der, C. J. KRAS: The Critical Driver and Therapeutic Target for Pancreatic Cancer. *Cold Spring Harb Perspect Med* **8**, doi:10.1101/cshperspect.a031435 (2018).

14 Corcoran, R. B. *et al.* STAT3 plays a critical role in KRAS-induced pancreatic tumorigenesis. *Cancer Res* **71**, 5020-5029, doi:10.1158/0008-5472.CAN-11-0908 (2011).

15 Aguirre, A. J. *et al.* Activated Kras and Ink4a/Arf deficiency cooperate to produce metastatic pancreatic ductal adenocarcinoma. *Genes Dev* **17**, 3112-3126, doi:10.1101/gad.1158703 (2003).

16 Bardeesy, N. *et al.* Smad4 is dispensable for normal pancreas development yet critical in progression and tumor biology of pancreas cancer. *Genes Dev* **20**, 3130-3146, doi:10.1101/gad.1478706 (2006).

17 Dias Carvalho, P. *et al.* KRAS Oncogenic Signaling Extends beyond Cancer Cells to Orchestrate the Microenvironment. *Cancer Res* **78**, 7-14, doi:10.1158/0008-5472.CAN-17-2084 (2018).

18 Zdanov, S. *et al.* Mutant KRAS Conversion of Conventional T Cells into Regulatory T Cells. *Cancer Immunol Res* **4**, 354-365, doi:10.1158/2326-6066.CIR-15-0241 (2016).

19 Busch, S. E. *et al.* Lung Cancer Subtypes Generate Unique Immune Responses. *J Immunol* **197**, 4493-4503, doi:10.4049/jimmunol.1600576 (2016).

20 Strobel, O. *et al.* In vivo lineage tracing defines the role of acinar-to-ductal transdifferentiation in inflammatory ductal metaplasia. *Gastroenterology* **133**, 1999-2009, doi:10.1053/j.gastro.2007.09.009 (2007).

21 Crawford, H. C., Scoggins, C. R., Washington, M. K., Matrisian, L. M. & Leach, S. D. Matrix metalloproteinase-7 is expressed by pancreatic cancer precursors and regulates acinar-to-ductal metaplasia in exocrine pancreas. *J Clin Invest* **109**, 1437-1444, doi:10.1172/JCI15051 (2002).

22 Lowenfels, A. B., Maisonneuve, P. & Whitcomb, D. C. Risk factors for cancer in hereditary pancreatitis. International Hereditary Pancreatitis Study Group. *Med Clin North Am* **84**, 565-573, doi:10.1016/s0025-7125(05)70240-6 (2000).

23 Grippo, P. J., Nowlin, P. S., Demeure, M. J., Longnecker, D. S. & Sandgren, E. P. Preinvasive pancreatic neoplasia of ductal phenotype induced by acinar cell targeting of mutant Kras in transgenic mice. *Cancer Res* **63**, 2016-2019 (2003).

24 Terhune, P. G., Phifer, D. M., Tosteson, T. D. & Longnecker, D. S. K-ras mutation in focal proliferative lesions of human pancreas. *Cancer Epidemiol Biomarkers Prev* **7**, 515-521 (1998).

25 Wagner, M. *et al.* A murine tumor progression model for pancreatic cancer recapitulating the genetic alterations of the human disease. *Genes Dev* **15**, 286-293, doi:10.1101/gad.184701 (2001).

26 Schmid, R. M. Acinar-to-ductal metaplasia in pancreatic cancer development. *J Clin Invest* **109**, 1403-1404, doi:10.1172/JCI15889 (2002).

27 He, P., Yang, J. W., Yang, V. W. & Bialkowska, A. B. Kruppel-like Factor 5, Increased in Pancreatic Ductal Adenocarcinoma, Promotes Proliferation, Acinar-to-Ductal Metaplasia, Pancreatic Intraepithelial Neoplasia, and Tumor Growth in Mice. *Gastroenterology* **154**, 1494-1508 e1413, doi:10.1053/j.gastro.2017.12.005 (2018).

28 David, C. J. *et al.* TGF-beta Tumor Suppression through a Lethal EMT. *Cell* **164**, 1015-1030, doi:10.1016/j.cell.2016.01.009 (2016).

29 Hingorani, S. R. *et al.* Trp53R172H and KrasG12D cooperate to promote chromosomal instability and widely metastatic pancreatic ductal adenocarcinoma in mice. *Cancer Cell* **7**, 469-483, doi:10.1016/j.ccr.2005.04.023 (2005).

30 Bournet, B. *et al.* KRAS G12D Mutation Subtype Is A Prognostic Factor for Advanced Pancreatic Adenocarcinoma. *Clin Transl Gastroenterol* **7**, e157, doi:10.1038/ctg.2016.18 (2016).

31 Izeradjene, K. *et al.* Kras(G12D) and Smad4/Dpc4 haploinsufficiency cooperate to induce mucinous cystic neoplasms and invasive adenocarcinoma of the pancreas. *Cancer Cell* **11**, 229-243, doi:10.1016/j.ccr.2007.01.017 (2007).

32 Blando, J. *et al.* Comparison of immune infiltrates in melanoma and pancreatic cancer highlights VISTA as a potential target in pancreatic cancer. *Proc Natl Acad Sci U S A* **116**, 1692-1697, doi:10.1073/pnas.1811067116 (2019).

33 Erkan, M. *et al.* The activated stroma index is a novel and independent prognostic marker in pancreatic ductal adenocarcinoma. *Clin Gastroenterol Hepatol* **6**, 1155-1161, doi:10.1016/j.cgh.2008.05.006 (2008).

34 Torphy, R. J. *et al.* Stromal Content Is Correlated With Tissue Site, Contrast Retention, and Survival in Pancreatic Adenocarcinoma. *JCO Precis Oncol* **2018**, doi:10.1200/PO.17.00121 (2018).

35 Ohlund, D. *et al.* Distinct populations of inflammatory fibroblasts and myofibroblasts in pancreatic cancer. *J Exp Med* **214**, 579-596, doi:10.1084/jem.20162024 (2017).

36 Elyada, E. *et al.* Cross-Species Single-Cell Analysis of Pancreatic Ductal Adenocarcinoma Reveals Antigen-Presenting Cancer-Associated Fibroblasts. *Cancer Discov* **9**, 1102-1123, doi:10.1158/2159-8290.CD-19-0094 (2019).

37 Ware, M. B., El-Rayes, B. F. & Lesinski, G. B. Mirage or long-awaited oasis: reinvigorating T-cell responses in pancreatic cancer. *J Immunother Cancer* **8**, doi:10.1136/jitc-2020-001100 (2020).

38 Olive, K. P. *et al.* Inhibition of Hedgehog signaling enhances delivery of chemotherapy in a mouse model of pancreatic cancer. *Science* **324**, 1457-1461, doi:10.1126/science.1171362 (2009).

39 Owen, K. A. *et al.* Regulation of lamellipodial persistence, adhesion turnover, and motility in macrophages by focal adhesion kinase. *J Cell Biol* **179**, 1275-1287, doi:10.1083/jcb.200708093 (2007).

40 Rhim, A. D. *et al.* Stromal elements act to restrain, rather than support, pancreatic ductal adenocarcinoma. *Cancer Cell* **25**, 735-747, doi:10.1016/j.ccr.2014.04.021 (2014).

41 Ozdemir, B. C. *et al.* Depletion of carcinoma-associated fibroblasts and fibrosis induces immunosuppression and accelerates pancreas cancer with reduced survival. *Cancer Cell* **25**, 719-734, doi:10.1016/j.ccr.2014.04.005 (2014).

42 Biffi, G. *et al.* IL1-Induced JAK/STAT Signaling Is Antagonized by TGFbeta to Shape CAF Heterogeneity in Pancreatic Ductal Adenocarcinoma. *Cancer Discov* **9**, 282-301, doi:10.1158/2159-8290.CD-18-0710 (2019).

43 Dominguez, C. X. *et al.* Single-Cell RNA Sequencing Reveals Stromal Evolution into LRRC15(+) Myofibroblasts as a Determinant of Patient Response to Cancer Immunotherapy. *Cancer Discov* **10**, 232-253, doi:10.1158/2159-8290.CD-19-0644 (2020).

44 Kim, Y. I. *et al.* Management of isolated recurrence after surgery for pancreatic adenocarcinoma. *Br J Surg* **106**, 898-909, doi:10.1002/bjs.11144 (2019).

45 Le Large, T. Y. S. *et al.* Key biological processes driving metastatic spread of pancreatic cancer as identified by multi-omics studies. *Semin Cancer Biol* **44**, 153-169, doi:10.1016/j.semcancer.2017.03.008 (2017).

46 Avula, L. R., Hagerty, B. & Alewine, C. Molecular mediators of peritoneal metastasis in pancreatic cancer. *Cancer Metastasis Rev*, doi:10.1007/s10555-020-09924-4 (2020).

47 Lee, J. W. *et al.* Hepatocytes direct the formation of a pro-metastatic niche in the liver. *Nature* **567**, 249-252, doi:10.1038/s41586-019-1004-y (2019).

48 Farren, M. R. *et al.* Systemic Immune Activity Predicts Overall Survival in Treatment-Naive Patients with Metastatic Pancreatic Cancer. *Clin Cancer Res* **22**, 2565-2574, doi:10.1158/1078-0432.CCR-15-1732 (2016).

49 Mace, T. A., Bloomston, M. & Lesinski, G. B. Pancreatic cancer-associated stellate cells: A viable target for reducing immunosuppression in the tumor microenvironment. *Oncoimmunology* **2**, e24891, doi:10.4161/onci.24891 (2013).

50 Mace, T. A. *et al.* IL-6 and PD-L1 antibody blockade combination therapy reduces tumour progression in murine models of pancreatic cancer. *Gut*, doi:10.1136/gutjnl-2016-311585 (2016).

51 Lenk, L. *et al.* The hepatic microenvironment essentially determines tumor cell dormancy and metastatic outgrowth of pancreatic ductal adenocarcinoma. *Oncoimmunology* **7**, e1368603, doi:10.1080/2162402X.2017.1368603 (2017).

52 Nielsen, S. R. *et al.* Macrophage-secreted granulin supports pancreatic cancer metastasis by inducing liver fibrosis. *Nat Cell Biol* **18**, 549-560, doi:10.1038/ncb3340 (2016).

53 Hwang, R. F. *et al.* Cancer-associated stromal fibroblasts promote pancreatic tumor progression. *Cancer Res* **68**, 918-926, doi:10.1158/0008-5472.CAN-07-5714 (2008).

54 O'Reilly, E. M. *et al.* Durvalumab With or Without Tremelimumab for Patients With Metastatic Pancreatic Ductal Adenocarcinoma: A Phase 2 Randomized Clinical Trial. *JAMA Oncol*, doi:10.1001/jamaoncol.2019.1588 (2019).

55 Royal, R. E. *et al.* Phase 2 trial of single agent Ipilimumab (anti-CTLA-4) for locally advanced or metastatic pancreatic adenocarcinoma. *J Immunother* **33**, 828-833, doi:10.1097/CJI.0b013e3181eec14c (2010).

56 Brahmer, J. R. *et al.* Safety and activity of anti-PD-L1 antibody in patients with advanced cancer. *N Engl J Med* **366**, 2455-2465, doi:10.1056/NEJMoa1200694 (2012).

57 Beatty, G. L. *et al.* Safety and antitumor activity of chimeric antigen receptor modified T cells in patients with chemotherapy refractory metastatic pancreatic cancer. *Journal of Clinical Oncology* **33**, doi:DOI 10.1200/jco.2015.33.15_suppl.3007 (2015).

58 Le, D. T. *et al.* Evaluation of ipilimumab in combination with allogeneic pancreatic tumor cells transfected with a GM-CSF gene in previously treated pancreatic cancer. *J Immunother* **36**, 382-389, doi:10.1097/CJI.0b013e31829fb7a2 (2013).

59 Le, D. T. *et al.* Safety and survival with GVAX pancreas prime and Listeria Monocytogenes-expressing mesothelin (CRS-207) boost vaccines for metastatic pancreatic cancer. *J Clin Oncol* **33**, 1325-1333, doi:10.1200/JCO.2014.57.4244 (2015).

60 Moretta, L., Webb, S. R., Grossi, C. E., Lydyard, P. M. & Cooper, M. D. Functional analysis of two human T-cell subpopulations: help and suppression of B-cell responses by T cells bearing receptors for IgM or IgG. *J Exp Med* **146**, 184-200, doi:10.1084/jem.146.1.184 (1977).

61 Tada, T., Takemori, T., Okumura, K., Nonaka, M. & Tokuhisa, T. Two distinct types of helper T cells involved in the secondary antibody response: independent and synergistic

effects of Ia- and Ia+ helper T cells. *J Exp Med* **147**, 446-458, doi:10.1084/jem.147.2.446 (1978).

62 Kung, P., Goldstein, G., Reinherz, E. L. & Schlossman, S. F. Monoclonal antibodies defining distinctive human T cell surface antigens. *Science* **206**, 347-349, doi:10.1126/science.314668 (1979).

63 Evans, R. L., Lazarus, H., Penta, A. C. & Schlossman, S. F. Two functionally distinct subpopulations of human T cells that collaborate in the generation of cytotoxic cells responsible for cell-mediated lympholysis. *J Immunol* **120**, 1423-1428 (1978).

64 Durda, P. J. & Gottlieb, P. D. Sequential precipitation of mouse thymocyte extracts with anti-Lyt-2 and anti-Lyt-3 sera. I. Lyt-2.1 and Lyt-3.1 antigenic determinants reside on separable molecular species. *J Immunol* **121**, 983-989 (1978).

65 Hollander, N., Pillemer, E. & Weissman, I. L. Blocking effect of lyt-2 antibodies on T cell functions. *J Exp Med* **152**, 674-687, doi:10.1084/jem.152.3.674 (1980).

66 Shinohara, N. & Sachs, D. H. Mouse alloantibodies capable of blocking cytotoxic T-cell function. I. Relationship between the antigen reactive with blocking antibodies and the Lyt-2 locus. *J Exp Med* **150**, 432-444, doi:10.1084/jem.150.3.432 (1979).

67 Cantor, H. & Boyse, E. A. Functional subclasses of T lymphocytes bearing different Ly antigens. II. Cooperation between subclasses of Ly+ cells in the generation of killer activity. *J Exp Med* **141**, 1390-1399, doi:10.1084/jem.141.6.1390 (1975).

68 Shiku, H. *et al.* Expression of T-cell differentiation antigens on effector cells in cell-mediated cytotoxicity in vitro. Evidence for functional heterogeneity related to the surface phenotype of T cells. *J Exp Med* **141**, 227-241, doi:10.1084/jem.141.1.227 (1975).

69 Howard, M. *et al.* Identification of a T cell-derived b cell growth factor distinct from interleukin 2. *J Exp Med* **155**, 914-923, doi:10.1084/jem.155.3.914 (1982).

70 Isakson, P. C., Pure, E., Vitetta, E. S. & Krammer, P. H. T cell-derived B cell differentiation factor(s). Effect on the isotype switch of murine B cells. *J Exp Med* **155**, 734-748, doi:10.1084/jem.155.3.734 (1982).

71 Mosmann, T. R., Cherwinski, H., Bond, M. W., Giedlin, M. A. & Coffman, R. L. Two types of murine helper T cell clone. I. Definition according to profiles of lymphokine activities and secreted proteins. *J Immunol* **136**, 2348-2357 (1986).

72 Coffman, R. L. *et al.* The role of helper T cell products in mouse B cell differentiation and isotype regulation. *Immunol Rev* **102**, 5-28, doi:10.1111/j.1600-065x.1988.tb00739.x (1988).

73 Stevens, T. L. *et al.* Regulation of antibody isotype secretion by subsets of antigen-specific helper T cells. *Nature* **334**, 255-258, doi:10.1038/334255a0 (1988).

74 Do, J. S. *et al.* Committed memory effector type 2 cytotoxic T (Tc2) cells are ineffective in protective anti-tumor immunity. *Immunol Lett* **95**, 77-84, doi:10.1016/j.imlet.2004.06.006 (2004).

75 Takeuchi, A. & Saito, T. CD4 CTL, a Cytotoxic Subset of CD4(+) T Cells, Their Differentiation and Function. *Front Immunol* **8**, 194, doi:10.3389/fimmu.2017.00194 (2017).

76 Hsieh, C. S., Heimberger, A. B., Gold, J. S., O'Garra, A. & Murphy, K. M. Differential regulation of T helper phenotype development by interleukins 4 and 10 in an alpha beta T-cell-receptor transgenic system. *Proc Natl Acad Sci U S A* **89**, 6065-6069, doi:10.1073/pnas.89.13.6065 (1992).

77 Hsieh, C. S. *et al.* Development of TH1 CD4+ T cells through IL-12 produced by Listeria-induced macrophages. *Science* **260**, 547-549, doi:10.1126/science.8097338 (1993).

78 Yamamoto, J. *et al.* Differential expression of the chemokine receptors by the Th1- and Th2-type effector populations within circulating CD4+ T cells. *J Leukoc Biol* **68**, 568-574 (2000).

79 Groom, J. R. & Luster, A. D. CXCR3 in T cell function. *Exp Cell Res* **317**, 620-631, doi:10.1016/j.yexcr.2010.12.017 (2011).

80 Al-Banna, N. A., Vaci, M., Slauenwhite, D., Johnston, B. & Issekutz, T. B. CCR4 and CXCR3 play different roles in the migration of T cells to inflammation in skin, arthritic joints, and lymph nodes. *Eur J Immunol* **44**, 1633-1643, doi:10.1002/eji.201343995 (2014).

81 Yoshie, O. & Matsushima, K. CCR4 and its ligands: from bench to bedside. *Int Immunol* **27**, 11-20, doi:10.1093/intimm/dxu079 (2015).

82 Szabo, S. J. *et al.* A novel transcription factor, T-bet, directs Th1 lineage commitment. *Cell* **100**, 655-669, doi:10.1016/s0092-8674(00)80702-3 (2000).

83 Koch, M. A. *et al.* The transcription factor T-bet controls regulatory T cell homeostasis and function during type 1 inflammation. *Nat Immunol* **10**, 595-602, doi:10.1038/ni.1731 (2009).

84 Zheng, W. & Flavell, R. A. The transcription factor GATA-3 is necessary and sufficient for Th2 cytokine gene expression in CD4 T cells. *Cell* **89**, 587-596, doi:10.1016/s0092-8674(00)80240-8 (1997).

85 Rincon, M., Anguita, J., Nakamura, T., Fikrig, E. & Flavell, R. A. Interleukin (IL)-6 directs the differentiation of IL-4-producing CD4+ T cells. *J Exp Med* **185**, 461-469, doi:10.1084/jem.185.3.461 (1997).

86 Cua, D. J. *et al.* Interleukin-23 rather than interleukin-12 is the critical cytokine for autoimmune inflammation of the brain. *Nature* **421**, 744-748, doi:10.1038/nature01355 (2003).

87 Murphy, C. A. *et al.* Divergent pro- and antiinflammatory roles for IL-23 and IL-12 in joint autoimmune inflammation. *J Exp Med* **198**, 1951-1957, doi:10.1084/jem.20030896 (2003).

88 Langrish, C. L. *et al.* IL-23 drives a pathogenic T cell population that induces autoimmune inflammation. *J Exp Med* **201**, 233-240, doi:10.1084/jem.20041257 (2005).

89 Harrington, L. E. *et al.* Interleukin 17-producing CD4+ effector T cells develop via a lineage distinct from the T helper type 1 and 2 lineages. *Nat Immunol* **6**, 1123-1132, doi:10.1038/ni1254 (2005).

90 Knochelmann, H. M. *et al.* When worlds collide: Th17 and Treg cells in cancer and autoimmunity. *Cell Mol Immunol* **15**, 458-469, doi:10.1038/s41423-018-0004-4 (2018).

91 Gershon, R. K. & Kondo, K. Cell interactions in the induction of tolerance: the role of thymic lymphocytes. *Immunology* **18**, 723-737 (1970).

92 Sakaguchi, S., Takahashi, T. & Nishizuka, Y. Study on cellular events in postthymectomy autoimmune oophoritis in mice. I. Requirement of Lyt-1 effector cells for oocytes damage after adoptive transfer. *J Exp Med* **156**, 1565-1576, doi:10.1084/jem.156.6.1565 (1982).

93 Sakaguchi, S., Sakaguchi, N., Asano, M., Itoh, M. & Toda, M. Immunologic self-tolerance maintained by activated T cells expressing IL-2 receptor alpha-chains (CD25). Breakdown of a single mechanism of self-tolerance causes various autoimmune diseases. *J Immunol* **155**, 1151-1164 (1995).

94 Chen, W. *et al.* Conversion of peripheral CD4+CD25- naive T cells to CD4+CD25+ regulatory T cells by TGF-beta induction of transcription factor Foxp3. *J Exp Med* **198**, 1875-1886, doi:10.1084/jem.20030152 (2003).

95 Fontenot, J. D., Gavin, M. A. & Rudensky, A. Y. Foxp3 programs the development and function of CD4+CD25+ regulatory T cells. *Nat Immunol* **4**, 330-336, doi:10.1038/ni904 (2003).

96 Hori, S., Nomura, T. & Sakaguchi, S. Control of regulatory T cell development by the transcription factor Foxp3. *Science* **299**, 1057-1061, doi:10.1126/science.1079490 (2003).

97 Kasprowicz, D. J., Smallwood, P. S., Tyznik, A. J. & Ziegler, S. F. Scurfin (FoxP3) controls T-dependent immune responses in vivo through regulation of CD4+ T cell effector function. *J Immunol* **171**, 1216-1223, doi:10.4049/jimmunol.171.3.1216 (2003).

98 Khattri, R., Cox, T., Yasayko, S. A. & Ramsdell, F. An essential role for Scurfin in CD4+CD25+ T regulatory cells. *Nat Immunol* **4**, 337-342, doi:10.1038/ni909 (2003).

99 Ramsdell, F. Foxp3 and natural regulatory T cells: key to a cell lineage? *Immunity* **19**, 165-168, doi:10.1016/s1074-7613(03)00207-3 (2003).

100 Sakaguchi, S. The origin of FOXP3-expressing CD4+ regulatory T cells: thymus or periphery. *J Clin Invest* **112**, 1310-1312, doi:10.1172/JCI20274 (2003).

101 Walker, M. R. *et al.* Induction of FoxP3 and acquisition of T regulatory activity by stimulated human CD4+CD25- T cells. *J Clin Invest* **112**, 1437-1443, doi:10.1172/JCI19441 (2003).

102 Korn, T. *et al.* IL-6 controls Th17 immunity in vivo by inhibiting the conversion of conventional T cells into Foxp3+ regulatory T cells. *Proc Natl Acad Sci U S A* **105**, 18460-18465, doi:10.1073/pnas.0809850105 (2008).

103 Rudensky, A. Y. Regulatory T cells and Foxp3. *Immunol Rev* **241**, 260-268, doi:10.1111/j.1600-065X.2011.01018.x (2011).

104 Ahmed, S., Bradshaw, A. D., Gera, S., Dewan, M. Z. & Xu, R. The TGF-beta/Smad4 Signaling Pathway in Pancreatic Carcinogenesis and Its Clinical Significance. *J Clin Med* **6**, doi:10.3390/jcm6010005 (2017).

105 Aoki, H. *et al.* Autocrine loop between TGF-beta1 and IL-1beta through Smad3- and ERK-dependent pathways in rat pancreatic stellate cells. *Am J Physiol Cell Physiol* **290**, C1100-1108, doi:10.1152/ajpcell.00465.2005 (2006).

106 Aoki, H. *et al.* Existence of autocrine loop between interleukin-6 and transforming growth factor-beta1 in activated rat pancreatic stellate cells. *J Cell Biochem* **99**, 221-228, doi:10.1002/jcb.20906 (2006).

107 Goumas, F. A. *et al.* Inhibition of IL-6 signaling significantly reduces primary tumor growth and recurrencies in orthotopic xenograft models of pancreatic cancer. *Int J Cancer*, doi:10.1002/ijc.29445 (2015).

108 Lesina, M. *et al.* Stat3/Socs3 activation by IL-6 transsignaling promotes progression of pancreatic intraepithelial neoplasia and development of pancreatic cancer. *Cancer Cell* **19**, 456-469, doi:10.1016/j.ccr.2011.03.009 (2011).

109 Mace, T. A. *et al.* Pancreatic cancer-associated stellate cells promote differentiation of myeloid-derived suppressor cells in a STAT3-dependent manner. *Cancer Res* **73**, 3007-3018, doi:10.1158/0008-5472.CAN-12-4601 (2013).

110 Mitsunaga, S. *et al.* Serum levels of IL-6 and IL-1beta can predict the efficacy of gemcitabine in patients with advanced pancreatic cancer. *Br J Cancer* **108**, 2063-2069, doi:10.1038/bjc.2013.174 (2013).

111 Principe, D. R. *et al.* TGFbeta Signaling in the Pancreatic Tumor Microenvironment Promotes Fibrosis and Immune Evasion to Facilitate Tumorigenesis. *Cancer Res* **76**, 2525-2539, doi:10.1158/0008-5472.CAN-15-1293 (2016).

112 Principe, D. R. *et al.* TGFbeta Blockade Augments PD-1 Inhibition to Promote T-Cell-Mediated Regression of Pancreatic Cancer. *Mol Cancer Ther* **18**, 613-620, doi:10.1158/1535-7163.MCT-18-0850 (2019).

113 Barilla, R. M. *et al.* Specialized dendritic cells induce tumor-promoting IL-10(+)IL-17(+) FoxP3(neg) regulatory CD4(+) T cells in pancreatic carcinoma. *Nat Commun* **10**, 1424, doi:10.1038/s41467-019-09416-2 (2019).

114 Jang, J. E. *et al.* Crosstalk between Regulatory T Cells and Tumor-Associated Dendritic Cells Negates Anti-tumor Immunity in Pancreatic Cancer. *Cell Rep* **20**, 558-571, doi:10.1016/j.celrep.2017.06.062 (2017).

115 Shevchenko, I. *et al.* Low-dose gemcitabine depletes regulatory T cells and improves survival in the orthotopic Panc02 model of pancreatic cancer. *Int J Cancer* **133**, 98-107, doi:10.1002/ijc.27990 (2013).

116 Muranski, P. *et al.* Tumor-specific Th17-polarized cells eradicate large established melanoma. *Blood* **112**, 362-373, doi:10.1182/blood-2007-11-120998 (2008).

117 Diehl, S. & Rincon, M. The two faces of IL-6 on Th1/Th2 differentiation. *Mol Immunol* **39**, 531-536, doi:10.1016/s0161-5890(02)00210-9 (2002).

118 Szabo, S. J. *et al.* Distinct effects of T-bet in TH1 lineage commitment and IFN-gamma production in CD4 and CD8 T cells. *Science* **295**, 338-342, doi:10.1126/science.1065543 (2002).

119 Chen, H. *et al.* Anti-CTLA-4 therapy results in higher CD4+ICOShi T cell frequency and IFN-gamma levels in both nonmalignant and malignant prostate tissues. *Proc Natl Acad Sci U S A* **106**, 2729-2734, doi:10.1073/pnas.0813175106 (2009).

120 Bailey, J. M. *et al.* Sonic hedgehog promotes desmoplasia in pancreatic cancer. *Clin Cancer Res* **14**, 5995-6004, doi:10.1158/1078-0432.CCR-08-0291 (2008).

121 Hingorani, S. R. *et al.* HALO 202: Randomized Phase II Study of PEGPH20 Plus Nab-Paclitaxel/Gemcitabine Versus Nab-Paclitaxel/Gemcitabine in Patients With Untreated, Metastatic Pancreatic Ductal Adenocarcinoma. *J Clin Oncol* **36**, 359-366, doi:10.1200/JCO.2017.74.9564 (2018).

122 Infante, J. R. *et al.* Phase 1 trials of PEGylated recombinant human hyaluronidase PH20 in patients with advanced solid tumours. *Br J Cancer* **118**, e3, doi:10.1038/bjc.2017.438 (2018).

123 Sato, N., Cheng, X. B., Kohi, S., Koga, A. & Hirata, K. Targeting hyaluronan for the treatment of pancreatic ductal adenocarcinoma. *Acta Pharm Sin B* **6**, 101-105, doi:10.1016/j.apsb.2016.01.002 (2016).

124 Scheller, J., Chalaris, A., Schmidt-Arras, D. & Rose-John, S. The pro- and anti-inflammatory properties of the cytokine interleukin-6. *Biochim Biophys Acta* **1813**, 878-888, doi:10.1016/j.bbamcr.2011.01.034 (2011).

125 Johnson, D. E., O'Keefe, R. A. & Grandis, J. R. Targeting the IL-6/JAK/STAT3 signalling axis in cancer. *Nat Rev Clin Oncol* **15**, 234-248, doi:10.1038/nrclinonc.2018.8 (2018).

126 Sahin, I. H., Elias, H., Chou, J. F., Capanu, M. & O'Reilly, E. M. Pancreatic adenocarcinoma: insights into patterns of recurrence and disease behavior. *BMC Cancer* **18**, 769, doi:10.1186/s12885-018-4679-9 (2018).

127 Neesse, A. *et al.* Stromal biology and therapy in pancreatic cancer. *Gut* **60**, 861-868, doi:10.1136/gut.2010.226092 (2011).

128 Mahadevan, D. & Von Hoff, D. D. Tumor-stroma interactions in pancreatic ductal adenocarcinoma. *Mol Cancer Ther* **6**, 1186-1197, doi:10.1158/1535-7163.MCT-06-0686 (2007).

129 Xu, Z. *et al.* Role of pancreatic stellate cells in pancreatic cancer metastasis. *Am J Pathol* **177**, 2585-2596, doi:10.2353/ajpath.2010.090899 (2010).

130 Connolly, M. K. *et al.* Distinct populations of metastases-enabling myeloid cells expand in the liver of mice harboring invasive and preinvasive intra-abdominal tumor. *J Leukoc Biol* **87**, 713-725, doi:10.1189/jlb.0909607 (2010).

131 Toh, B. *et al.* Mesenchymal transition and dissemination of cancer cells is driven by myeloid-derived suppressor cells infiltrating the primary tumor. *PLoS Biol* **9**, e1001162, doi:10.1371/journal.pbio.1001162 (2011).

132 Vonlaufen, A. *et al.* Pancreatic stellate cells: partners in crime with pancreatic cancer cells. *Cancer Res* **68**, 2085-2093, doi:10.1158/0008-5472.CAN-07-2477 (2008).

133 Konen, J. *et al.* Image-guided genomics of phenotypically heterogeneous populations reveals vascular signalling during symbiotic collective cancer invasion. *Nat Commun* **8**, 15078, doi:10.1038/ncomms15078 (2017).

134 Sousa, C. M. *et al.* Pancreatic stellate cells support tumour metabolism through autophagic alanine secretion. *Nature* **536**, 479-483, doi:10.1038/nature19084 (2016).

135 Zhao, H. *et al.* Tumor microenvironment derived exosomes pleiotropically modulate cancer cell metabolism. *Elife* **5**, e10250, doi:10.7554/eLife.10250 (2016).

136 Kim, H. W. *et al.* Serum interleukin-6 is associated with pancreatic ductal adenocarcinoma progression pattern. *Medicine (Baltimore)* **96**, e5926, doi:10.1097/MD.0000000000005926 (2017).

137 Lee, J. W. *et al.* Hepatocytes direct the formation of a pro-metastatic niche in the liver. *Nature*, doi:10.1038/s41586-019-1004-y (2019).

138 Affara, N. I. *et al.* B cells regulate macrophage phenotype and response to chemotherapy in squamous carcinomas. *Cancer Cell* **25**, 809-821, doi:10.1016/j.ccr.2014.04.026 (2014).

139 Ai, L. *et al.* Prognostic role of myeloid-derived suppressor cells in cancers: a systematic review and meta-analysis. *BMC Cancer* **18**, 1220, doi:10.1186/s12885-018-5086-y (2018).

140 Bayne, L. J. *et al.* Tumor-derived granulocyte-macrophage colony-stimulating factor regulates myeloid inflammation and T cell immunity in pancreatic cancer. *Cancer Cell* **21**, 822-835, doi:10.1016/j.ccr.2012.04.025 (2012).

141 Chang, Q. *et al.* The IL-6/JAK/Stat3 feed-forward loop drives tumorigenesis and metastasis. *Neoplasia* **15**, 848-862 (2013).

142 Dysthe, M. & Parihar, R. Myeloid-Derived Suppressor Cells in the Tumor Microenvironment. *Adv Exp Med Biol* **1224**, 117-140, doi:10.1007/978-3-030-35723-8_8 (2020).

143 Gabitass, R. F., Annels, N. E., Stocken, D. D., Pandha, H. A. & Middleton, G. W. Elevated myeloid-derived suppressor cells in pancreatic, esophageal and gastric cancer are an independent prognostic factor and are associated with significant elevation of the Th2 cytokine interleukin-13. *Cancer Immunol Immunother* **60**, 1419-1430, doi:10.1007/s00262-011-1028-0 (2011).

144 Liu, Q. *et al.* Targeting interlukin-6 to relieve immunosuppression in tumor microenvironment. *Tumour Biol* **39**, 1010428317712445, doi:10.1177/1010428317712445 (2017).

145 Markowitz, J. *et al.* Patients with pancreatic adenocarcinoma exhibit elevated levels of myeloid-derived suppressor cells upon progression of disease. *Cancer Immunol Immunother* **64**, 149-159, doi:10.1007/s00262-014-1618-8 (2015).

146 Wang, X. *et al.* Cancer-FOXP3 directly activated CCL5 to recruit FOXP3+Treg cells in pancreatic ductal adenocarcinoma. *Oncogene* **36**, 3048-3058, doi:10.1038/onc.2016.458 (2017).

147 Wu, P. *et al.* gammadeltaT17 cells promote the accumulation and expansion of myeloid-derived suppressor cells in human colorectal cancer. *Immunity* **40**, 785-800, doi:10.1016/j.immuni.2014.03.013 (2014).

148 Castino, G. F. *et al.* Spatial distribution of B cells predicts prognosis in human pancreatic adenocarcinoma. *Oncoimmunology* **5**, e1085147, doi:10.1080/2162402X.2015.1085147 (2016).

149 Lee, K. E. *et al.* Hif1a Deletion Reveals Pro-Neoplastic Function of B Cells in Pancreatic Neoplasia. *Cancer Discov* **6**, 256-269, doi:10.1158/2159-8290.CD-15-0822 (2016).

150 Pylayeva-Gupta, Y. *et al.* IL35-Producing B Cells Promote the Development of Pancreatic Neoplasia. *Cancer Discov* **6**, 247-255, doi:10.1158/2159-8290.CD-15-0843 (2016).

151 Lakins, M. A., Ghorani, E., Munir, H., Martins, C. P. & Shields, J. D. Cancer-associated fibroblasts induce antigen-specific deletion of CD8 (+) T Cells to protect tumour cells. *Nat Commun* **9**, 948, doi:10.1038/s41467-018-03347-0 (2018).

152 Ene-Obong, A. *et al.* Activated pancreatic stellate cells sequester CD8+ T cells to reduce their infiltration of the juxtatumoral compartment of pancreatic ductal adenocarcinoma. *Gastroenterology* **145**, 1121-1132, doi:10.1053/j.gastro.2013.07.025 (2013).

153 Ferdek, P. E. & Jakubowska, M. A. Biology of pancreatic stellate cells-more than just pancreatic cancer. *Pflugers Arch* **469**, 1039-1050, doi:10.1007/s00424-017-1968-0 (2017).

154 Fujita, H. *et al.* alpha-Smooth Muscle Actin Expressing Stroma Promotes an Aggressive Tumor Biology in Pancreatic Ductal Adenocarcinoma. *Pancreas*, doi:10.1097/MPA.0b013e3181dbf647 (2010).

155 Ottaviano, M., De Placido, S. & Ascierto, P. A. Recent success and limitations of immune checkpoint inhibitors for cancer: a lesson from melanoma. *Virchows Arch* **474**, 421-432, doi:10.1007/s00428-019-02538-4 (2019).

156 Tan, E. & El-Rayes, B. Pancreatic Cancer and Immunotherapy: Resistance Mechanisms and Proposed Solutions. *J Gastrointest Cancer* **50**, 1-8, doi:10.1007/s12029-018-0179-z (2019).

157 Gorchs, L. *et al.* Human Pancreatic Carcinoma-Associated Fibroblasts Promote Expression of Co-inhibitory Markers on CD4(+) and CD8(+) T-Cells. *Front Immunol* **10**, 847, doi:10.3389/fimmu.2019.00847 (2019).

158 Dienz, O. & Rincon, M. The effects of IL-6 on CD4 T cell responses. *Clin Immunol* **130**, 27-33, doi:10.1016/j.clim.2008.08.018 (2009).

159 Boj, S. F. *et al.* Organoid models of human and mouse ductal pancreatic cancer. *Cell* **160**, 324-338, doi:10.1016/j.cell.2014.12.021 (2015).

160 Bengsch, F., Knoblock, D. M., Liu, A., McAllister, F. & Beatty, G. L. CTLA-4/CD80 pathway regulates T cell infiltration into pancreatic cancer. *Cancer Immunol Immunother* **66**, 1609-1617, doi:10.1007/s00262-017-2053-4 (2017).

161 Diehl, S. *et al.* Induction of NFATc2 expression by interleukin 6 promotes T helper type 2 differentiation. *J Exp Med* **196**, 39-49, doi:10.1084/jem.20020026 (2002).

162 Loetscher, M. *et al.* Chemokine receptor specific for IP10 and mig: structure, function, and expression in activated T-lymphocytes. *J Exp Med* **184**, 963-969, doi:10.1084/jem.184.3.963 (1996).

163 Loetscher, M., Loetscher, P., Brass, N., Meese, E. & Moser, B. Lymphocyte-specific chemokine receptor CXCR3: regulation, chemokine binding and gene localization. *Eur J Immunol* **28**, 3696-3705, doi:10.1002/(SICI)1521-4141(199811)28:11<3696::AID-IMMU3696>3.0.CO;2-W (1998).

164 Cole, K. E. *et al.* Interferon-inducible T cell alpha chemoattractant (I-TAC): a novel non-ELR CXC chemokine with potent activity on activated T cells through selective high affinity binding to CXCR3. *J Exp Med* **187**, 2009-2021, doi:10.1084/jem.187.12.2009 (1998).

165 Lu, B. *et al.* Structure and function of the murine chemokine receptor CXCR3. *Eur J Immunol* **29**, 3804-3812, doi:10.1002/(SICI)1521-4141(199911)29:11<3804::AID-IMMU3804>3.0.CO;2-9 (1999).

166 Angevin, E. *et al.* A phase I/II, multiple-dose, dose-escalation study of siltuximab, an anti-interleukin-6 monoclonal antibody, in patients with advanced solid tumors. *Clin Cancer Res* **20**, 2192-2204, doi:10.1158/1078-0432.CCR-13-2200 (2014).

167 Kamath, S. D. *et al.* Ipilimumab and Gemcitabine for Advanced Pancreatic Cancer: A Phase Ib Study. *Oncologist*, doi:10.1634/theoncologist.2019-0473 (2019).

168 Lamano, J. B. *et al.* Glioblastoma-Derived IL6 Induces Immunosuppressive Peripheral Myeloid Cell PD-L1 and Promotes Tumor Growth. *Clin Cancer Res* **25**, 3643-3657, doi:10.1158/1078-0432.CCR-18-2402 (2019).

169 Li, J. *et al.* Targeting Interleukin-6 (IL-6) Sensitizes Anti-PD-L1 Treatment in a Colorectal Cancer Preclinical Model. *Med Sci Monit* **24**, 5501-5508, doi:10.12659/MSM.907439 (2018).

170 Tsukamoto, H. *et al.* Combined Blockade of IL6 and PD-1/PD-L1 Signaling Abrogates Mutual Regulation of Their Immunosuppressive Effects in the Tumor Microenvironment. *Cancer Res* **78**, 5011-5022, doi:10.1158/0008-5472.CAN-18-0118 (2018).

171 Alspach, E. *et al.* MHC-II neoantigens shape tumour immunity and response to immunotherapy. *Nature* **574**, 696-701, doi:10.1038/s41586-019-1671-8 (2019).

172 Liakou, C. I. *et al.* CTLA-4 blockade increases IFNgamma-producing CD4+ICOShi cells to shift the ratio of effector to regulatory T cells in cancer patients. *Proc Natl Acad Sci U S A* **105**, 14987-14992, doi:10.1073/pnas.0806075105 (2008).

173 Dunn, G. P., Koebel, C. M. & Schreiber, R. D. Interferons, immunity and cancer immunoediting. *Nat Rev Immunol* **6**, 836-848, doi:10.1038/nri1961 (2006).

174 Ikeda, H., Old, L. J. & Schreiber, R. D. The roles of IFN gamma in protection against tumor development and cancer immunoediting. *Cytokine Growth Factor Rev* **13**, 95-109, doi:10.1016/s1359-6101(01)00038-7 (2002).

175 Detjen, K. M., Farwig, K., Welzel, M., Wiedenmann, B. & Rosewicz, S. Interferon gamma inhibits growth of human pancreatic carcinoma cells via caspase-1 dependent induction of apoptosis. *Gut* **49**, 251-262, doi:10.1136/gut.49.2.251 (2001).

176 Chin, Y. E., Kitagawa, M., Kuida, K., Flavell, R. A. & Fu, X. Y. Activation of the STAT signaling pathway can cause expression of caspase 1 and apoptosis. *Mol Cell Biol* **17**, 5328-5337, doi:10.1128/mcb.17.9.5328 (1997).

177 Gao, J. *et al.* Loss of IFN-gamma Pathway Genes in Tumor Cells as a Mechanism of Resistance to Anti-CTLA-4 Therapy. *Cell* **167**, 397-404 e399, doi:10.1016/j.cell.2016.08.069 (2016).

178 Chow, M. T. *et al.* Intratumoral Activity of the CXCR3 Chemokine System Is Required for the Efficacy of Anti-PD-1 Therapy. *Immunity* **50**, 1498-1512 e1495, doi:10.1016/j.immuni.2019.04.010 (2019).

179 McLoughlin, R. M. *et al.* IL-6 trans-signaling via STAT3 directs T cell infiltration in acute inflammation. *Proc Natl Acad Sci U S A* **102**, 9589-9594, doi:10.1073/pnas.0501794102 (2005).

180 Uemura, M. *et al.* Selective inhibition of autoimmune exacerbation while preserving the anti-tumor clinical benefit using IL-6 blockade in a patient with advanced melanoma and Crohn's disease: a case report. *J Hematol Oncol* **9**, 81, doi:10.1186/s13045-016-0309-7 (2016).

181 Maude, S. L., Barrett, D., Teachey, D. T. & Grupp, S. A. Managing cytokine release syndrome associated with novel T cell-engaging therapies. *Cancer J* **20**, 119-122, doi:10.1097/PPO.0000000000000035 (2014).

182 Horisberger, A. *et al.* A severe case of refractory esophageal stenosis induced by nivolumab and responding to tocilizumab therapy. *J Immunother Cancer* **6**, 156, doi:10.1186/s40425-018-0481-0 (2018).

183 Bankhead, P. *et al.* QuPath: Open source software for digital pathology image analysis. *Sci Rep* **7**, 16878, doi:10.1038/s41598-017-17204-5 (2017).

184 Lin, J. H. *et al.* Type 1 conventional dendritic cells are systemically dysregulated early in pancreatic carcinogenesis. *J Exp Med* **217**, doi:10.1084/jem.20190673 (2020).

185 Ellyard, J. I., Simson, L. & Parish, C. R. Th2-mediated anti-tumour immunity: friend or foe? *Tissue Antigens* **70**, 1-11, doi:10.1111/j.1399-0039.2007.00869.x (2007).

186 Varricchi, G. *et al.* Eosinophils: The unsung heroes in cancer? *Oncoimmunology* **7**, e1393134, doi:10.1080/2162402X.2017.1393134 (2018).

187 Yalcindag, A. *et al.* The complement component C3 plays a critical role in both Th1 and Th2 responses to antigen. *J Allergy Clin Immunol* **117**, 1455-1461, doi:10.1016/j.jaci.2006.01.048 (2006).